



## 12° Workshop tematico di Telerilevamento

IL RUOLO DEI DATI COPERNICUS SENTINEL NEI PROCESSI DI CONOSCENZA E  
GESTIONE DEL TERRITORIO: STATO DELL'ARTE DEL TRASFERIMENTO  
TECNOLOGICO AL COMPARTO OPERATIVO

•PROCESSAMENTO •CARTOGRAFIA •ESTRAZIONE INFORMAZIONI •COSTI/BENEFICI



**25-26**  
giugno  
**2019**

**BOLOGNA**

Oratorio San Filippo Neri - Via Manzoni 5

A cura di Elena Candigliota e Francesco Immordino

ENEA

*Divisione Modelli e Tecnologie per la Riduzione degli Impatti Antropici e dei Rischi Naturali.  
Dipartimento Sostenibilità dei Sistemi Produttivi e Territoriali.*

*12° Workshop Tematico di Telerilevamento*

**Il ruolo dei dati Copernicus Sentinel nei processi di conoscenza e gestione del territorio: stato dell'arte del trasferimento tecnologico al comparto operativo**

*•processamento •cartografia •estrazione informazioni •costi/benefici*

Oratorio San Filippo Neri

Via Manzoni 5 - Bologna

**25-26 giugno 2019**

*Organizzazione*

*Gabriele Bitelli - Università di Bologna  
Elena Candigliota - ENEA Bologna  
Francesco Immordino - ENEA Bologna  
Livio Rossi - e-Geos*

*Comitato Scientifico*

*Gabriele Bitelli - Università di Bologna  
Elena Candigliota - ENEA Bologna  
Gherardo Chirici - Università di Firenze  
Maria Antonietta Dessena - ENAS, Cagliari  
Francesco Immordino - ENEA Bologna  
Emanuele Mandanici - Università di Bologna  
Maria Teresa Melis - Università di Cagliari  
Livio Rossi - e-Geos*

## Index

<b>Fusion of Sentinel-1 and Sentinel-2 derived ship detection for the extraction of the Maritime Patterns in the context of MSA (Maritime Situational Awareness)</b>	5
Filippo Daffinà, Dino Quattrocioni, Marco Corsi, Gianfausto Bottini, Torbjorn Stahl	
<b>A new index to assess tree vigour decline based on Sentinel-2 multi-temporal data</b>	6
Samuele De Petris, Roberta Berretti, Enrico Borgogno-Mondino	
<b>Remote Sensing to map coastal dunes of northern Adriatic: the Po River Delta</b>	9
Andrea Fiduccia, Luisa Cattozzo, Leonardo Marotta, Leonardo Filesi, Luca Gugliermetti, Carlo Terranova	
<b>Sentinel 1 data for fuel spill detection. The case of the ships collision near Corsica</b>	14
Francesca Franci, Francesca Trevisiol and Gabriele Bitelli	
<b>AWARE, a platform for monitoring assets and infrastructure, through the integration of EO and in situ data: moving from data to information</b>	19
Elena Francioni, Dino Quattrocioni	
<b>Sentinel-1 data for ground deformation monitoring: the SNAP-StaMPS workflow</b>	20
Francesca Grassi, Francesco Mancini	
<b>Slow evolution landslides monitoring from processing of SAR interferometric data through the Rheticus platform and in situ validation</b>	26
Francesco Immordino, Elena Candigliota, Claudio Puglisi, Augusto Screpanti, Giuseppe Forenza, Vincenzo Massimi	
<b>A geomatic application for water management in precision farming for a LIFE European project</b>	33
Alessandro Lambertini, Gabriele Bitelli, Emanuele Mandanici, Luca Vittuari	
<b>ENVI Deep Learning: un nuovo tool per la risoluzione di problemi geospaziali</b>	37
Andrea Marchesi, Paola Filippi	
<b>Supporting Forest Planning and Management by Sentinel 2 data aimed at forest Basal Area Estimation</b>	38
Enrico Borgogno Mondino, Roberta Berretti, Evelyn Momo	
<b>Assessing Earthquake-induced Urban Rubbles by means of multiplatform Remotely sensed data</b>	40
Maurizio Pollino, Sergio Cappucci, Ludovica Giordano, Domenico Iantosca, Luigi De Cecco, Danilo Bersan, Vittorio Rosato, Flavio Borfecchia	
<b>Rheticus® Network Alert supporting critical infrastructures: a case study for ACEA</b>	46
<b>- utility operator - within SCIRES project.</b>	46
Angelo Amodio, Giuseppe Forenza, Daniela Drimaco, Vincenzo Massimi, Francesca Albanese, Christian Bignami, Matteo Albano, Maurizio Pollino, Vincenzo Rosato, Cristiano Cialone	
<b>The Hyperspectral PRISMA Mission and its first results</b>	53
Rosa Loizzo, Rocchina Guarini, Maria Girolamo Daraio, Ettore Lopinto	
<b>Copernicus S2 to support CAP control policies in agriculture</b>	59
Filippo Sarvia, Enrico Borgogno-Mondino	
<b>SAR Remote Sensing techniques applied to tectonic and volcanic processes investigation</b>	62
Matteo Albano, Simone Atzori, Christian Bignami, Marco Moro, Marco Polcari, Stefano Salvi, Cristiano Tolomei and Salvatore Stramondo	
<b>Ottawa Flooding 2019 April/May– Processing of Sentinel-1 imagery with PCI Geomatica for hydraulic risk management</b>	66
Vera Costantini	
<b>EO multitemporal data for semi-automatic agricultural monitoring: the new Common Agricultural Policy application</b>	67
Fabio Volpe, Livio Rossi	
<b>Sentinel – 1 and Sentinel – 2 applications in coastal areas</b>	68
Sara Zollini, María Cuevas-González, Donatella Dominici, Oriol Monserrat, Maria Alicandro	





## **Fusion of Sentinel-1 and Sentinel-2 derived ship detection for the extraction of the Maritime Patterns in the context of MSA (Maritime Situational Awareness)**

Filippo Daffinà, Dino Quattrocioni, Marco Corsi, Gianfausto Bottini, Torbjorn Stahl

*e-geos, Roma*

In Maritime Situational Awareness (MSA) context, the most complete maritime scenario is guaranteed by the fusion of all the information made available by heterogeneous sources. The growing availability of open satellite images (Sentinel-1 and Sentinel-2 constellations), possibly integrated with images acquired from commercial space missions with higher spatial and/or temporal resolution (eg. COSMO-SkyMed) enables new possibilities to monitor, in a systematic and recurrent way, areas of interest that are difficult to monitor with the traditional assets. The affirmation of Big Data Analytics and object detection techniques based on Deep Learning and Convolutional Neural Network (CNN), also allows to effectively manage the huge amount of Earth Observation data and to extract the Maritime Patterns. The combination of these data with the information provided by the cooperative systems (e.g. AIS) also makes it possible to characterize the behavioral profiles by different boats co-operation level (focusing attention on the dark ships), type of boats (fishing, oil tankers, cargo etc) and by type of their activity (eg navigation, fishing, anchoring). The presentation will show how this EO multisource system works on a dedicated platform.

# A new index to assess tree vigour decline based on Sentinel-2 multi-temporal data

Samuele De Petris, Roberta Berretti, Enrico Borgogno-Mondino

*DISAFA-Dipartimento di scienze agrarie, forestali ed alimentari - University of Torino*

Corresponding author: Samuele De Petris [Samuele.depetris@unito.it](mailto:Samuele.depetris@unito.it)

Keywords: Tree vigour trend, Sentinel-2, phenology.

## 1. Introduction

Forest managers need to know where, when and why certain agents cause changes in structure, composition, growth and development of forest (Franklin, 2001; Stoszek, 1988). In this way, remote sensing can give significant contributions to forest management, especially concerning prediction or detection of incipient biotic/abiotic disturbances. Monitoring of forest resources in time requires that uniform and comparable indices are used. Vegetation Indices (VIs) are well known to be related to vegetation cover/status and consequently are often used to assess biomass productivity and tree health conditions (Asner, 1998).

In the remote sensing context, generally, only the effect of plant/forest disturbance (i.e. crown dieback) is considered with no focus about the cause of a given spectral anomaly, therefore resulting in a wrong management of many situations. Conversely, it is necessary to face the problem in a more phyto-pathological way. Tree vigour anomalies can be generated by:

- (i) transitory problems caused by edaphic deficiencies, leaf diseases or defoliator insect attacks, determining a loss of photosynthetically biomass (and so VI lower values) that, in general, are followed by a new VI increasing;
- (ii) chronic and gradual decreasing of photosynthetically biomass generated by plant pathology that determine a peculiar negative trend in the VI time series.

These anomalies produce similar effects on plants, inducing lower VI values, but require different management strategies. Detection and monitoring of vigour's decline is certainly useful for forest managers, permitting them to operate predictions to base future interventions on. In this work we propose a new spectral index, hereinafter called "Vegetation Vigor's Decline Index (VVDI), specifically designed to measure tree vigour's decline and based on Sentinel-2 image time series.

## 2. Materials and Methods

### 2.1 Study area

The study area is located in La Mandria Regional Park (Piemonte, NW-Italy) sited near to Torino. Broadleaves with dominance of pedunculate oak (*Quercus robur* L.) are the main vegetation type. We focused on an area close to the main park entrance, that sizes about 13 ha with a tree-lined boulevard (composed of sixty 200 years old trees) sizing 7.7 ha and a forested area of 5.3 ha.

### 2.2 Available Dataset

267 Sentinel-2 (A/B) multispectral images, level 2A, were obtained from CNES-Theia provider covering a sensing period between 27<sup>th</sup> May 2015 and 7<sup>th</sup> October 2018. Level 2A dataset are orthoprojected and calibrated in at-the-ground reflectance and supplied with mask layers of clouds, shadows, water and snow.

A ground survey was also conducted to collect a reference dataset by Field-map © (Zambarda, Černý, & Vopěnka, 2010) measuring the following parameters: tree position, species, tree age, planimetric crown projection (P).

### 2.3 Method developed

Starting from the 267 downloaded images, the correspondent NDVI maps were generated and stacked along a NDVI Time series (NTS). Since many scenes were affected by cloud cover a self-developed routine was implemented in IDL vs. 8.0 to mask out bad observations and regularize them with a time step of 5 days, resulting in a new NTS made of 73 images/year. A further filtering, based on FFT (Fast Fourier Transform), was finally applied to minimize NDVI fluctuations, caused by remaining outliers, and emphasize periodic fluctuations of the phenological trend. Trend interpretation was finally achieved at year level to overcome the limitation given by a single time NDVI observation (instantaneous approach) that simply shows the state of vegetation relative to a single moment forgetting about actual

biomass changes that occur along the entire growing season. Since physiopathologies, or pests attacks, can change their magnitude during the year, a phenology-based approach is certainly more robust to explore vegetation behaviour. With these premises, a new vegetation index, hereinafter called i-NDVI (Integral of Normalized Vegetation Index), was computed according to equation 1

$$(1) \quad iNDVI = \frac{\sum_{SOS}^{EOS} NDVI}{LOS}$$

where SOS and EOS are respectively the start and the end of the phenological season (Start Of Season; End Of Season). LOS is the duration of the vegetative season (Length Of Season) and is calculated as difference between EOS and SOS. SOS and EOS were calculated starting from the yearly NTS finding the moment when the second derivative is zero (inflection points) during the ascending and descending traits of NDVI profiles (Testa, Soudani, Boschetti, & Mondino, 2018). Theoretically, this new index expresses average vigor of crown in a given vegetative period. The normalization for the duration of the vegetative season (LOS) allows to more robustly compare iNDVI between different years minimizing the problems related to unequal observations in the annual NTS. Assuming iNDVI as a proxy of plant average annual health status, the analysis trend over time of this index provides useful information for interpretation of latent or chronic phenomena of vigor's decline.

Four iNDVI maps were therefore generated for the considered years (2015-2018). With reference to the surveyed crown projections (recorded as polygon vector layer), the correspondent zonal statistics (mean value) were computed from iNDVI maps.

For each crown polygon, with reference to the above mentioned statistics, a iNDVI trend line was modelled by regression (first order polynomial) for the 2015-2018 period. Its gain value (VVDI) was assumed as proxy of the average vigor change rate during the 4 years of observation. To investigate the variability of this index, the theoretical range within which it can be move was analytically calculated. Taking into account that a vegetated surface ordinarily shows NDVI values ranging between 0.3 and 1 (Burgan & Hartford, 1993; Gao, 1996; Ormsby, Choudhury, & Owe, 1987; Zhang et al., 2003) a 0.7 NDVI range of variation was considered, the steepest line relating time (4 years) and iNDVI is given by the ratio  $0.7/4 = 0.175$ . Accordingly, VVDI can therefore be said to vary between -0.175 to + 0.175.

To make it easily interpretable, the index was further normalized between 0 and 1 to compute nVVDI. Values of nVVDI lower than 0.5 can be interpreted as loss of vegetation vigour; values higher than 0.5 can be interpreted as increasing of vigour; values around 0.5 can be interpreted as no variation in vigor strength during the considered period (4 years).

### 3. Results and discussions

A nVVDI map was finally generated for the whole study area. A nVVDI mean value of 0.546 (snDI = 0.043) was found. To assess the accuracy of this index we assumed that tree age was a good predictor of crown vigour decline (generally associated with low VI value). We correlated tree age and nVVDI value founding a high correlation ( $r = -0.88$  @  $p < 0.001$ ). This result demonstrates that high nVVDI values correspond to young trees and reasonably to an increasing vigor related to tree growth. Differently, low nVVDI values are related to old trees that show a decline of vigor due to crown biomass regression (Li, Kräuchi, & Dobbertin, 2006; Marshall & Waring, 1986). It's authors' opinion that such correlation demonstrate that nVVDI is a predictor of tree vigor trend. Maps of nVVDI can represent a useful tool to detect incipient vegetative anomalies especially in extensive context, permitting a better focus over the area to address primarily controls. A definitive validation is not possible at the moment due to the lack of ground truth data. Future developments will be expected to achieve this problem collecting aeriels (RPAS) multispectral data with high temporal resolution.

### Bibliografia

- Asner, G. P. 1998. Biophysical and biochemical sources of variability in canopy reflectance. *Remote sensing of Environment*, 64(3), 234–253.
- Burgan, R. E., & Hartford, R. A. 1993. Monitoring vegetation greenness with satellite data. *Gen. Tech. Rep. INT-GTR-297. Ogden, UT: US Department of Agriculture, Forest Service, Intermountain Research Station*. 13 p., 297.
- Franklin, S. E. 2001. *Remote sensing for sustainable forest management*. CRC press.
- Gao, B.-C. 1996. NDWI—A normalized difference water index for remote sensing of vegetation liquid water from space. *Remote sensing of environment*, 58(3), 257–266.
- Li, M.-H., Kräuchi, N., & Dobbertin, M. 2006. Biomass distribution of different-aged needles in young and old Pinus cembra trees at highland and lowland sites. *Trees*, 20(5), 611–618.
- Marshall, J. D., & Waring, R. H. 1986. Comparison of methods of estimating leaf-area index in old-growth Douglas-fir.

- Ecology*, 67(4), 975–979.
- Ormsby, J. P., Choudhury, B. J., & Owe, M. 1987. Vegetation spatial variability and its effect on vegetation indices. *International Journal of Remote Sensing*, 8(9), 1301–1306.
- Stoszek, K. J. 1988. Forests under stress and insect outbreaks. *Northwest Environmental Journal*, 4(2), 247–261.
- Testa, S., Soudani, K., Boschetti, L., & Mondino, E. B. 2018. MODIS-derived EVI, NDVI and WDRVI time series to estimate phenological metrics in French deciduous forests. *International journal of applied earth observation and geoinformation*, 64, 132–144.
- Zambarda, A., Černý, M., & Vopěnka, P. 2010. Field-map-the new technology designed by IFER for the collection and processing of forest inventory data. *Sherwood-Foreste ed Alberi Oggi*, (167), 33–38.
- Zhang, X., Friedl, M. A., Schaaf, C. B., Strahler, A. H., Hodges, J. C., Gao, F., ... Huete, A. 2003. Monitoring vegetation phenology using MODIS. *Remote sensing of environment*, 84(3), 471–475.

## Remote Sensing to map coastal dunes of northern Adriatic: the Po River Delta

Andrea Fiduccia<sup>1</sup>, Luisa Cattozzo<sup>2</sup>, Leonardo Marotta<sup>3</sup>, Leonardo Filesì<sup>2</sup>, Luca Gugliermetti<sup>1</sup>, Carlo Terranova<sup>4</sup>

<sup>1</sup> Department of Astronautical, Electrical and Energy Engineering (DIAEE), Sapienza, University of Rome, Via Eudossiana 18, 00184, Rome, Italy;

<sup>2</sup> Department of Architecture and Arts, IUAV University, Santa Croce 1957, Ca' Tron, 30135, Venice, Italy;

<sup>3</sup> Studio Associato Entropia, via F. Corridoni 3, Recanati, 62019, Italia

<sup>4</sup> National Geoportal, Italian Ministry for Environment, Land and Sea, Italy

Corresponding author: andrea.fiduccia@uniroma1.it

Keywords: Remote Sensing, Coastal Dunes, ICZM, Spatial Decision Support Systems

### Abstract

The aim of the paper is to illustrate the progress of an active research line at the DIAEE - Department of Astronautical, Electrical and Energy Engineering of the University of Rome "Sapienza" in collaboration with Department of Architecture and Arts of IUAV (Venice, Italy) related to the analysis of remote sensing data and Spatial Decision Support Systems for Integrated Coastal Zone Management (ICZM) strategies and policies. The methodology uses the Copernicus Sentinel 1 and 2 satellite images but also foresees the use of the PRISMA images to increase the capability for thematic mapping.

The study area is the northern Adriatic coast of Italy and the test site of the methodology is the Delta of Po River (Italy).

### 1. Introduction. A general methodology for ICZM

In 2010, Marotta et al. proposed a framework based on a landscape approach to define a sustainability state for the coast. It follows several steps:

Definition of homogeneous Environmental Management Units, and analysis of spatial and temporal structure, hierarchy and dynamics over multiple scales. This step requires the production of a habitat map based on landscape ecology.

Analysis of land-use changes in the coastal system based on remote sensing techniques.

Implementation of spatial indices characterizing each landscape patch type and state.

Conservation-gaps analysis. The step is focused in the assessment of ecosystem health, cumulative impacts and habitat loss in coastal ecotones (Thrush et al., 2008). An urban and infrastructure index has been used as evaluation tool (Marotta et al., 2004, 2008).

Assessment of coastal conflicts using a coastal conflict index following the work of Vallega (1999).

Multi Criteria Analysis (MCA) in order to minimize conflicts over a set of values and constraints.

Currently the DIAEE-IUAV' research group is working to improve the methodology. From the remote sensing point of view the original methodology was based on Landsat images. The current workflow is based on Sentinel 2 images.

A second and important improvement is the ongoing setup of a "lean" version of the whole methodology. In fact, the Marotta (2010) workflow is very reliable from a scientific point of view, but it has a drawback in its complexity and in a set of indices and indicators hard to understand for non-technicians people and harder to implement and update.

Dunes are a fundamental component of the coastal ecosystem. This component is taken into consideration for the environmental regeneration projects that constitute the scenarios evaluated by the methodology. For this reason, they have been the subject of a specific study aimed at their identification and monitoring using satellite images.

### 2. The ecological value of sandy coastal dunes

A dune is the coastal or sub-coastal sector usually narrow and parallel to the coast characterized by small reliefs. These reliefs (in Italy from 0.5 m to 12 m height) are formed by the accumulation of incoherent sediments due to wind action. The sand dunes are those consisting of almost incoherent sands, depending both on their different age, and on the vegetation present, able to make at least a certain percentage of the

most superficial materials compact.

There are three factors that interact in the formation of a dune: sand, wind and vegetation. The wind, the sea breeze, moves the sand inward. The vegetation that grows on the sand causes further accumulation of sand. Deposition and erosion due to the wind are balanced and this process adjusts the height of the dune. The Italian Adriatic coasts is a long sandy shore that extends from Monfalcone to the Gargano, with the exception of the Conero promontory (Ancona) and some areas between Ortona and Vasto. The northern part of this sandy coastline, interrupted by the Grado-Marano and Venezia-Chioggia lagoons, represents the widest Italian dune system and consists of a series of sandy coasts almost continuous from Grado to Rimini. The dune system of Northern Adriatic is still today the largest Italian beach system. These beaches in recent decades have been the subject of important tourist activities. The price of well-being for these malarial areas and with low population density is the risk of environmental degradation.

The dune is a very special environment from an ecological point of view. The sand particles are not able to retain water and therefore the plants must adapt to a substrate almost devoid of water but which can reach high temperatures due to the action of the sun. The salinity is low because the salt carried by the marine aerosol is washed away by the rains.

Because of the peculiar environmental and microclimatic conditions, the ecosystems of the coastal beaches and sandy dunes are characterized by simplified animal and plant communities and with a low number of species compared to those of other terrestrial habitats. The same limiting abiotic parameters combined with conditions of environmental stress have selected highly specialized plant and animal species, often present only in those environments.

Therefore, the naturalistic value of sandy coastal dunes is given not by species richness - which is rather low - but by the coexistence of elements of different biogeographical origin. They are characterized by high levels of trophic specialization, exclusivity and loyalty to the habitat. This makes them good indicators of the biological quality of the ecosystems in which they are present.

Coastal ecosystems are complex and dynamic entities whose imbalances are related both to the marine and terrestrial component and to socio-economic and cultural causes (Grignetti et al., 2004). To understand the risks affecting dunes, we must state the "three laws of sandy shores" (Ruffo, 2002):

1. Beaches and dunes need waves, tides and sea winds;
2. The sand of the beaches must be able to dry completely in the emerged part and the grains must remain non-adherent to each other;
3. If the natural self-healing mechanisms have been unbalanced, artificial interventions can only delay damage but never resolve them.

Therefore, the risks faced by the dunes are:

- Macroclimatic risks and consequent sea level rise;
- Risks related to subsidence;
- Risks due to water pollution (marine, lagoon and river) and agricultural activities:
  - Non-biodegradable solid and coarse materials;
  - Biodegradable materials;
  - Inert materials with very fine granulometry;
  - Substances carried by sea aerosol and ground winds;
  - Fuel oils;
- Risks associated with erosion and removal of sand or imbalances in its transport to the sea;
- Risks associated with the construction of piers, artificial reefs and tide control barriers;
- Risks associated with urbanization and coastal construction, stabilization of dunes and planting of tree and shrub plant species;
- Risks associated with the introduction of alien plant species;
- Risks associated with bathing activities.

### **3. Remote Sensing techniques for mapping Coastal Dunes**

Remote Sensing is an alternative approach to traditional ground survey for mapping coastal dunes (Davis et al., 1991).

Landsat imagery has been used to map coastal vegetation, at the broad community level, but due to its medium spatial resolution, the use of Landsat imagery in mapping of smaller coastal environments has proven to be difficult (Klemas, 2011; Xie et al., 2008; Özdemir et al., 2005).

Berberoglu, Alphan, and Yilmaz (2003) used IKONOS imagery studying the coastal dunes of the Eastern



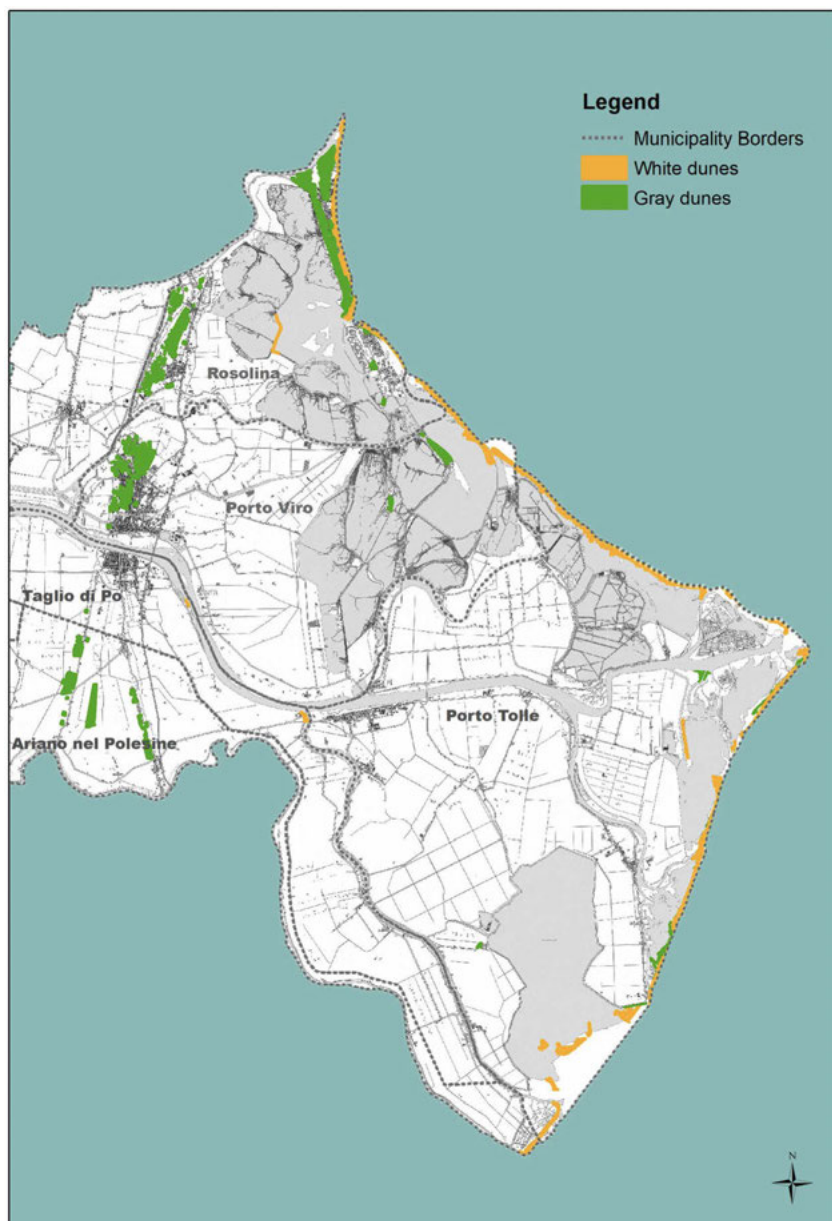


Figure 1. Test Area

Mediterranean in Turkey. They reached an overall classification accuracy of 84%. Timm and McGarigal (2012) used QuickBird data integrated by multispectral orthophotography to accurately map coastal dune and salt marsh ecosystems at Cape Cod National Seashore.

Shanmugam et al. (2003), Lucas et al. (2002), and Zhang et al. (2012) used CASI hyperspectral data (288 bands) to map coastal dune vegetation at Kenfig National Nature Reserve in the United Kingdom obtaining high classification accuracies (e.g., 85-90% or greater).

Brownnett and Mills (2017) using CASI data integrated by LIDAR data successfully mapped 11 coastal sites in UK within Special Areas of Conservation (SAC) and Sites of Special Scientific Interest (SSSI). Lalimi et al. (2017) used a ProSpecTIR VIS hyperspectral imaging spectrometer (SpecTIR Corp., Reno, NV, USA - 128 bands) integrated by LIDAR data to quantitatively characterize ecotopographic patterns of coastal dunes in Hog Island, Virginia.

Grignetti et al. (2004) mapped changes 1950-2002 of dunes in the coast near Rome (Italy) using aerial photos, Quickbird images and MIVIS hyperspectral data (102 bands).

Traditional aerial photographs can be enhanced by scanning in multispectral 3-bands dataset. Dech et al. (2005) obtained such a multispectral data set from color aerial photographs to classify

land cover of a Lake Huron sand dune system within Pinery Provincial Park (Ontario).

Panchromatic stereographic aerial photographs were used by Brown and Arbogast (1999) to monitor dynamic dune systems of Ludington State Park in Michigan using digital photogrammetric techniques. The availability of LIDAR technology was the natural evolution of the "volumetric monitoring" (i.e. Hantson et al., 2012 and Kempeneers et al., 2009).

From the algorithms point of view, mapping Land Use/ Land Cover (LULC) of coastal dunes is very challenging due to the problem of spectral mixing. In Shanmugam et al. (2003) there is a comparison analysis of the accuracy achievable using per-pixel classification techniques (Minimum Distance, Maximum Likelihood, Mahalanobis Distance) and sub-pixel techniques (Linear Mixture Model, Fuzzy-C Means, Multilayer Positron): in coastal areas conventional per-pixel algorithms can only map broad habitat categories.

However, according to Gonçalves et al. (2014), it is possible to obtain good performance in detection of dunes using synthetic bands from Landsat ETM+ and OLI:

1. Modification of Normalized Difference Water Index ( $MNDWI = ((Green - MIR) / (Green + MIR))$ );
2.  $NDVI = (NIR - Red) / (NIR + Red)$ .
3. Normalized Difference Built Up Index ( $NDBI = ((MIR - NIR) / (MIR + NIR))$ );
4. First principal component (PC1);
5. Second principal component (PC2).

Finally, Hussain et al. (2013) and Strasser and Lang (2015) showed Object Based Image Analysis (OBIA) produces higher accuracy results than traditional pixel based methods. OBIA has been successfully used by large detailed habitat mapping studies (Lucas et al. 2011).



#### 4. Test site, data and methods.

The north-Adriatic sandy coastal system plays a very important role for nature and biodiversity conservation in the whole Mediterranean basin, because of its particular geomorphologic, climatic and phytogeographic features. One of the most important traits is the richness of endemites, together with Mediterranean, dealpine and eastern species, in a system where a specialized but widely distributed flora generally occurs (Buffa et al., 2007).

The Po Delta is located in the northern Adriatic and belongs to two Italian Regions: the Veneto and Emilia-Romagna.

The Venetian part of the delta involves various municipalities in the Province of Rovigo, and the testing area of the methodology focused on the territories of the Municipalities of Rosolina, Porto Viro and Porto Tolle. The area in which the study area is located is flat, bordered by the seven branches of the river Po which characterize its delta morphology with a dense hydrographic network. The river routes are characterized by raised banks and the territory develops towards the lagoon and the sea, marked by fossil dunes and bordered towards the coast by "scanni" (strips of sand that separate the lagoon from the sea).

The entire system in which the study area is located is characterized by resources of inestimable environmental value in terms of fauna, vegetation and landscape, as well as what they represent at an ecosystem level. Here, in fact, vast wetlands alternate with agricultural extensions of considerable importance, made possible by large hydraulic drainage works, which still guarantee the survival of lands located a few meters below the average sea level.

For the test area, the DIAEE-IUAV' working group has a detailed field survey that constituted the ground truth for the classifications of remote sensing data (Figure 1).

The data used for the test are Sentinel 2 images, the color orthophoto and the GIS topographical vector database of the Veneto Region.

The dune identification test is in progress using the OBIA technique according to the workflow proposed in Brownnett and Mills (2017):

- Step 1: Initial Segmentation and Classification
  - Chessboard Segmentation at pixel Size 1
  - Identification of Intertidal Areas
  - Identification of Area of Interest
  - Classification of Classes Vegetation/ Non Vegetation
- Step 2: Creation of Detailed Level and Multiresolution Segmentation
- Step 3: Classification of Non Vegetation Classes
- Step 4: Classification of Vegetation Classes
- Step 5: Merge Process and Export as Feature Class.

#### 5. Future developments

The work program will proceed with the extension of dune mapping throughout the northern Adriatic using Sentinel 2 data and an in-depth study of landscape ecology indicators and geo-ecological patterns using the hyperspectral images (250 bands) of the PRISMA satellite of Italian Space Agency (ASI).

#### References

- Berberoglu, S., Alphan, H., and Yilmaz, K. T., 2003. A remote sensing approach for detecting agricultural encroachment on the eastern Mediterranean coastal dunes of Turkey. *Turkish Journal of Agriculture and Forestry* 27(3): 135-144.
- Brown, D. G., and Arbogast, A. F., 1999. Digital photogrammetric change analysis as applied to active coastal dunes in Michigan. *Photogrammetric Engineering and Remote Sensing* 65(4), 467-474.
- Brownnett, J.M. & Mills, R.S., 2017. The development and application of remote sensing to monitor sand dune habitats. *J Coast Conserv* (2017) 21:643–656.
- Buffa, G., Filesì, L., Gamper, U., Sburlino, G., 2007. Qualità e grado di conservazione del paesaggio vegetale del litorale sabbioso del Veneto (Italia settentrionale). *Fitosociologia* vol. 44 (1): 49-58.
- Davis, F.W., Quattarochi, D.A., Ridd, M.K, Lam, N.S.W., Walsh, S.J., Michaelsen, J.C., Franklin, J., Stow, D.A., Johannaen, C.J., Johnston, C.A., 1991. Environmental analysis using integrated GIS and remotely sensed data: some research needs and priorities. *Photogrammetric Engineering and Remote Sensing*, 57 (6). 689-697.
- Dech, J. P., Maun, M. A., and Pazner, M. I., 2005. Blowout dynamics on Lake Huron sand dunes: Analysis of digital multispectral data from colour air photos. *Catena* 60(2):165-180.
- Gonçalves, G. Duro, N., Sousa, E., Pinto, L., and Figueiredo, I., 2014. Detecting changes on coastal primary

- sand dunes using multi-temporal Landsat Imagery. *Proceedings. SPIE 9244, Image and Signal Processing for Remote Sensing XX*, 924420 (October 29, 2014).
- Grignetti, A., Casacchia, R., Salvatori, R. 2004. Studio dei cambiamenti di un sistema dunale mediante integrazione di fotoaeree e immagini MIVIS e Quickbird. *Studi Costieri*, 8. 111-120.
- Hantson, W., Kooistra, L., and Slim, P. A., 2012. Mapping invasive woody species in coastal dunes in the Netherlands: a remote sensing approach using LIDAR and high-resolution aerial photographs. *Applied Vegetation Science* 15(4): 536-547.
- Hussain, M., Chen, D., Cheng, A., Wei, H., Standley, D., 2013. Change detection from remotely sensed images: from pixel-based to object-based approaches. *ISPRS J Photogramm Remote Sens* 80:91–106.
- Kempeneers, P., Deronde, B., Provoost, S., and Houthuys, R., 2009. Synergy of airborne digital camera and Lidar data to map coastal dune vegetation. *Journal of Coastal Research Special Issue* 53: 73-82.
- Klemas, V., 2011. Remote sensing techniques for studying coastal ecosystem: An overview. *Journal of Coastal Research* 27(1): 2-17.
- Lucas, N. S., Shanmugam, S., and Barnsley, M., 2002. Sub-pixel habitat mapping of a coastal dune ecosystem. *Applied Geography* 22(3): 253-270.
- Lucas, R., Medcalfe, K., Brown, A., Bunting, P., Breyer, J., Clewley, D., Keyworth, S., Blackmore, P., 2011. Updating the phase 1 habitat map of Wales, UK, using satellite sensor data. *ISPRS J Photogramm Remote Sens* 66:81–102.
- Marotta, L., 2004. *Ecologia Urbana e sistemi costieri*. 2 In: Bettini, V. (ed) *Ecologia Urbana*. UTET, Torino, 419–454.
- Marotta, L., Ceccaroni, L., Matteucci, G., Rossini, P., Guerzoni, S., 2010. A decision-support system in ICZM for protecting the ecosystems: integration with the habitat directive. *Journal of Coastal Conservation*, 15, 393-415.
- Marotta, L., Cecchi, A., Ridolfi, E., Breton, F., Ceccaroni, L., 2008. Downscaling indicators of integrated coastal zone management in the Mediterranean Sea. In: *Proc Littoral , CORILA/EUCC*, Venice (2008).
- Özdemir, I., Asan, U., Koch, B., Yesil, A., Özkan, U. Y., and Hemphill, S., 2005. Comparison of Quickbird-2 and Landsat-7 ETM+ data for mapping of vegetation cover in Fethiye- Kumluova coastal dune in the Mediterranean region of Turkey. *Fresenius Environmental Bulletin* 14: 823-831.
- Ruffo, S. (a cura di), 2002. *Dune e Spiagge Sabbiose – Ambienti tra terra e mare*, Ministero dell’Ambiente e della Tutela del Territorio, Quaderni Habitat, 4.
- Shanmugam, S., Lucas, N., Phipps, P., Richards, A., and Barnsley, M., 2003. Assessment of remote sensing techniques for habitat mapping in coastal dune ecosystems. *Journal of Coastal Research* 19(1): 64-75.
- Strasser, T., Lang, S., 2015. Object-based class modelling for multi-scale riparian forest habitat mapping. *Int J Appl Earth Obs Geoinf* 37:29– 37.
- Timm, B. C., and McGarigal, K., 2012. Fine-scale remotely-sensed cover mapping of coastal dune and salt marsh ecosystems at Cape Code National Seashore using Random Forests. *Remote Sensing of Environment* 127: 106-117.
- Thrush, S. F., Halliday, J., Hevit, J. E., Lohrer, A. M., 2008. The effects of habitat loss, fragmentation, and community homogenization on resilience, in estuaries. *Ecol Appl* 18(1), 12–21.
- Vallega, A., 1999. *Fundamental of coastal zone management*. Kluwer, Dordrecht, 263 p.
- Xie, Y., Sha, Z., and Yu, M., 2008. Remote sensing imagery in vegetation mapping: a review. *Journal of Plant Ecology* 1(1): 9-23.
- Yousefi Lalimi, F., Silvestri, S., Moore, L. J., and Marani, M., 2017. Coupled topographic and vegetation patterns in coastal dunes: Remote sensing observations and ecomorphodynamic implications, *J. Geophys. Res. Biogeosci.*, 122, 119–130.
- Zhang, L., and Baas, A. C. W., 2012. Mapping functional vegetation abundance in a coastal dune environment using a combination of LSMA and MLC: A case study of Kenfig NNR, Wales. *International Journal of Remote Sensing* 33(16): 5043-5071.

## Sentinel 1 data for fuel spill detection. The case of the ships collision near Corsica

Francesca Franci, Francesca Trevisiol and Gabriele Bitelli

Department of Civil, Chemical, Environmental and Materials Engineering, University of Bologna.

Corresponding author: francesca.trevisiol2@unibo.it

Key words: Sentinel 1, fuel spill detection, semi-automatic classification, object-based technique, fuel spill monitoring.

Satellite remote sensing for environmental monitoring is developing fast in the last years, both for land and water resources. Thanks to the availability of data from various sensors with different spatial, temporal, radiometric and spectral resolutions, remote sensing data has become an essential source for a wide range of applications.

In the field of the maritime environment surveillance, the detection and mapping of oil on the water surface is one of the common use of the satellite images (Bhangale, Durbha, King, Younan, & Vatsavai, 2017; Kolokoussis & Karathanassi, 2018). The location of the spill should be obtained very precisely by means of image processing. It is nowadays standard practice to use Synthetic Aperture Radar (SAR) for producing this kind of thematic maps (Alpers et al., 2017). In fact, the capability to acquire images in day-night and all-weather conditions, covering large areas with frequent overpass, makes the active sensors the best for oil spill detection (Silva et al., 2017).

In this study, we focused on the potential of the SAR data collected by the European Earth observation program Copernicus. Copernicus offers free radar satellite images with high spatial and temporal resolution. In particular, Sentinel-1 mission meets the features required by marine surveillance tools. Sentinel-1A and the Sentinel-1B satellites collect SAR images with a swath of 250 km in Interferometric Wide (IW) mode, covering wide area with high spatial resolution (10 m pixel size). The two-satellite constellation offers a repeat cycle of 6 days and a repeat frequency, considering ascending and descending orbit directions, of 1- 3 days in accordance with the latitude (ESA - European Space Agency, 2016). The Sentinel-1 data are available for the Copernicus services within one hour of acquisition.

In the present work, Sentinel-1 images have been processed to map the oil spill caused by the ships collision occurred near Corsica coasts in October 2018 (Figure 1). For the SAR data classification, a near-real time procedure was developed through the Object-Based Image Analysis (OBIA).

The case study was offered by the ships collision occurred early in the morning of the 7<sup>th</sup> October 2018 off the coast of Corsica, in the Mediterranean Sea. The Tunisian freighter Ulysse rammed into a Cyprus-registered container ship CSL Virginia anchored about 20 miles off the northern tip of Corsica causing a heavy fuel oil spill. The spill was estimated to be around 600 m<sup>3</sup> of heavy fuel oil (AFP, 2018).

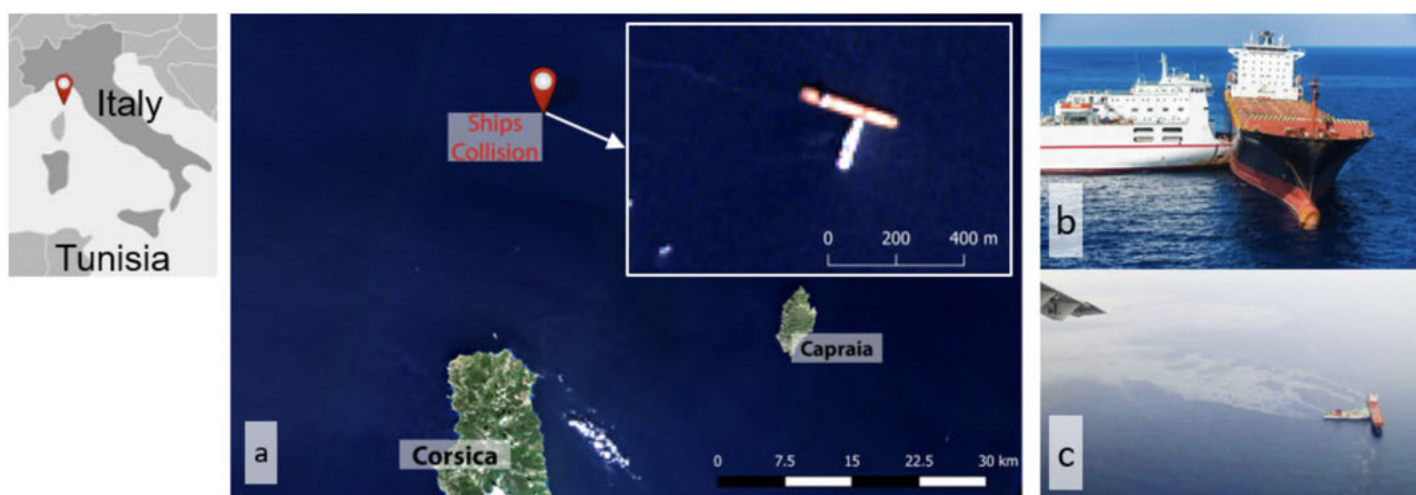


Figure 1. The point of the ships collision between Corsica and Italy. The collision captured by the S2 satellite on 9th October 2018 (a). Pictures of the collision. b) The freighter rammed into the container ship (Source: Alexandre Groyer/French Marine Nationale. c) The spreading fuel slick seen from the Italian Coast Guard airplane

SAR data can be effectively used to detect the presence of oil spills on the sea surface. Oil spills stand out because of their reflectivity in relation to the water. Oil slicks reduces the backscattering energy so that they appear as dark areas on radar images while ocean waves affected by wind appear brighter (Alpers et al., 2017; Fingas & Brown, 2017).

The area of the collision (Area Of Interest – AOI) was captured by the Sentinel-1 satellites on the days after the event. In particular, six radar images acquired between the 8th and the 15th October have been processed. Figure 2 groups the input data used for the fuel spill delineation. Sentinel-1 images were acquired in Interferometric Wide swath mode. The level-1 Ground Range Detected (GRD) products at 10 m of spatial resolution have been used. The VV polarisation was considered for the classification procedure since it is more effective in detecting oil spill (Arslan, 2018; Prastyani & Basith, 2018). The specifications of the Sentinel-1 scenes are listed in the Table 1.

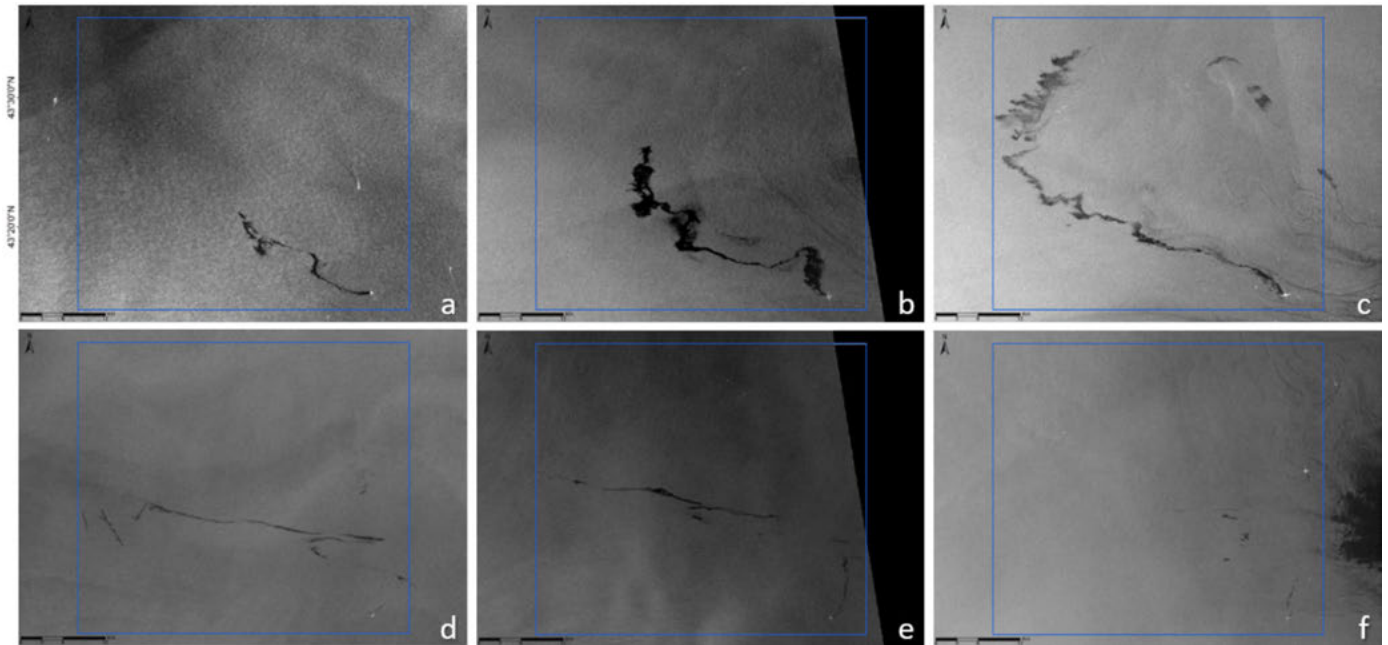


Figure 2. The Area Of Interest (blue rectangle) captured by the Sentinel-1 satellites on the 8<sup>th</sup> October a) at 5:27 UTC and b) 17:21 UTC, c) on the 9<sup>th</sup> October at 17:14 UTC, on the 14<sup>th</sup> October d) at 5:27 UTC and e) 17:22 UTC and on the 15<sup>th</sup> October at 17:13 UTC. The VV polarization of each image is shown

SATELLITE	DATE	TIME	LEVEL	POLARIZATION	PASS DIRECTION
S1A	08/10/2018	05:27 UTC	GRD	VV	Descending
S1B	08/10/2018	17:21 UTC	GRD	VV	Ascending
S1A	09/10/2018	17:14 UTC	GRD	VV	Ascending
S1B	14/10/2018	05:27 UTC	GRD	VV	Descending
S1A	14/10/2018	17:22 UTC	GRD	VV	Ascending
S1B	15/10/2018	17:13 UTC	GRD	VV	Ascending

Table 1. Specifications of the Sentinel-1 products used in the present study

Figure 3 shows the flowchart of the fuel spill extent delineation performed by means of the Sentinel-1 data processing. Firstly, speckle filtering has been applied to reduce the “salt and pepper” appearance of the radar images. The Lee Sigma filter with kernel size of 7 x 7 was used to for the speckle noise suppression (Lee et al., 2009). Pre-processing steps also comprised the geometric correction of the Sentinel-1 images. Since the AOI is located over the sea, i.e. flat areas without topographic variations, the Sentinel-1 data has been processed with the Ellipsoid Correction-Geolocation Grid ensuring the same projected coordinate



Figure 3. Flowchart showing the methodology of the fuel spill extent delineation by means of the Sentinel-1 images



reference system (WGS 1984/UTM zone 32N) for all the images (Schubert & Small, 2008). Finally, the pixel values were converted using the decibels scale in order to improve the image contrast. These pre-processing procedures were performed using the SNAP software (ESA, 2018).

An Object-Based Image Analysis (OBIA) was performed on the Sentinel-1 data to map the fuel oil spill. A semi-automatic procedure was developed using the commercial software eCognition (Trimble, 2014). The OBIA consisted of a rule set including the segmentation and the classification phases (Figure 4) (Bitelli et al., 2017; Franci et al., 2016; Franci & Spreafico, 2016). The multiresolution segmentation algorithm was used to generate the image objects. It is a bottom-up region growing technique which takes into account both spectral and shape heterogeneity through user-defined colour and shape parameters (Baatz & Schäpe, 2000). The scale parameter was set for defining the level of heterogeneity: a larger scale results in larger objects than setting small scale values. The thresholding classification based on Amplitude values was then applied to the image objects to identify those belonging to “Sure” and “Possible” oil slicks. The first class indicates the presence of spilled oil with a very high confidence level. The second one is used for mapping the residual traces of oil. Those could be due to the floating with the current of the oil spill. Therefore, in correspondence of areas belonging to “Possible” class, more detailed analyses should be required.

Threshold values have been chosen considering the Amplitude profiles along paths through oil and non-oil spill zones. Each Sentinel-1 image was processed with the same rule set changing only Amplitude threshold values.

Thanks to the developed workflow a near-real time procedure was obtained, just depending on the image availability.

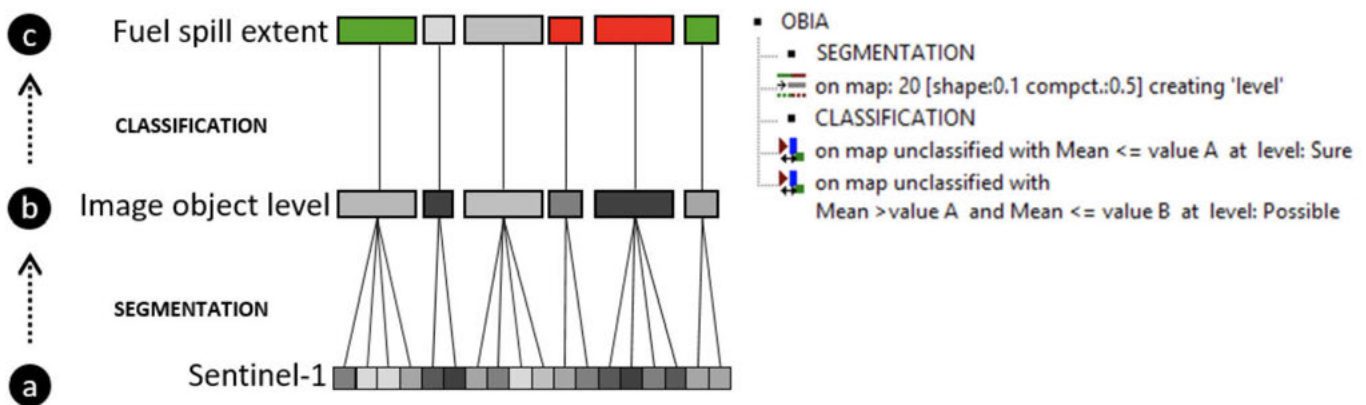


Figure 4. Phases of the semi-automatic OBIA procedure applied to each Sentinel-1 scene (left) and the rule set developed within the eCognition software environment (right)

The multitemporal maps of the fuel spill obtained are shown in Figure 5. Moreover, the extent of the “Sure” and “Possible” oil slicks was computed over the time (Figure 6). On the 8<sup>th</sup> October at 5:27 UTC, the main oil slick was about 22 km long with a linear shape. After twelve hours, the slick distorted its shape increasing the affected area from 20 to 52 km<sup>2</sup>. Despite the response activities, the fuel leakage spread until the 9<sup>th</sup> October reaching the maximum extent. The clean-up operation results can be observed a week after the collision, when slicks totally covered less than 20 km<sup>2</sup>. On the 15<sup>th</sup> October, the AOI seems to be not affected by fuel spills.

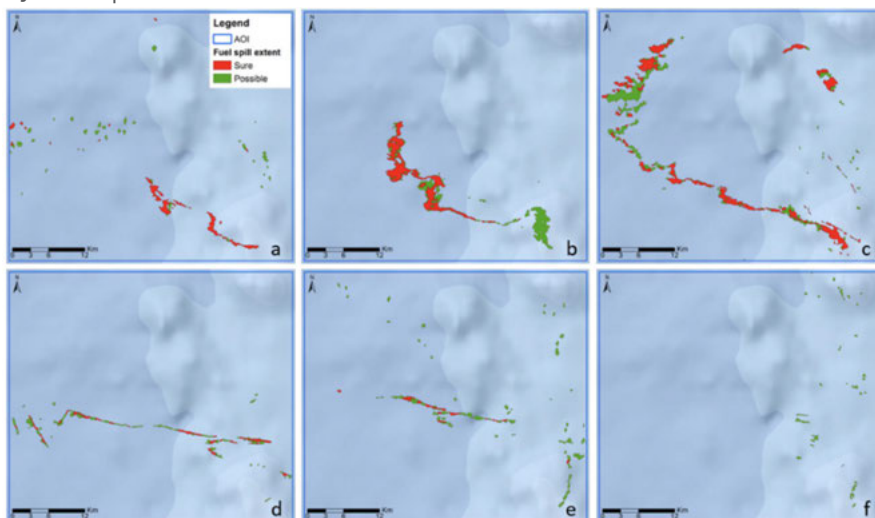


Figure 5. The fuel spill extent maps obtained by the classification of the Sentinel-1 acquired on the 8<sup>th</sup> October a) at 5:27 UTC and b) 17:21 UTC, c) on the 9<sup>th</sup> October at 17:14 UTC, on the 14<sup>th</sup> October d) at 5:27 UTC and e) 17:22 UTC and on the 15<sup>th</sup> October at 17:13 UTC

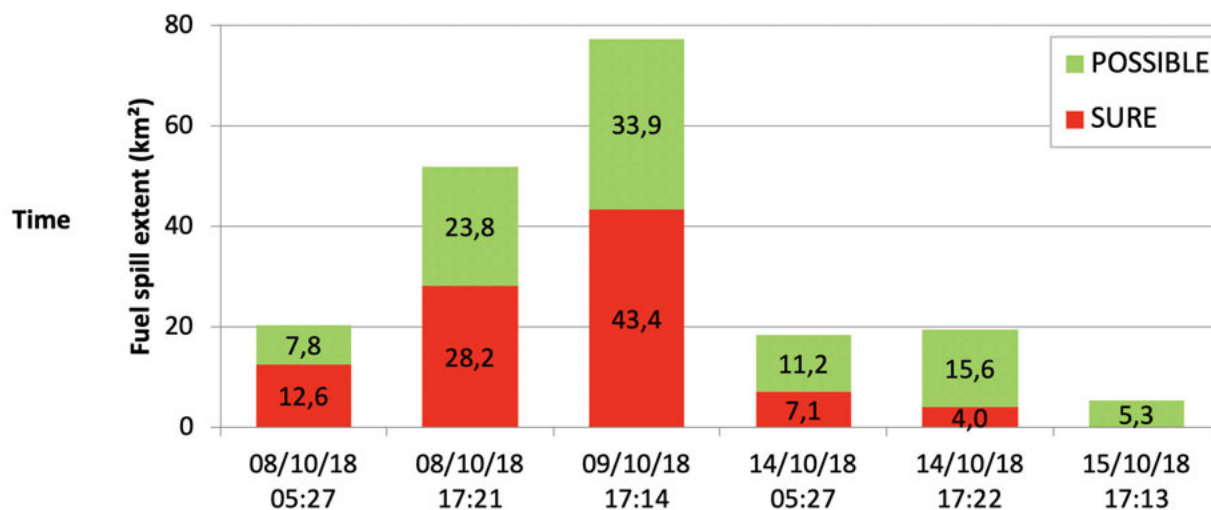


Figure 6. The Fuel spill extent computed thanks to the multitemporal maps

The accuracy of the presented approach was assessed using visual criteria therefore a rigorous validation procedure will be necessary.

As a first conclusion, this work confirms that Sentinel-1 routine operations makes these satellite images particularly suitable for mapping and monitoring the oil traces over the time. The multitemporal maps of the fuel slicks extent have been produced by processing the freely available scenes by means of a semi-automatic classification procedure. In particular, an object-based technique, comprising the segmentation and the thresholding classification phases, was performed using the eCognition software. The developed ruleset allowed to implement a near real time procedure for Sentinel-1 processing, just depending on the images' availability.

The presented approach could be useful in the different phases of the oil spill management. During the response, the processing of the first post event acquisition allows to rapidly locate the affected zone and to identify the leakage origin. In the days after the accident, near real time monitoring of the oil extent is given by the multitemporal analyses that also permit to assess the effectiveness of the clean-up activities. This information can support the marine surveillance after the event for the recovery purpose. This is a crucial point to reduce as much as possible the long-term pollution.

Secondly, the obtained thematic maps could be employed to validate numerical models devoted to simulate the oil spilled trajectory. Moreover, a variety of dataset provided by different sources should be integrated to achieve an efficient tool for the complete knowledge of the phenomenon.

## Bibliografia

- AFP. (2018). Fuel cleanup begins after cargo ships collide off Corsica.
- Alpers, W., Holt, B., & Zeng, K. (2017). Oil spill detection by imaging radars: Challenges and pitfalls. *Remote Sensing of Environment*, 201, 133–147. <https://doi.org/10.1016/j.rse.2017.09.002>
- Arslan, N. (2018). Assessment of oil spills using Sentinel 1 C-band SAR and Landsat 8 multispectral sensors. *Environmental Monitoring and Assessment*, 190(11), 637. <https://doi.org/10.1007/s10661-018-7017-4>
- Baatz, M., & Schäpe, A. (2000). Multiresolution segmentation: an optimization approach for high quality multi-scale image segmentation. In J. Strobl, T. Blaschke, & G. Griesebner (Eds.), *Angewandte Geographische Informationsverarbeitung XII AGIT symposium* (Vol. 58, pp. 12–23). Salzburg, Germany.
- Bhangale, U., Durbha, S. S., King, R. L., Younan, N. H., & Vatsavai, R. (2017). High performance GPU computing based approaches for oil spill detection from multi-temporal remote sensing data. *Remote Sensing of Environment*, 202, 28–44. <https://doi.org/10.1016/j.rse.2017.03.024>
- Bitelli, G., Eleias, M., Franci, F., & Mandanici, E. (2017). VHR satellite imagery for humanitarian crisis management: A case study. In *Proceedings of SPIE - The International Society for Optical Engineering* (Vol. 10444). <https://doi.org/10.1117/12.2279185>
- ESA. (2018). STEP Scientific Toolbox Exploitation Platform. Retrieved December 12, 2018, from <http://step.esa.int/main/toolboxes/snap/>
- ESA - European Space Agency. (2016). SENTINEL-1 User Guide.
- Fingas, M., & Brown, C. (2017). A Review of Oil Spill Remote Sensing. *Sensors*, 18(2), 91. <https://doi.org/10.3390/s18010091>

- Franci, F., Bitelli, G., Mandanici, E., Hadjimitsis, D., & Agapiou, A. (2016). Satellite remote sensing and GIS-based multi-criteria analysis for flood hazard mapping. *Natural Hazards*, 83. <https://doi.org/10.1007/s11069-016-2504-9>
- Franci, F., & Spreafico, M. C. (2016). Processing of remote sensing data for the estimation of rock block size distribution in landslide deposits. In *Landslides and Engineered Slopes. Experience, Theory and Practice* (pp. 935–942). CHAP, CRC Press. <https://doi.org/doi:10.1201/b21520-110>
- Kolokoussis, P., & Karathanassi, V. (2018). Oil Spill Detection and Mapping Using Sentinel 2 Imagery. *Journal of Marine Science and Engineering*, 6(1), 4. <https://doi.org/10.3390/jmse6010004>
- Lee, J.-S., Lee, J.-S., Wen, J.-H., Ainsworth, T. L., Chen, K.-S., & Chen, A. J. (2009). Improved Sigma Filter for Speckle Filtering of SAR Imagery. *IEEE Transactions on Geoscience and Remote Sensing*, 47(1), 202–213. <https://doi.org/10.1109/TGRS.2008.2002881>
- Prastyani, R., & Basith, A. (2018). Utilisation of Sentinel-1 SAR Imagery for Oil Spill Mapping: A Case Study of Balikpapan Bay Oil Spill. *JGISE: Journal of Geospatial Information Science and Engineering*, 1(1). <https://doi.org/10.22146/jgise.38533>
- Schubert, A., & Small, D. (2008). Guide to ASAR Geocoding. Remote Sensing Laboratories.
- Silva, A., Branco, W., Silva, D., Habl, L., Sarmiento, T., & Pascual, M. (2017). Semi-automatic Oil Spill Detection in Sentinel-1 SAR Images at Brazil's Coast. In *GEOProcessing 2017* (Ed.), The Ninth International Conference on Advanced Geographic Information Systems, Applications, and Services (pp. 1–5).
- Trimble. (2014). eCognition Developer 9.0 Reference Book. München, Germany: Trimble Germany GmbH.



## **AWARE, a platform for monitoring assets and infrastructure, through the integration of EO and in situ data: moving from data to information**

Elena Francioni, Dino Quattrocioni

*e-geos, Roma*

AWARE is a suite of technological solutions for supporting monitoring and management of critical infrastructures and strategic assets, starting from SAR satellite data.

The solution leverages on e-GEOS products portfolio adding value-added enablers for supporting planning, management and maintenance of infrastructures and strategic assets: Power Supply Utilities, Transport and Infrastructures, Mining, Oil & Gas, Natural Resources Management.

AWARE is structured in three main families to cover all main needs of the asset management:

- Health: Deformations & movements identification by the use of Satellite interferometric products, GNSS monitoring, IoT technology, RPAS video
- Control: Monitoring the assets and infrastructure changes and activities in the surrounding by the use of specific Encroachment and Change detection analysis, spatial analysis, RPAS video, high resolution cartography and 3D models to monitor the surrounding area
- Operations: Supporting the day by day management with GIS platform for continuous data management, integration and analysis

The presentation will describe hints of the "suite" solutions and the real advantages both for administrative and private users

Francesca Grassi, Francesco Mancini

*DIEF Dipartimento di Ingegneria "Enzo Ferrari", Università degli Studi di Modena e Reggio Emilia, francesca.grassi.fg@gmail.com;  
francesco.mancini@unimore.it*

Corresponding author: francesco.mancini@unimore.it

Keywords: Copernicus, Sentinel, SNAP, PSInSAR, Ground deformation

## Abstract

During the last decades, radar interferometry has become an effective technique able to provide reliable information in a variety of applications such as geodesy, natural hazards assessment, ground deformations and monitoring. With the beginning of Copernicus Earth Observation program, new chances in Earth Observation field arose. For instance, Sentinel-1A and -1B provide synthetic aperture radar acquisitions over very large areas at average spatial resolution and very short revisit time, thus increasing the opportunities offered by existing radar satellite. In this work we assess the potentialities of Sentinel-1 data by the generation of displacements maps through the PSInSAR techniques and a processing workflow including the free Sentinel Application Platform (SNAP) and Stanford Method for Persistent Scatterers (StaMPS) software package. Results are referred to a couple of areas affected by ground deformation.

## 1. Introduction

During the last decades, satellite radar interferometry has proven to be an effective technique able to provide useful information about phenomena occurring on the Earth's surface because of the ability to depict kinematic processes at very high accuracy level (mm/yr) and unprecedented spatial resolution (few meters, depending also on the satellite platform). Many research fields focused on hazards assessment, ground deformations, investigations on polar caps dynamics, slope failures and instability processes took advantage of such methodology [1]. The main limitations of this technique are linked to spatial and temporal decorrelation, due to varying field and atmospheric conditions, discontinuities in satellite data acquisitions and the geometry of acquisitions, more sensitive towards actual ground displacements along the vertical and east-west direction.

Besides the dismissed (ERS1-2, Envisat, Radarsat 1) and active (Radarsat 2, TerraSAR-X, Alos Palsar, Cosmo Sky-Med) satellite radar missions, the Copernicus Earth Observation program offered new chances in global monitoring by spaceborne radar sensors thanks to its constellations of Sentinel satellites. In particular, by the launch of Sentinel-1A and Sentinel-1B satellites in 2014 and 2016 respectively, Copernicus started to provide free-access synthetic aperture radar (SAR) acquisitions over very large areas at average spatial resolution and very short revisiting time, opening new perspectives for continuous ground surface monitoring.

Recent studies have shown that Sentinel-1A and -1B data processed with well-known interferometric SAR (InSAR), differential interferometric SAR (DInSAR) and permanent scatterers (PS-InSAR) methods allows to detect the Earth's surface displacements and the generation of time series for ground deformation monitoring at the mentioned level of accuracy [2, 3, 4]. In addition, the users have now the opportunity to process the radar data with toolboxes for interferograms generation, as in free software SNAP (Sentinel Application Platform) complemented by SNAPHU (Statistical cost Network flow Algorithm for Phase Unwrapping) by the European Space Agency. Moreover, displacement history of selected PS, showing high coherence across time of satellite passages, can be derived by the free StaMPS (Stanford Method for Persistent Scatterers) package which requires output products from SNAP.

This work introduces some experiences about the processing of Sentinel-1A and -1B radar data for ground displacement investigations by the PS method and a workflow composed of routines included in the open software SNAP and StaMPS.

The PSInSAR technique was applied on two selected areas where remarkable and well-documented ground displacements are occurring due to different reasons: the areas surrounding Campi Flegrei (Pozzuoli, Italy) and the city of Ravenna (Italy).

## 2. The Sentinel-1A and -1B platform: characteristics and data access

Sentinel-1A and -1B, committed to European company Thales Alenia Space, were launched respectively on 3 April 2014 and 25 April 2016. As for the whole Sentinel constellation, the majority of data and

information delivered by the Copernicus Space infrastructure are made available and accessible to any citizen and any organisation around the world on a free, full and open access basis. The European Commission is funding the deployment of five cloud-based platforms providing centralised access to Copernicus data and information, as well as to processing tools. These platforms are known as the DIAS (Data and Information Access Services) and offer a complement to existing data access portals that will continue to operate.

Data from all Sentinel missions are freely accessible through the Sentinel Scientific Data Hub ([scihub.copernicus.eu](https://scihub.copernicus.eu)) by using an interactive graphical user interface (GUI). Depending on the Sentinel mission the users are interested in, the GUI allows the selection of a list of parameters to find the more appropriate image dataset for their studies. With particular reference to the Sentinel-1 dataset, the following are prompted: wave polarization (HH, VV, HV, VH, HH+HV, VV+VH); Relative Orbit Number (in a repeated cycle); Product type (the Single Look Complex, SLC, format is required for interferometric analysis); Sensor Mode (the Interferometric Wide Swath Mode, IW, was selected). See also Table 1 and Figure 1 for a list of characteristics and acquisition modes.

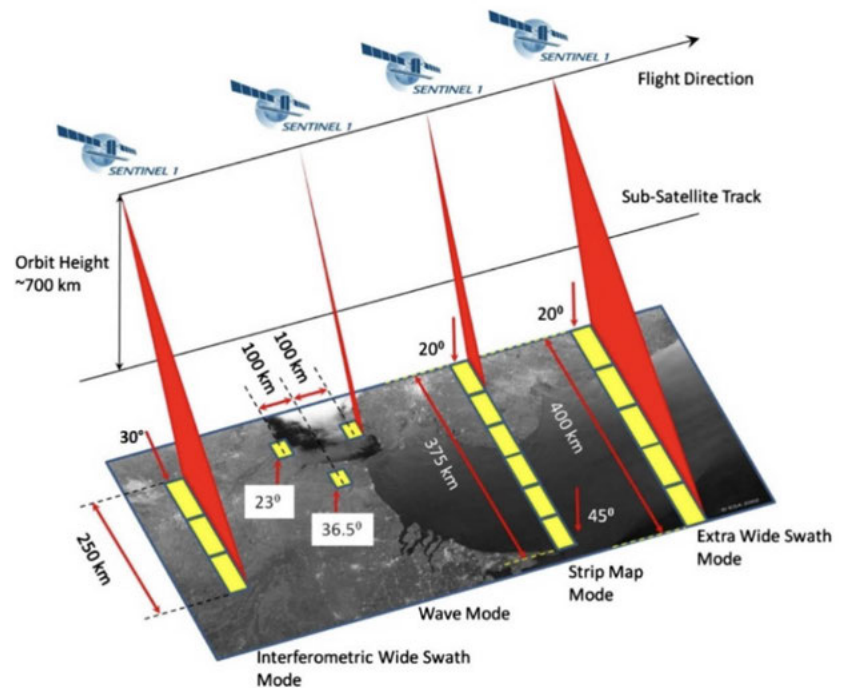


Figure 1. Sentinel-1 acquisition modes [5]

#### ***Sentinel-1 satellite characteristics***

<i>Type of orbit</i>	Near-polar Sun-synchronous
<i>Inclination</i>	98.18°
<i>Orbits per cycle</i>	175
<i>Revolutions per day and orbital period</i>	14.59, 98.6 minutes
<i>Repeat cycle</i>	12 days (6 days in the S1 and S2 ensembled orbits)
<i>Altitude</i>	693 km
<i>Radar band</i>	C band, Frequency range: 4-8 GHz, Wavelength range: 37.5-75 mm
<b><i>IW SLC image features</i></b>	
<i>Nominal resolution (azimuth x range)</i>	20 m x 5 m
<i>Ground swath width</i>	250 km
<i>Incidence angle</i>	32.9 °(IW1); 38.3°(IW2); 43.1°(IW3)
<i>Polarisation</i>	Single (HH or VV) or Dual (HH+HV or VV+VH)

Table 1. Main characteristics of the Sentinel-1 satellite and SLC images

The designed IW mode supports the single and dual polarisation option and makes the Sentinel-1 data very suitable for medium-resolution applications with a wide swath of 250 km and medium-spatial resolution (5m x 20m along the ground-range and azimuth directions).

The Interferometric Wide swath (IW) mode implements a new type ScanSAR mode called Terrain Observation with Progressive Scan (TOPS). The basic principle of TOPSAR is the shrinking of the azimuth antenna pattern (along track direction). This is obtained by steering the antenna from aft to the fore at a constant rate. The antenna beam is also switched cyclically among the three sub-swaths. The TOPSAR acquisition mode is reported in Figure 2.

As a result, all targets on ground are observed by the entire azimuth antenna pattern: this eliminates almost entirely the scalloping effect (caused by inaccurate estimation of doppler centroid mean frequency) and leads to constant azimuth ambiguities and signal-to-noise ratio (SNR) along azimuth [6]. As drawback, the fast azimuth beam steering reduces the target dwell time, and as such, the spatial resolution in azimuth. Moreover, several sub-swaths are acquired quasi-simultaneously by sub-swath switching from burst to burst. Through the TOPSAR the mentioned spatial resolution of 5m x 20m across the 250km-wide swath

is achieved. Sentinel-1 satellites are able to deliver data within an hour after reception by the ground station for the near-real time service and 24 hours from archive. This is thanks to the ESA facilities located in Darmstadt (Germany) and ESRIN in Frascati (Italy).

Level-1 SLC images are obtained from Level-0 after focusing and represent the starting products for interferometric processing. SLC products consist of focused and geo-referenced data (provided in zero-Doppler slant-range geometry) where the phase information is preserved.

In the IW mode, SLC products are composed by three subswaths and by three images in single polarisation and six images for dual polarisation. Each of the sub-swath consists of a series of bursts in azimuth. The individually focused complex burst data are included, in azimuth-time order, into a single sub-swath image, with black-fill demarcation in between. To have contiguous coverage of the ground, single bursts partially overlap in azimuth and range. Images for all bursts in all sub-swaths in IW and EW SLC products are resampled to a common pixel spacing grid in both reference directions. Burst synchronisation is maintained for both IW and EW products to ensure that interferometry between pairs of products acquired in different periods can be performed. The Swath Timing data set record in SLC products contains information about the bursts including dimensions, timing and location that can be used to merge the bursts and swaths together.

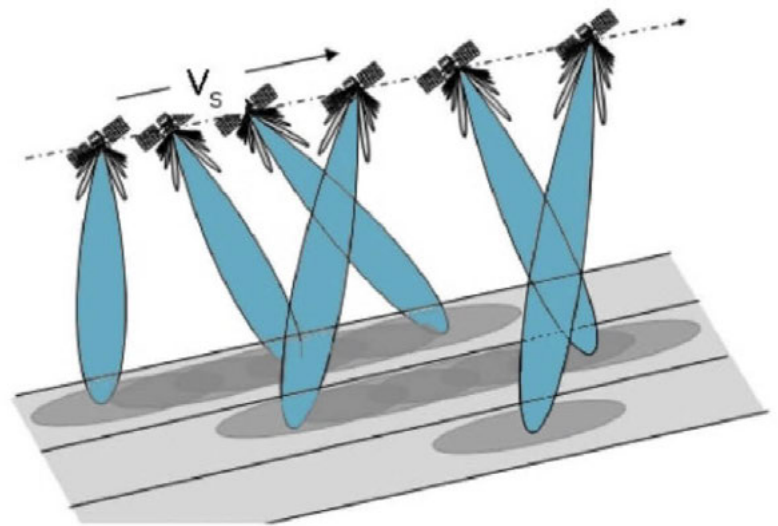


Figure 2. The TOPSAR mode of acquisition ([sentinel.esa.int](http://sentinel.esa.int))

### 3. Free toolboxes for interferometric data analysis: SNAP-StaMPS workflow

This section describes the free toolboxes and processing workflows used to generate interferograms and displacement maps. SNAP architecture has been developed for Earth Observation processing and allows the analysis of data collected by the constellation of Sentinel satellites. Sentinel-1 toolbox includes the fundamental processing steps for satellite radar data from ESA SAR missions (Sentinel-1, ERS-1, ERS-2 and ENVISAT) and from third party SAR missions (COSMO SkyMed, Radarsat-2, TerraSAR-X and ALOS PALSAR).

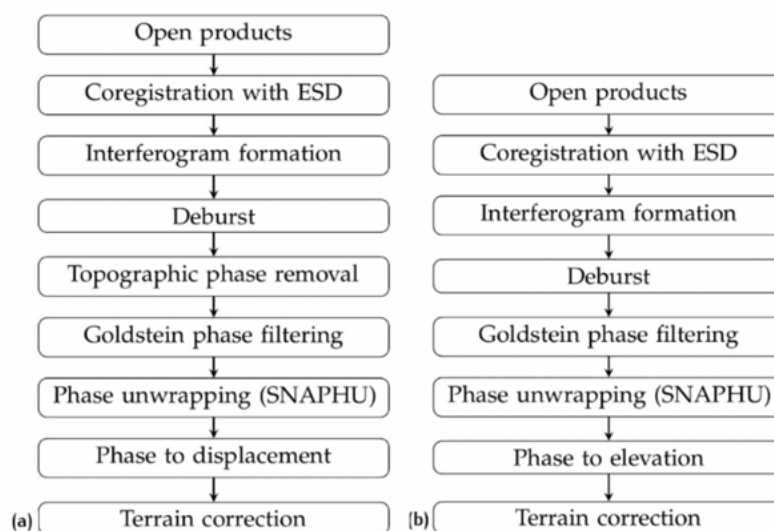


Figure 3. shows the workflow adopted in the interferometric data analysis for the detection of displacements (a) and generation of elevation models (b)



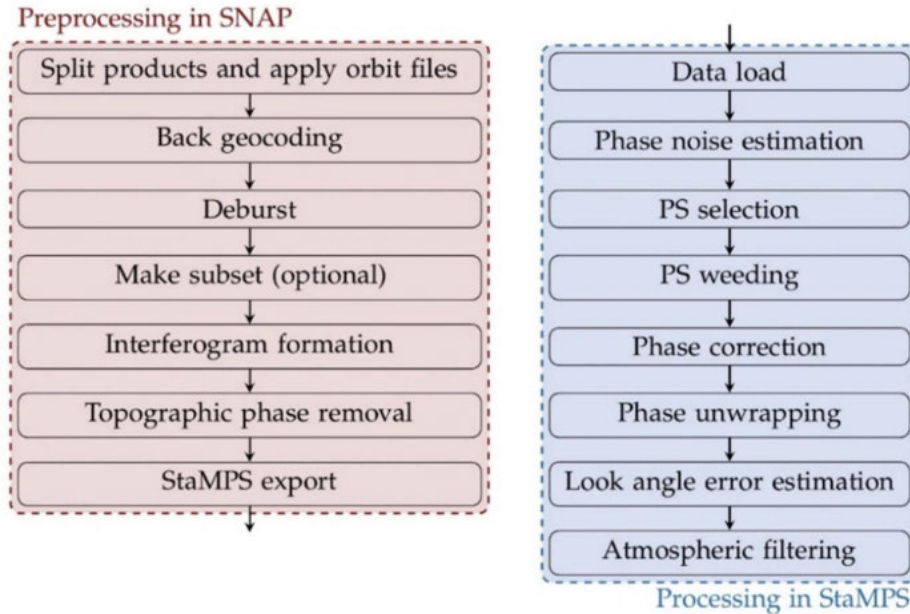


Figure 4. Combining SNAP and StaMPS workflows for displacement analysis using PS interferometry

Table 2 lists a short description of the main steps included in the workflow.

StaMPS, by Stanford University (Stanford, USA), University of Iceland (IS), Delft University (NL) and University of Leeds (GB) implements PSInSAR method to extract ground displacements from time series of synthetic aperture radar acquisitions.

There are two pre-processing steps: focusing of the raw data (if required) and interferograms formation from SLC products. This pre-processing can be accomplished by SNAP and results exported for successive processing by StaMPS. The StaMPS processing steps are summarized in Figure 4 and described in Table 2.

Step	Description
<i>Product splitting</i>	Splitting subswath with selected bursts and polarisation. For coregistration steps, the same subswath and bursts have to be selected for each product
<i>Orbit files application</i>	Correction of orbital parameters
<i>Coregistration</i>	Co-registration of one or more slave images with a master
<i>Subset creation</i>	Spatial or spectral subset to focus on a dataset and speed up the processing
<i>Interferogram formation</i>	Computation of complex interferograms
<i>Deburst</i>	Merging of adjacent bursts in the azimuth direction according to their zero Doppler time with resampling to a common pixel spacing
<i>Topographic phase removal</i>	Estimation and subtraction of topographic phase from the interferograms
<i>Phase filtering</i>	Implementation of a non-linear adaptive algorithm in order to reduce the residues and enhance the accuracy in the phase unwrapping step
<i>Phase unwrapping</i>	Recovering of unambiguous phase from wrapped phase by SNAPHU
<i>Phase to displacement</i>	Conversion of an interferometric product with phase proportional to the relative terrain displacement to a displacement map
<i>Phase to elevation</i>	Conversion of the unwrapped interferometric phase to the heights in the radar coded system
<i>Terrain correction</i>	Compensation of distances distortions in the SAR images due to topographic variations of a scene and to the tilt of the satellites' sensor
<i>StaMPS export</i>	Preparation of StaMPS folders starting from 1) coregistered and deburst image, 2) deburst interferogram with topographic phase removed
<i>Data load</i>	Preparation and saving of the data for the PS processing in MATLAB workspaces
<i>Phase noise estimation</i>	Estimation of the phase noise value for each candidate pixel in every interferogram
<i>PS selection</i>	Selection of eligible PS pixels on a noise characteristics basis
<i>PS weeding</i>	Discard of noisy PS or PS affected by signal contribution from neighbouring elements
<i>Phase correction</i>	Correction of the wrapped phase for spatially-uncorrelated look angle error
<i>Look angle error estimation</i>	Computation of spatially-correlated look angle error
<i>Atmospheric filtering</i>	Atmospheric filtering exploiting triangle mesh generator and Delaunay triangulator

Table 2. Brief description of main tools used in the processing of Sentinel-1 data by SNAP and StaMPS

#### 4. Ground displacements from Sentinel-1 data and SNAP-StaMPS workflow

A comprehensive discussion of ground deformation phenomena is not within the aim of this work. The following displacement maps have been generated for a couple of case studies as proof of the reliability of the discussed workflows. Those two areas have been selected because of the known and notable phenomena they are subjected to.

In particular, Figure 5 depicts the ground displacements through the PSInSAR methodology in a wide area surrounding the city of Ravenna (Italy) and the coastal areas facing the northern Adriatic Sea.

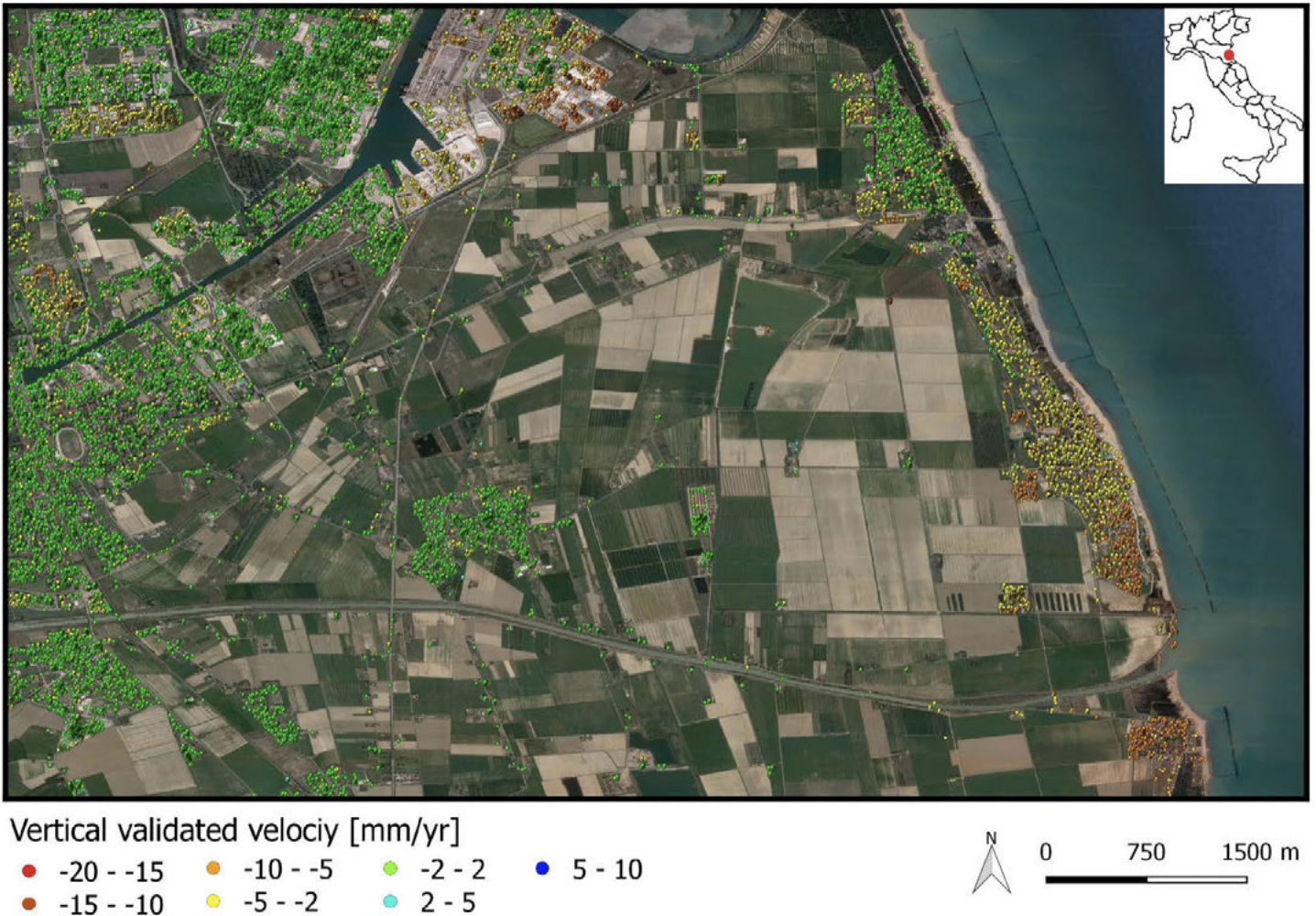


Figure 5. Displacements map (vertical direction, descending orbit, from October 2014 to February 2019) in Ravenna (Italy) and nearby coastal areas of data validated with GNSS measurements

We report the processing outcomes from a second case study represented by the intense ground deformation processes occurring at Campi Flegrei (Naples, Italy). In this area results from levelling data, geological investigations and satellite studies evidenced uplift and subsidence due to the presence of the so-called bradyseism [7]. Nowadays, the deformation monitoring in the area is made with continuous GNSS, the NeVoCGPS (Neapolitan Volcanoes Continuous GPS) network. In Figure 6 the LOS-oriented (descending orbit) is compared with long time series provided by a selection of the GNSS stations.

#### Conclusion

Although during the last decades the processing of satellite radar data with low-budget represented the main limitation to the extensive and timely use of SAR data for large scale mapping and monitoring, with the free access of Sentinel-1 data and processing tools the users are able to generate interferometric products for tailored applications.

Especially the Sentinel-1 mission can be considered a breakthrough due to the short revisiting time (that brings to high coherence interferograms) and average to high spatial resolution. In particular, the enhanced temporal resolution and the regularity of TOPSAR acquisitions are paving the way to the use of the InSAR technique for early detection of movements in places where ground-based techniques would be unfeasible. This work reported some applications about ground deformation monitoring in which the joint use of SNAP and StaMPS tools allowed the detection of displacements at the typical level of accuracy (mm/yr) achievable by PSInSAR technique.



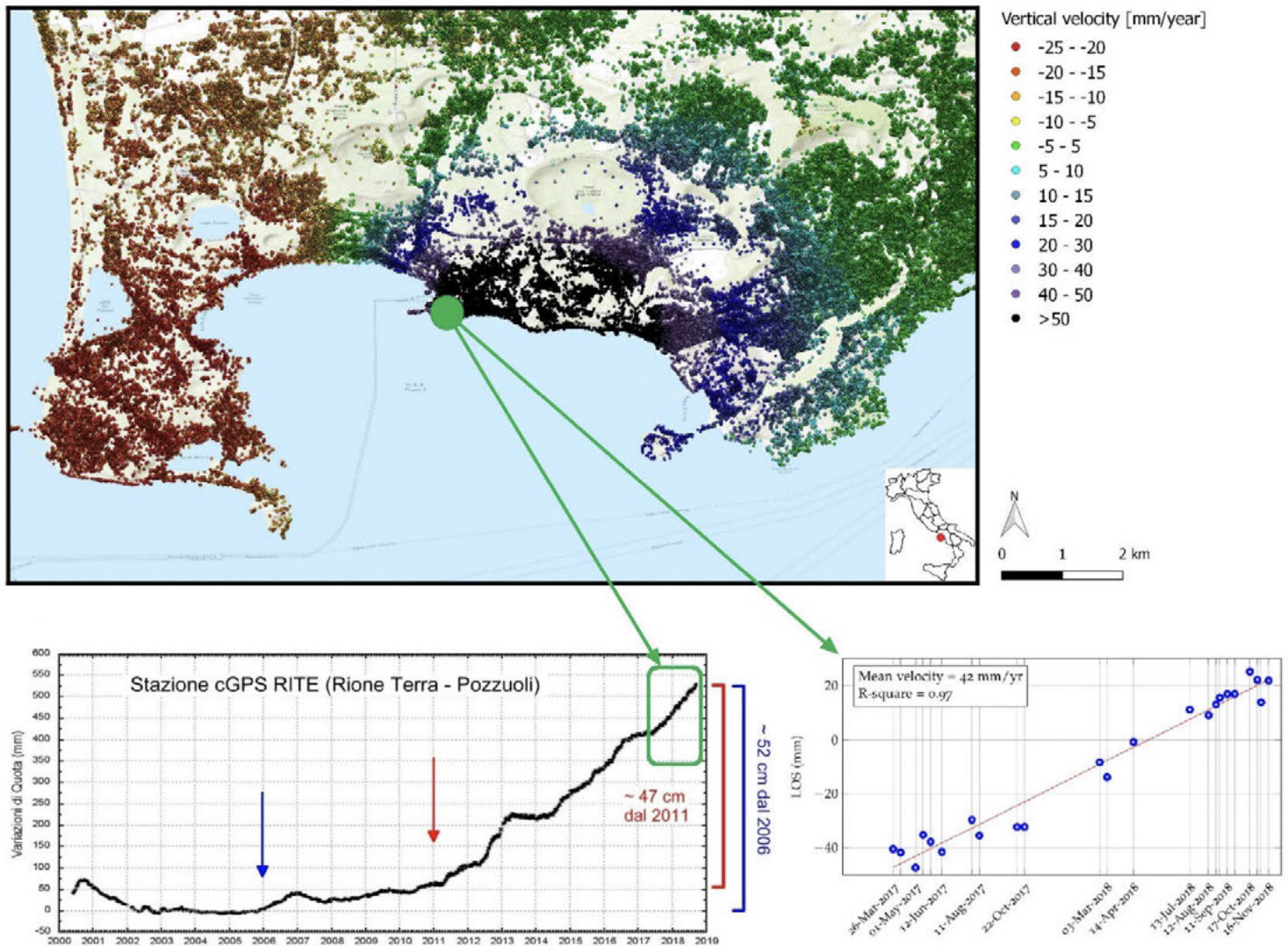


Figure 6. Displacements map (vertical direction, descending orbit, from March 2017 to November 2018) in the area of Campi Flegrei (Naples, Italy) and comparison with velocity provided by GNSS stations

## References

- [1] A. Moreira, P. Prats-Iraola, M. Younis, G. Krieger, I. Hajnsek, and K. P. Papathanassiou (2013). A tutorial on synthetic aperture radar. *IEEE Geoscience and remote sensing magazine*, 1(1), 6–43.
- [2] A. Rucci, A. Ferretti, A. M. Guarnieri, and F. Rocca (2012). Sentinel 1 SAR interferometry applications: The outlook for submillimeter measurements. *Remote Sensing of Environment*, 120, 156–163.
- [3] N. Devan  ry, M. Crosetto, O. Monserrat, M. Cuevas-Gonz  lez, and B. Crippa (2018). Deformation monitoring using Sentinel-1 SAR data," in *Multidisciplinary Digital Publishing Institute Proceedings*, 2(7), p. 344.
- [4] J. M. Delgado Blasco, M. Fomelis, C. Stewart, and A. Hooper (2019). Measuring urban subsidence in the Rome metropolitan area (Italy) with Sentinel-1 SNAP-StaMPS persistent scatterer interferometry," *Remote Sensing*, vol. 11, no. 2, p. 129.
- [5] D. Geudtner, R. Torres, P. Snoeij, M. Davidson, and B. Rommen (2014). Sentinel-1 system capabilities and applications. In *2014 IEEE Geoscience and Remote Sensing Symposium*, 1457–1460.
- [6] F. De Zan and A. M. Guarnieri (2006). TopSAR: Terrain observation by progressive scans. *IEEE Transactions on Geoscience and Remote Sensing*, 44(9), 2352–2360.
- [7] M. Dolce, G. Brandi, G. Scarpato, and P. D. Martino (2018). La Rete NeVoCGPS (Neapolitan Volcanoes Continuous GPS), per il monitoraggio delle deformazioni del suolo nell'area vulcanica napoletana. p. 6.



# Slow evolution landslides monitoring from processing of SAR interferometric data through the Rheticus platform and in situ validation

Francesco Immordino<sup>1</sup>, Elena Candigliota<sup>1</sup>, Claudio Puglisi<sup>2</sup>, Augusto Screpanti<sup>2</sup>, Giuseppe Forenza<sup>3</sup>, Vincenzo Massimi<sup>3</sup>

<sup>1</sup>ENEA, Territorial and Production Systems Sustainability Department, Bologna Research Centre

<sup>2</sup>ENEA, Territorial and Production Systems Sustainability Department, Casaccia Research Centre

<sup>3</sup>Planetek Italia, Bari

Corresponding author: francesco.immordino@enea.it

Keywords: INSAR, Landslides, Rheticus

## 1. Introduction

A study about movements of two landslides, in Sicilia region, Italy, by means of SAR interferometry KosmoSkyMed data is in progress. The paper presents the methodology and preliminary data.

The ENEA activities concerns: the displacements historical analysis through Advanced Satellite SAR Interferometry with Persistent Scatterer (PS) methodology on COSMO-SkyMed images in 2011-2018 and 2019-2021 period; movements monitoring using Advanced Interferometry SAR Persistent Scatterer (PS) with COSMO-SkyMed images through the in the period 2019-2021; movements evaluation through surveys in situ with differential GPS measurement.

## 2. Interferometric data and Rheticus Displacement platform service.

The landslides under study are located in the municipalities of Messina, in Altolia locality, and Niscemi (province of Caltanissetta) in Sicilia island.

In relation to the activity of historical evaluation of the landslide movements in the Altolia and Niscemi areas, the two Municipalities are interested in a study of the area through satellite SAR Interferometry with PS methodology and COSMO-SkyMed images (CSK) for 2014-2018 and 2019-2021 period (Fig. 1 - Altolia).

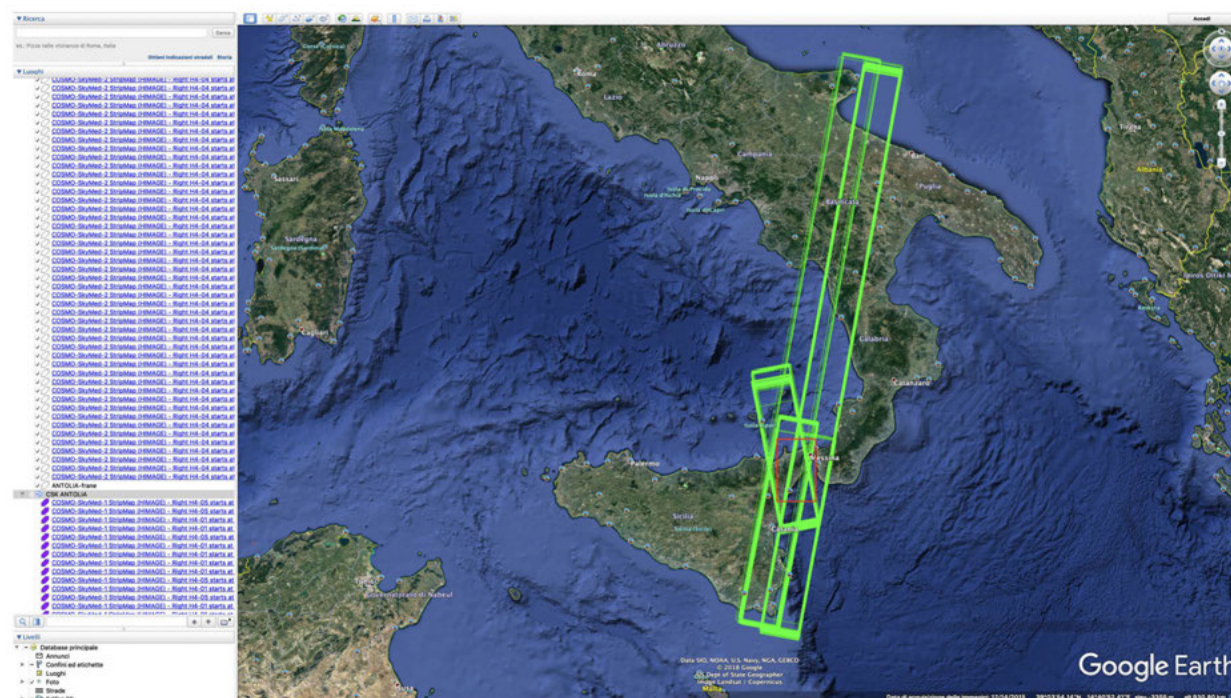


Figure 1. CosmoskyMed interferometric products acquisition (2014-2018) and study area (red box): Messina, Italy

The geomorphological conditions of the territory show a poorly evolved morphological stage that determines intense erosive activity. It developed during meteorological events that enhance the degradation of soils by surface waters, triggering slow landslides affecting the inhabited, ascribable to a slow evolution in substrate. The landslides movements will be evaluated with the support of Rheticus platform. Rheticus® is available for

various applications and businesses that include territorial changes, urban dynamics and land use changes, ground displacements (landslide and subsidence), infrastructure stability, new infrastructure and construction areas, wildfire burned areas or coastal seawaters quality, aquaculture. The service is updated with the availability of incoming data, and the refresh rate can range from monthly to daily frequency depending on the service characteristics (Tab. 1). The service update is guaranteed using satellite images, mapping data and environmental information available online as open data.

Rheticus® Displacement is the solution for the monitoring of ground surface movements, infrastructure stability and areas subject to subsidence or landslides. Subscribed users can access to timely and accurate information in form of dynamic maps, reports and alerts, fundamental for organizations and professionals working in engineering, utilities management, civil protection, master plan management and insurance.

Service	Application
Rheticus® Displacement	Landslides identification and monitoring for infrastructures planning and management
Rheticus® Network Alert	Monitoring water and sewer networks for the detection of potential failures linked to ground movements and displacements
Rheticus® Safeway	Dynamic Roadway and Railway Networks Monitoring
Rheticus® Marine	Marine water quality monitoring, turbidity, chlorophyll and sea temperature
Rheticus® Aquaculture	Farm monitoring and identification of best harvesting times for optimizing aquaculture activities
Rheticus® UrbanDynamics	Land cover monitoring
Rheticus® Wildfires	Mapping and monitoring over the time of burned area
Rheticus® Oenoview	Vineyards monitoring to support the productivity & the improvement of the quality of wines.

Table 1. Rheticus Service and Application

## Geology and geomorphology

In the two areas under study there are similar phenomena of slope dynamics with slow landslides and deep sliding surfaces (80-100m) but in different geological contexts.

In the Altolia area mainly strongly tectonized metamorphic rocks emerge on morphologies with narrow and hanging valleys (Fig. 2); Niscemi, instead, develops on sandy, calcarenitic and clayey outcrops with an active dynamic tectonic.

### Altolia (Messina)

Geologically the site is represented by paragneisses passing through micaschists, with large intercalations of gneiss "occhiadino" with associated metagranitoids and less slow than basic rocks; redominantly paragneisses that pass laterally to paragneiss with a broad compositional spectrum. The substratum is characterized by soils consisting of alteration products present generally sands and ruditic size breccias and less percentage of silt and pebbles. The degraded basement of altered and sanded crystalline rocks can be assimilated to a conglomerate consisting of coarse elements of crystalline rocks in a sandy-silty-clay matrix.

The outcropping metamorphic substrate is made up of paragneiss and mica schists, with inside haplitic levels, which sometimes become crumbling due to the various systems of schistosity and fracturing, complicated by the root system of the plants and by an intense alteration, especially in the part exposed to exogenous agents, while in depth the state of alteration is reduced, although the state of fracturing remains.



The morphology is characterized by the geological and structural conditions of the various units and by the numerous tectonic discontinuities present in the territory. The main watershed is located in the NNE-SSW direction, and the short distance from the coast determines notably steep slopes, with embankment and watershed lines arranged orthogonally to the coast (Fig. 3). Where the metamorphic soils emerge, the area presents itself with very narrow and incised valleys, while in the other lands it appears with softer forms and slopes but with an engraved hydrographic network.



Figure 2. Altolia: litology and geomorphology; landslide effects in the historic centre

The regional uplift has highlighted relict morphologies of old abrasion surfaces and marine terraces, with consequent rejuvenation and deepening of the hydrographic network due to the continuous elevation of the area. The geomorphological conditions show a poorly developed geomorphological stage that determines an intense erosive activity, developed during meteorological events, enhancing the degradation of the soil by channelled and wild waters.

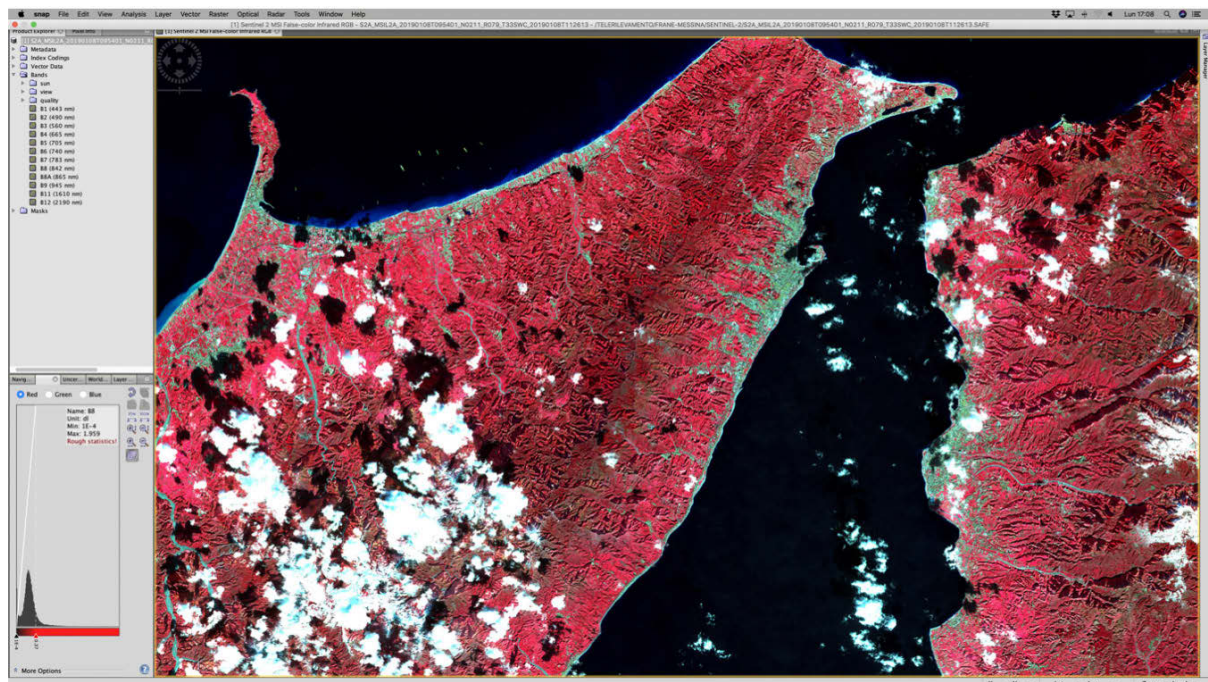


Figure 3. Sentinel 2 satellite image (MSIL2A product): the morphology is characterized by the geological and structural conditions of the various units and by the numerous tectonic discontinuities present in the territory. The main watershed is located in the NNE-SSW direction, and the short distance from the coast determines remarkably steep slopes, with watershed lines arranged orthogonally to the coast

The permeability of the lithotypes emerging in the monitoring area can be traced back to sands with gravels and is substantially primary (due to porosity). In the lithoid rocks (metamorphites) placed in bed (or in outcrops in neighboring areas) there is a discreet flow of superficial waters, while the presence of a secondary permeability due to fracturing favors the infiltration. In depth the metamorphic lithotypes, in the parts where it is not fractured or if present are not communicating, behave as an impermeable substrate.

## Niscemi

The Hyblean Plateau is the margin of the African shield colliding with the European one along the Apennine-Southern Arc; the front of the tectonic overthrust, known as Falda di Gela (Butler et al., 1992) passes about 1 km to the east from the landslide of Niscemi with a buried margin oriented NE-SW (fig. 4). Previous studies have described a series of faults with parallel course to the buried orogenic margin (Lentini et al., 1990; Butler et al., 1992; Catalano et al., 1995) and over-thrust activity during the Upper Pliocene-Lower Pleistocene (Catalano et al., 1995). Grasso et al. (1995) describe deformations, landslides and uplifts of the Pleistocene sedimentary coverages above the Falda di Gela, as consequences of compressive phenomena behind the front of the aquifer itself and testifying the activity in progress. Niscemi is located on a marine terrace consisting of a sequence of sand and limestone (middle Pleistocene) with a thickness of 50 m. The landslide sides are characterized by Pleistocenic clayey grounds surmounted by strips of sand dislocated on the marine terrace (Rizzo, 2004).

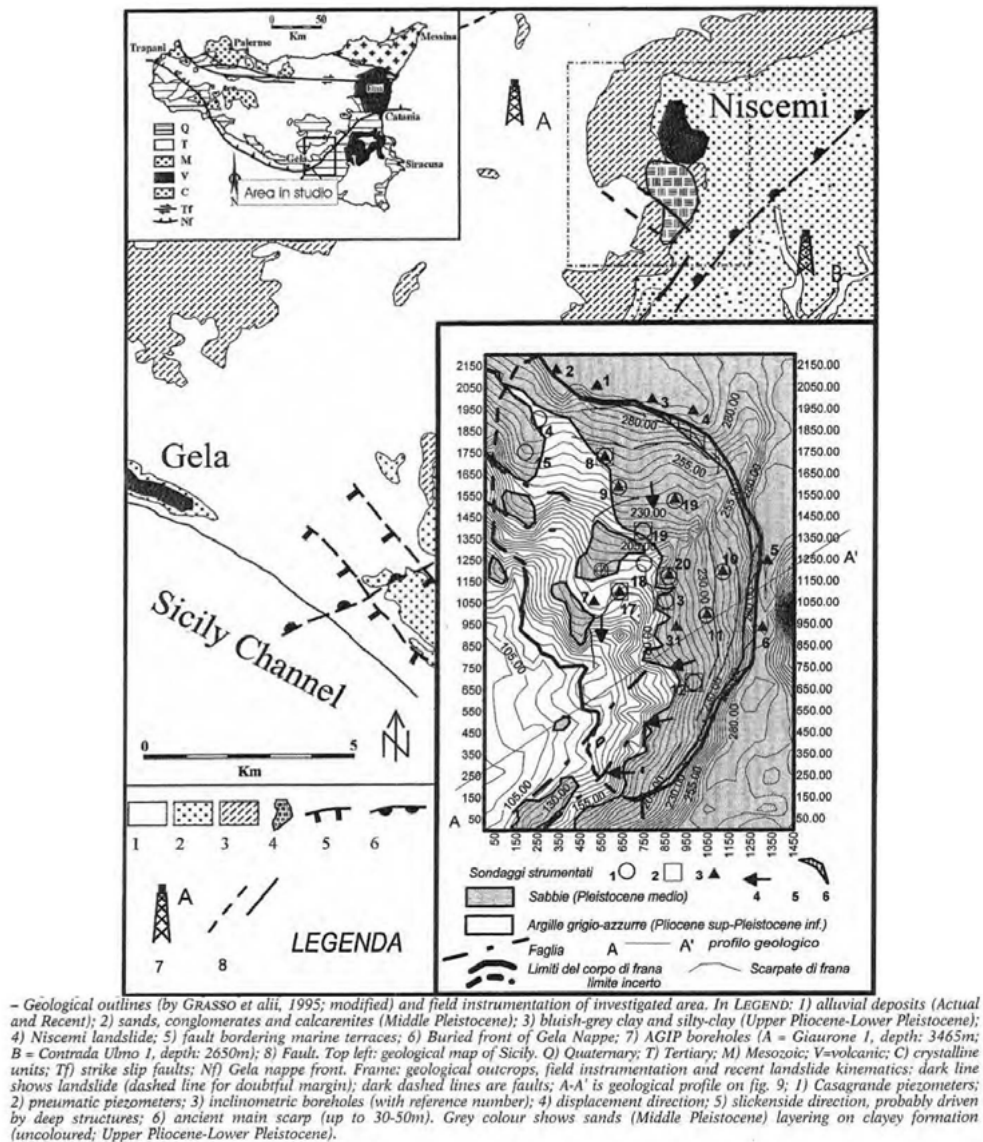


Figure 4. Geological Map (from: Rizzo, 2004)

The regressive series uplift deposited on the Falda di Gela in addition to the structures described, determined the formation of the slightly inclinator terrace on a regional scale. At Niscemi, the terrace has a marked curvature, in which the body landslide is placed.

Rizzo (2004) describes a morphogenesis conditioned by structural dislocations and by previous landslide movements (elongated escarpments, ditches, cracks) rather than by the action of erosion of watercourses. Badlands phenomena affects the clayey sedimentary sequence that emerges at the base of the slopes. Local morphogenesis, as also shown by the SENTINEL-2 satellite image and in situ survey (Fig. 5-6), is very active and causes a very irregular channeled erosive action conditioned by structural and morphological features that lead to erosive processes due to infiltration of rainwater inside of unstable masses. The underlying alluvial plain of the Gela River sometimes presents undulations and anomalous drainages with directions perpendicular to the general ones of the slope.



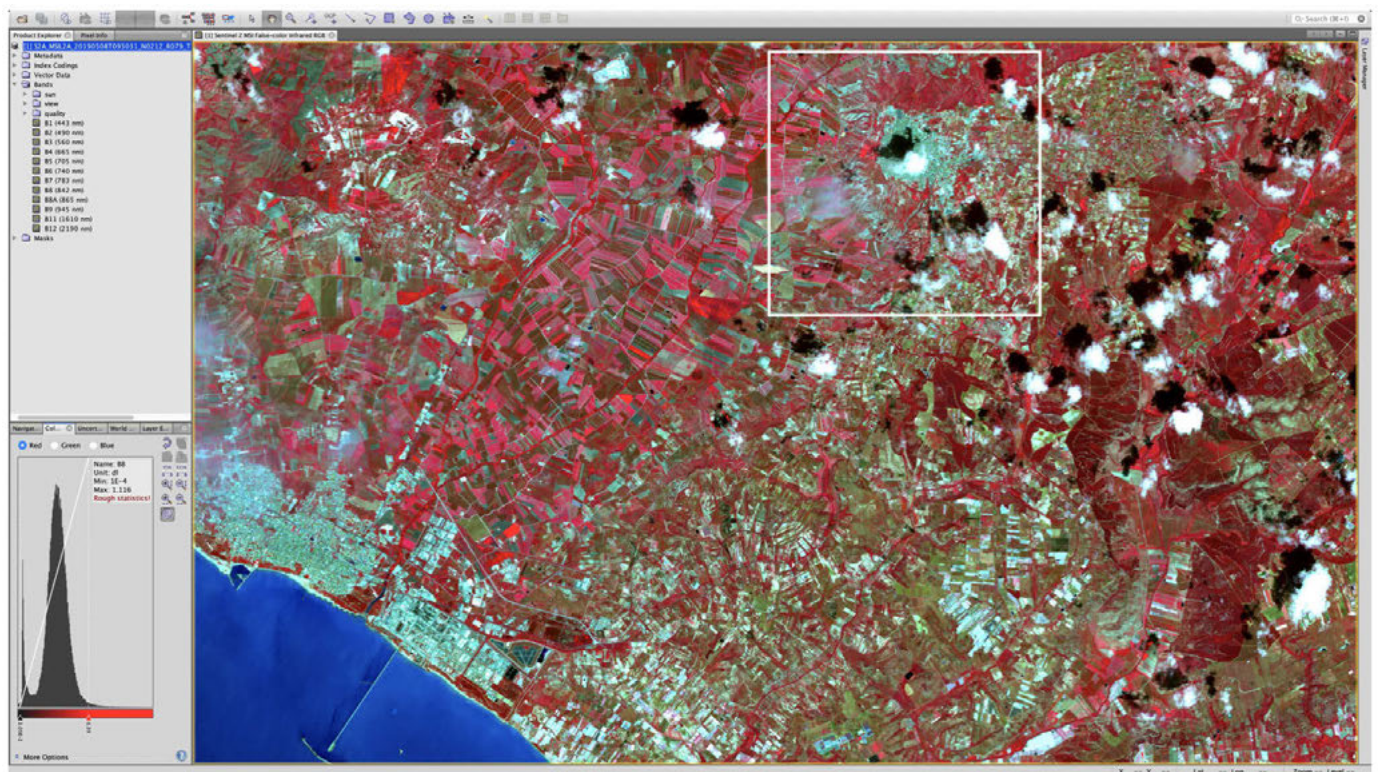


Figure 5. Sentinel 2 satellite image (MSIL2A product): the morphology is characterized by a hilly landscape set on sandy, conglomeratic, arenaceous and clayey lithologies. Local morphogenesis is very active and causes a very irregular channelled erosive action conditioned by structural and morphological features

### Interferometric data processing and mapping

The contribution of satellite Synthetic Aperture Radar (SAR) interferometry to landslide risk mitigation is well known in the scientific community and many encouraging results have been obtained (Herrera et al. 2009; Cigna et al. 2013; Crosetto et al. 2013; Raspini et al. 2013; Frangioni et al. 2014; Rocca et al. 2015).



Figure 6. Niscemi: landslide morphological features; a) top landslide view of the Gela fluvial plain; b) marine terrace affected by the landslide phenomenon; c) landslide effects; d) area below the Niscemi marine terrace

The data processed in Rheticus® Displacement are from SENTINEL-1 radar acquisitions (time range: 2014-2019), in ascending and descending orbit. The data were reported and processed in a GIS software (Fig. 7), mapping the precise values of V-LOS with a spatial analysis procedure (interpolation with IDW weighted inverse distance); the process allows to manipulate spatial information to extract new information and



meaning from the original information. In the IDW interpolation method, the sample points are weighed during interpolation so that the influence of each point with respect to the others decreases based on the distance from the unknown point to be created.

The figure 8 shows the map of the interpolated values in descending orbit and which gave the best results, probably related to the best exposure of the ground reflectors in the descending phase. The LOS values distribution highlights some areas (in red and yellow) that represent the lowest values (negative) found and that are concentrated in the most critical areas (as shown by in-situ surveys) represented by the structures present along the slopes and towards the foot of the landslide. In according to the bibliographic studies related to the area, the INSAR data confirm a morphogenesis conditioned by structural dislocations, previous landslide movements and probably by the erosion action of surficial water and deep infiltration phenomena.

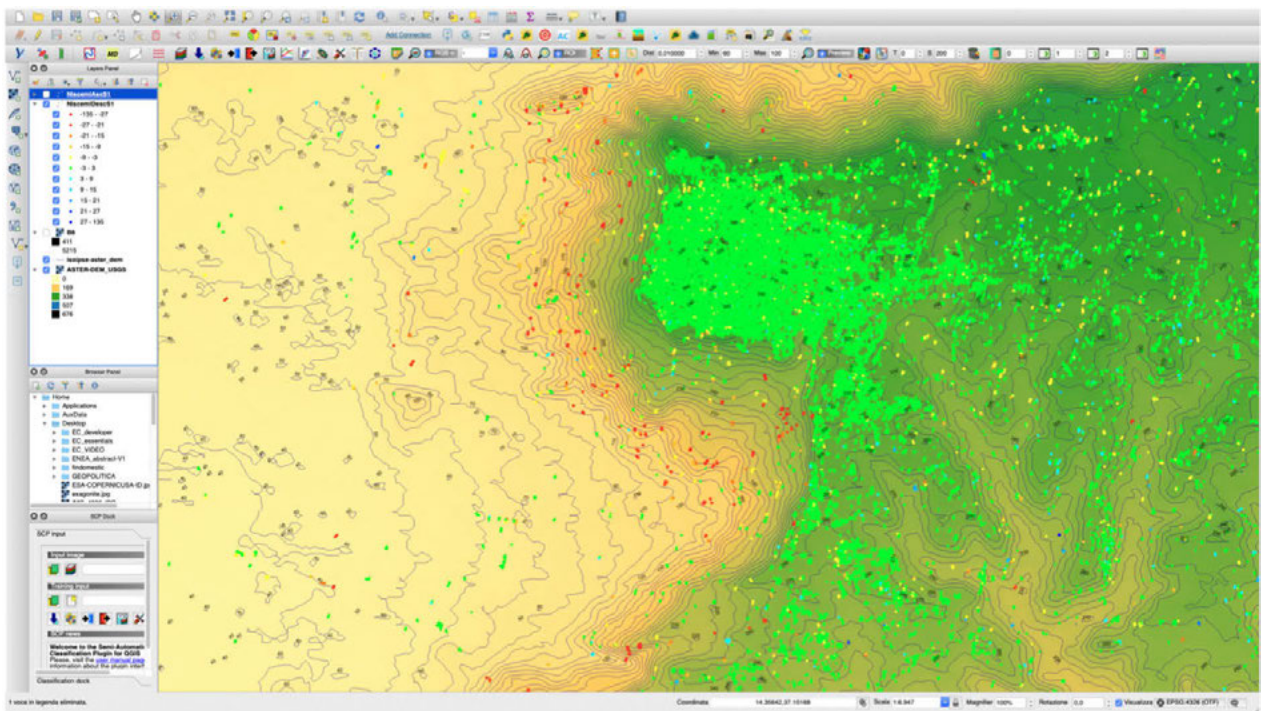


Figure 7. SENTINEL-1: INSAR data (descending orbit): the red points indicate the most critical (negative) values that are located in the most critical morpho-tectonic features

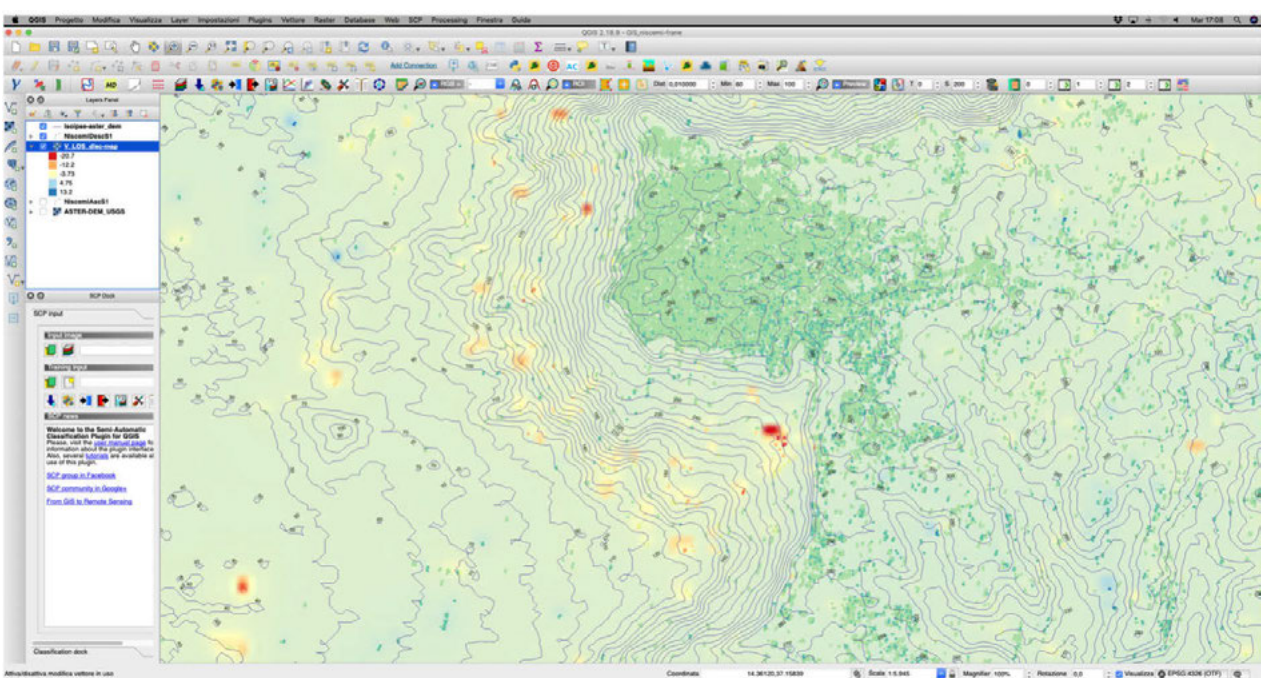


Figure 8. SENTINEL-1 INSAR data: interpolation processing of data (descending). In red most critical areas with high lowering values

## References

- Butler R.H.V., Grasso M., & La Manna F., 1995. Origin and Deformation of the Neogene-Recent Magherbian foredeep at the Gela Nappe, SE Sicily. *Journ. Geol. Soc. London*, 149, 547-556.
- Catalano R., Infuso S., & Sulli A., 1995. Tectonic History of the submerged Maghreb Chain from the Southern Tyrrhenian Sea to the Pealagian Foreland. *Terra Nova*, 7, 179-188.
- Cigna F, Bianchini S, Casagli N. 2013. How to assess landslide activity and intensity with Persistent Scatterer Interferometry (PSI): the PSI-based matrix approach. *Landslides*. 10:267\_283.
- Crosetto M, Gili JA, Monserrat O, Cuevas-Gonzalez M, Corominas J, Serral D. 2013. Interferometric SAR monitoring of the Vallcebre landslide (Spain) using corner reflectors. *Nat Hazard Earth Syst Sci*. 13:923\_933.
- Frangioni S, Bianchini S, Moretti S. 2014. Landslide inventory updating by means of persistent scatterer interferometry (PSI): The Setta basin (Italy) case study. *Geomat Nat Hazard Risk*. 6:419-438.
- Herrera G, Davalillo JC, Mulas J, Cooksley G, Monserrat O, Pancioli V. 2009. Mapping and monitoring geomorphological processes in mountainous areas using PSI data: Central Pyrenees case study. *Nat Hazard Earth Syst Sci*. 9:1587\_1598.
- Lentini F, Carbone S., Catalano R., & Monaco C., 1990. Tettonica e tectonica neogenica nella Catena Appenninico-Maghrebide: esempi dalla Lucania e dalla Sicilia. In: *Neogene Thrust Tectonics*, Boccaletti M., Deiana G., & Raspini F, Moretti S, Casagli N. 2013. Landslide mapping using SqueeSAR data: Giampilieri (Italy) case study. In *Landslide science and practice*. Berlin Heidelberg: Springer-Verlag; p. 147\_154.
- Rizzo V., 2004. Un vasto movimento gravitativo al fronte della falda di Gela: evidenze e problematiche in relazione alla tettonica (Frana di Niscemi, Sicilia Meridionale). *Boll. Soc. Geol.*, 123 (2004), 229-252, 15 ff., 1 tab.
- Rocca A, Mazzanti P, Bozzano F, Perissin D. 2015. Advanced characterization of a landslide-prone area by satellite a-DInSAR. In: *Engineering geology for society and territory*, Volume 5. Switzerland: Springer International Publishing; p. 177-181



## A geomatic application for water management in precision farming for a LIFE European project

Alessandro Lambertini, Gabriele Bitelli, Emanuele Mandanici, Luca Vittuari

*Dept. of Civil, Chemical, Environmental and Materials Engineering (DICAM), University of Bologna  
(alessandro.lambertini, gabriele.bitelli, emanuele.mandanici, luca.vittuari)@unibo.it*

Corresponding author: A. Lambertini

Keywords: UAV, GIS, precision farming, remote sensing, aerial thermography

### 1. Introduction

The activities and the approaches described in this work are carried out in the frame of the current European LIFE project AGROWETLANDS II (Principal Investigator: M. Speranza, University of Bologna). This multidisciplinary project aims at the integration of multi-source data, to provide a valuable support for a more efficient and sustainable management of territorial resources, through an innovative approach to precision farming.

The implementation of a smart irrigation management system is a central task of AGROWETLANDS II. A pilot system is operational in a study area located close to the Northern coast of the Adriatic Sea, in the Ravenna province (Italy). It is a farming area affected by soil and groundwater salinization, due to the ingression of sea water. The permanent monitoring network records several parameters for the weather, soil and groundwater. The expected results of the project include: a mitigation in the soil salinity, an improvement in the productivity of the crops, a reduction of the environmental impact and the implementation of a decision support system (DSS), which is able to advise farmers on the management of their agricultural activities (LIFE AGROWETLANDS II, 2019).

In fact, one of the main goals of the project is to reduce the water use for crop production and to ensure a sustainable water management for an efficient agricultural production. In order to achieve significant results in precision farming and water management, an accurate survey is needed to create precise numerical models which are the necessary base for each subsequent analysis.

### 2. Materials and methods

Several geomatic techniques were adopted at different scales of survey in the project area: satellite, aerial, UAV and terrestrial. As a first step, a single and continuous Digital Elevation Model (DEM) with 1 meter spatial-resolution was produced, covering the whole area of the project, integrating data obtained from airborne laser scanner survey (ALS LIDAR) and data obtained from bathymetric survey along the coastline. Furthermore, in order to detect the elevation of piezometers in the study area with a greater accuracy, a levelling campaign was planned. The survey was carried out through the combined use of geodetic GNSS receivers, total stations, and levels, and provided the orthometric height of each piezometer, enabling accurate analyses for the water level. The DEM was used to perform an analysis of the salt contamination in the area, based on the creation of a three-dimensional stratigraphic model (Lamberti et al., 2018).

Multidisciplinary teams working for the project contributed to the acquisition of heterogeneous geographical data. Each dataset collected was imported in a comprehensive GIS. The resulting database is described in the following chapter.

In the perspective of a high frequency monitoring of the crop status for the entire project area, an analysis was carried out to identify the most suitable multispectral data acquisition solution. The availability of free satellite data with high temporal resolution was the optimal and cost-effective solution compared to an aerial overflight.

In order to achieve the desired result, the sensor and acquisition specifications of the multispectral satellites covering the project area were reviewed. The goal was to identify the time and period of acquisition of the images that are suitable for the computation of relevant vegetation indexes. In a preliminary analysis, both Copernicus Sentinel-2 and USGS Landsat 8 were considered as input for multispectral data processing. Sentinel-2 was preferred for the better spatio-temporal resolution (5 days combining both Sentinel-2A and Sentinel-2B acquired data).

A series of thermal surveys to further assess crop health is ongoing at the time of writing. Previous experiences confirmed the possibility to identify spatial variation in crop water stress from thermal remote sensing (Tilling et al., 2007). Moreover, in a comprehensive review was found out that visible and near-infrared wavelengths

were widely used for the computation of soil properties, while mid-infrared and thermal-infrared regions were less commonly used (Yufeng et al., 2011). Nevertheless, recent availability of higher spatial-resolution thermal surveys from low-altitude UAV platforms may provide further possibilities to better understand and prevent soil and vegetation problems (Figure 1).

In this project, data will be acquired and processed both from satellite and UAV platforms, with different spatial-resolutions and coverages. For the UAV surveys, a significant sample area of 5 hectares spread among different crops was identified.

Even for low-altitude UAV flights, the atmospheric effects are relevant for an accurate thermal survey (Berni et al., 2009). In most cases it is difficult to obtain an adequate model of the atmospheric conditions at the time of the flight. Therefore, in order to avoid excessive accuracy losses, an approximate estimation of the atmospheric parameters is performed with data acquired from ground surveys of temperature and emissivity parameters (Bitelli et al., 2015; Mandanici et al., 2016). This is possible thanks to the meteorological data acquired continuously from the sensors of the permanent monitoring network displaced over the study area, integrated with further surface temperature measurement acquired on field using special targets easily detectable on the UAV imagery.

The thermal sensor used from the UAV platform was carefully chosen given the technical specifications needed for this particular survey. The chosen sensor has the ability to capture and record calibrated temperature measurements for each pixel, with a resolution of 0.3 megapixel (640 rows and 512 columns in the raster output). The flight parameters in the planning of the UAV survey were computed given the field size, the focal length of the camera, the sensor size and the desired Ground Sample Distance (GSD) of 0.15 meters. Custom thermal targets to be used as Ground Control Point (GCP) were created using aluminum foils in order to make them visible from the UAV platform with sufficient temperature contrast and an appropriate size compared to the GSD (Figure 2).

The parameters for an automated UAV flight over the 5 hectares area were computed considering also the UAV flight autonomy with the survey payload configuration and the necessary overlap between subsequent flight lines. The placement of GCPs was particularly challenging due to the farming activities to be carried out in the fields. The limited number of stable natural or manmade surfaces offered only a few possibilities to identify permanent reference points, measured with RTK GNSS, to be used as a target in the UAV survey (Figure 3).

The UAV flights are scheduled to match Landsat 8 overpasses. Landsat 8 satellite, indeed, can acquire thermal data over the entire study area with its TIRS (Thermal Infrared Sensor). Thanks to the availability of satellite orbit information, it was possible to predict well in advance each satellite acquisition during the whole agricultural season.



Figure 1. The UAV platform and sensors used for the survey



Figure 2. Example of a thermal Ground Control Point (GCP)

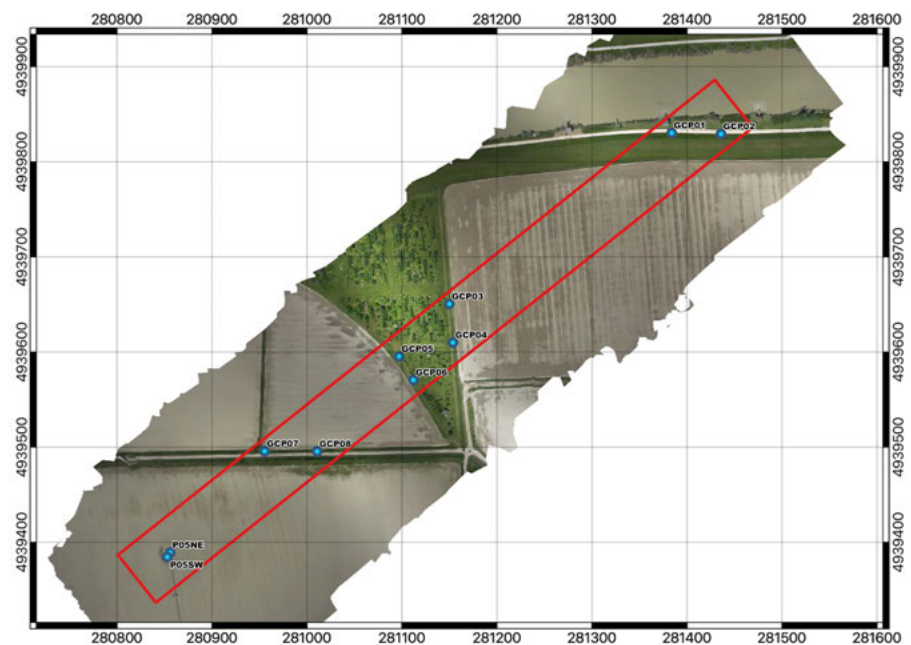


Figure 3. Ground Control Points (in blue) placed over the 5 hectares UAV survey area (in red).



### 3. Results and discussion

In the context of the project, currently in progress, all the outputs of the geomatic procedures and techniques described in the previous section was integrated in a unique database. This database was designed to serve as a common platform to share and combine all the heterogeneous geographical data, acquired for each different discipline involved in the project, encompassing the analysis of soil, climate, water and environment. The aim is to gather information within a unified platform, usable for further analysis. The database structure is tuned to deliver data and metadata in compliance with the INSPIRE directive, using Free and Open-Source Software (FOSS). Each thematic layer containing geographic information is appropriately added in a GIS environment and converted into a unique coordinate reference system defined for the whole project (European Terrestrial Reference System 1989 in UTM zone 33N) (Figure 4).

At the time of writing, a complete series of at least 30 multispectral images were acquired from Copernicus Sentinel-2 during the main agricultural season in 2018 with less than 10% cloud cover. NDVI was processed from the images providing straightforward information about health and phase of each crop (Figure 5). The same procedure will be repeated for 2019 season.

The UAV thermal survey is planned for the entire 2019 agricultural season and is expected to provide the first results at the end of the summer. Among the interesting preliminary results, it is worthwhile to mention the complexity of the processing of accurate high-resolution thermal orthomosaics. In fact, it is a challenging task due to the low resolution of thermal sensors and their low dynamic range. Furthermore, some best practices were recently discussed for an automated generation of thermal orthomosaics with Structure from Motion techniques (Conte et al., 2018) and are going to be adapted for the present

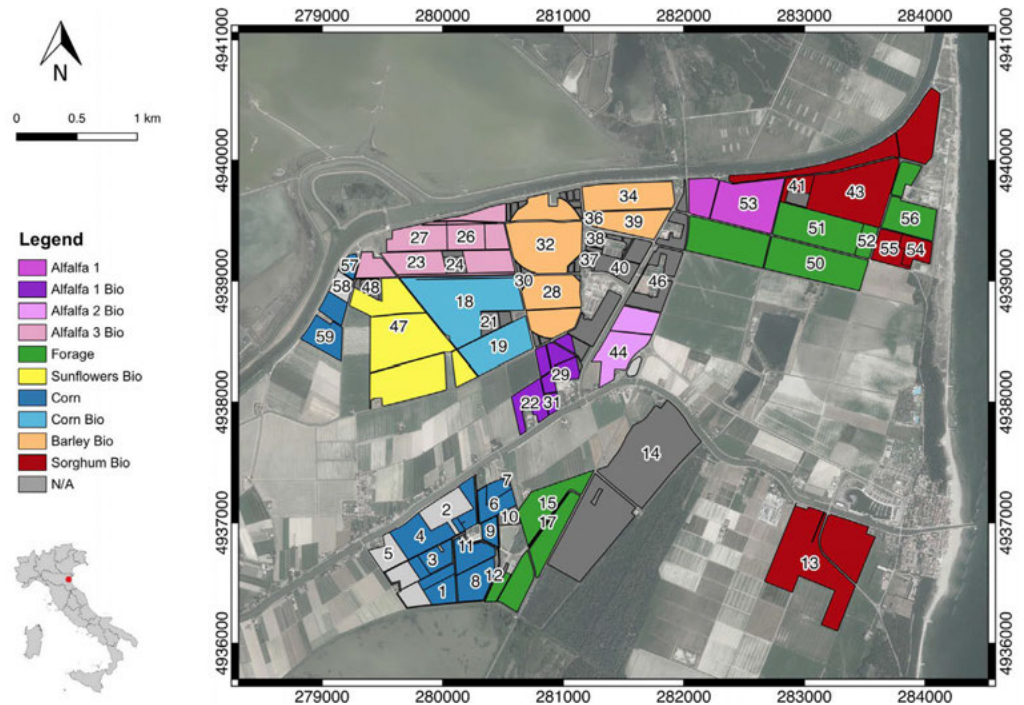


Figure 4. Thematic map produced from the GIS database in the study area

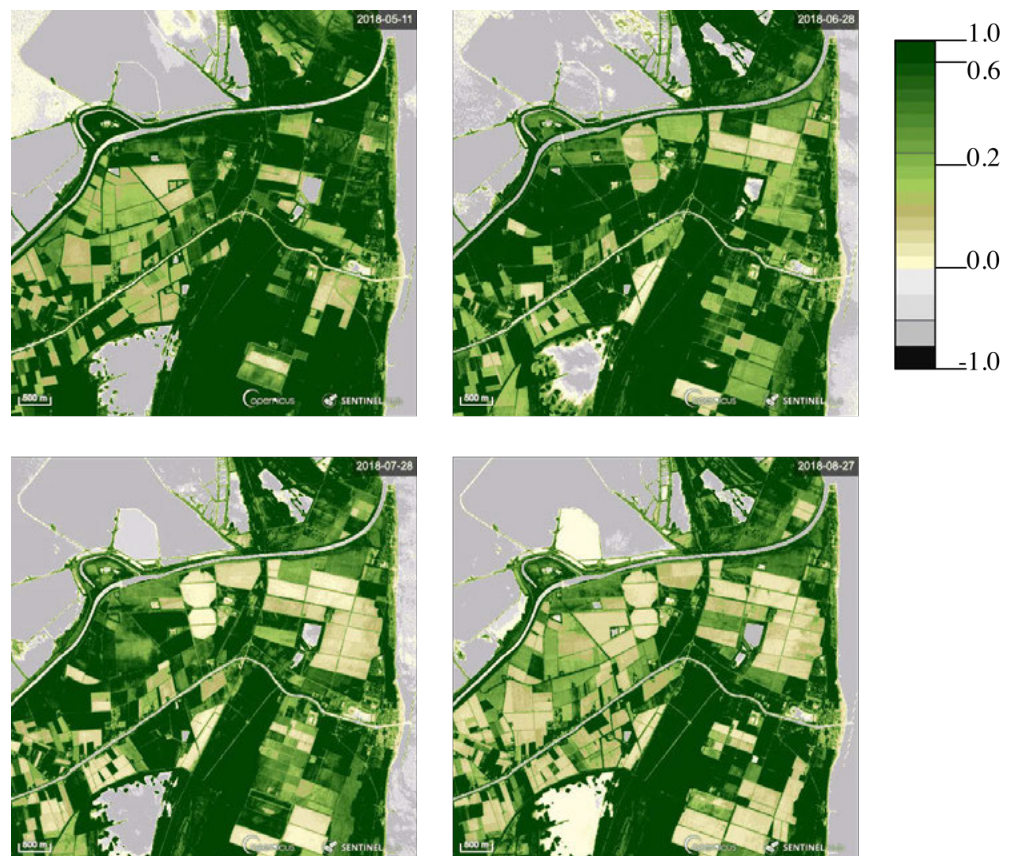


Figure 5. NDVI change over the studied area during 2018 crop season, in a series of maps sorted in chronological order from left to right and from top to bottom, acquired from Sentinel Hub, Sinergise Ltd.

application. These and other practices are to be taken into account during the entire workflow of this project, starting from the survey to the processing of thermal datasets.

### Acknowledgments

This work is partially funded by the LIFE Programme 2014-2020 project LIFE AGROWETLANDS II - LIFE15 ENV/IT/000423.

The authors would like to thank the components of the project and their colleagues Maria Alessandra Tini and Luca Poluzzi for their help during the survey activities.

### References

- Berni, J. A. J., Zarco-Tejada, P. J., Suarez, L., Fereres, E., 2009. Thermal and Narrowband Multispectral Remote Sensing for Vegetation Monitoring From an Unmanned Aerial Vehicle. *IEEE Transactions on Geoscience and Remote Sensing*, 47(3), 722–738. doi:10.1109/TGRS.2008.2010457.
- Bitelli, G., Conte, P., Csoknyai, T., Franci, F., Girelli, V. A., Mandanici, E., 2015. Aerial Thermography for Energetic Modelling of Cities. *Remote Sensing*, 7(2), 2152–2170. doi:10.3390/rs70202152.
- Conte, P., Girelli, V. A., Mandanici, E., 2018. Structure from Motion for aerial thermal imagery at city scale: Pre-processing, camera calibration, accuracy assessment. *ISPRS Journal of Photogrammetry and Remote Sensing*, 146, 320–333. doi:10.1016/j.isprsjprs.2018.10.002.
- Lamberti, A., Masina, M., Lambertini, A., Borgatti, L., 2018. La contaminazione salina nella fascia costiera tra i fiumi Reno e Lamone: influenza delle condizioni geomorfologiche per l'ingressione di acqua marina. IDRA 2018 – XXXVI Convegno Nazionale di Idraulica e Costruzioni Idrauliche, Ancona (Italy) 12-14/09/2018.
- LIFE AGROWETLANDS II, 2019. Available online: <http://www.lifeagrowetlands2.eu> [Accessed 31 May 2019].
- Mandanici, E., Conte, P., Girelli, V. A., 2016. Integration of Aerial Thermal Imagery, LiDAR Data and Ground Surveys for Surface Temperature Mapping in Urban Environments. *Remote Sensing*, 8(10), 880. doi:10.3390/rs8100880.
- Tilling, A. K., O'Leary, G. J., Ferwerda, J. G., Jones, S. D., Fitzgerald, G. J., Rodriguez, D., Belford, R., 2007. Remote sensing of nitrogen and water stress in wheat. *Field Crops Research*, 104(1–3), 77–85. doi:10.1016/j.fcr.2007.03.023.
- Yufeng, G., Thomasson, J. A., Ruixiu, S., 2011. Remote sensing of soil properties in precision agriculture: A review. *Frontiers of Earth Science*, 5(3), 229–238. doi:10.1007/s11707-011-0175-0.



## ENVI Deep Learning: un nuovo tool per la risoluzione di problemi geospaziali

Andrea Marchesi, Paola Filippi

*Harris Geospatial Solutions Italia*

Corresponding author: [andrea.marchesi@harris.com](mailto:andrea.marchesi@harris.com)

Keywords: Deep Learning, Classificazione, Soluzioni Enterprise, Big Data, ENVI

### **Abstract**

L'innovazione tecnologica, la sempre maggiore disponibilità di missioni e immagini satellitari, la necessità di estrarre informazioni utili in modo semplice e veloce, sono tutti elementi che implicano un nuovo approccio metodologico e nuovi strumenti di analisi.

In questo Workshop sarà presentata l'ultima novità nel campo dell'intelligenza artificiale, ENVI Deep Learning, un nuovo modulo sviluppato da Harris che, grazie alla sua facilità di utilizzo, permette rapidamente di individuare, classificare e contare differenti "oggetti" all'interno di qualsiasi immagine digitale con valori di accuratezza difficilmente ottenibili con i classici algoritmi di classificazione. L'integrazione del nuovo modulo all'interno della piattaforma ENVI e la possibilità di combinare differenti algoritmi in ENVI Modeler, permette inoltre di creare velocemente applicazioni verticali, pubblicarle in ambiente cloud e offrire un servizio in grado di soddisfare molteplici esigenze in svariati settori.

## Supporting Forest Planning and Management by Sentinel 2 data aimed at forest Basal Area Estimation

Enrico Borgogno Mondino, Roberta Berretti, Evelyn Momo

DISAFA - University of Torino

*enrico.borgogno@unito.it, roberta.berretti@unito.it, evelyn.momo@edu.unito.it*

This work is part of a project dealing with the problem of the socio-economic marginality of forest sector for wood production. The Regional Forestry Plan of Piemonte Region (NW Italy) blamed this marginality mainly due to the high costs of wood extraction and its corresponding low market value. Costs could be reduced supporting the forest biomass estimation by remote sensing, limiting the ordinary workflow based on field surveys, thus resulting highly time consuming. Furthermore, in some cases stands of interest can be difficultly accessed inducing additive costs.

Many studies dealing with both climate change and sustainability of forest management based on remotely sensed data can be found in literature (Dube et al., 2016). Many of them propose different methods for the estimation of forest biomass-related features (volume, basal area, above ground biomass and forest carbon stocks). A wide variety of approaches have been used (optical, LiDAR and RADAR are the most frequently used), including parametric (e.g. regression models) and nonparametric algorithms such as K-Nearest Neighbour (K-NN), Artificial Neural Network (ANN), random forest, support vector machine (SVM), and Maximum Entropy (MaxEnt) (Fassnacht et al., 2014; Lu et al., 2016). Nonparametric approaches, in recent years, have become more prevalent because of their higher potential to identify complex nonlinear relationships compared to regression model (Haywood et al., 2018). Optical images are widely employed because of their accessibility and affordability (Dube et al., 2016). In some studies the native spectral bands are used to calibrate a regression model with the biomass (Muukkonen and Heiskanen, 2005; Vacchiano et al., 2018; Zhao et al., 2016); in others vegetation indexes are employed (Freitas et al., 2005; Pandit et al., 2018). There are a lot of cases where optical data are associated to LiDAR or RADAR data (Jiménez et al., 2017; Morin et al., 2018; Wittke et al., 2019).

The quality of the estimation is depends on the error. In literature it is possible to find studies that refer to the absolute error, making difficult any comparison. Others uses rRMSE (Relative Root Mean Squared Error) referring the absolute value of the error to the value of the measure itself, therefore introducing a sort of normalization. rRMSE proves to vary between 8 and 50 %, but these values have to be compared with caution because the validation sets were generated in very different ways (Dittman et al., 2017).

Allometric approaches for biomass estimation based on field measurements are certainly more accurate, but time consuming (Dittmann et al., 2017) and cannot provide a continuous spatial distribution of the data at a large scale (Vacchiano et al., 2018). As a consequence, they are suitable for a small area application only. RADAR based methods appear to be efficient on a large area scale, but suitable for homogenous stands only (Dittmann et al., 2017); they also proved to saturate in forest characterized by a high level of biomass (Dube et al., 2016). LiDAR based approaches appear to be the most efficient and accurate ones for medium sized area applications. Differently, multispectral imagery appears to be appropriate for large area monitoring; unfortunately, in general, they give a coarse estimation of homogeneous stands, and some further limitations can be observed in mountain regions (Dittmann et al., 2017).

This work is aimed at exploring the possibility of defining a methodology for the estimation of the Forest Basal Area (BA) of conifers based on freely available satellite imagery. BA is said to be a good dendrometric parameters to synthesize the structure of the forest stands. The procedure is, in fact, intended to support local forest management in a more effective and economic way with special focus on forest inventory instances. In particular a preliminary and experimental procedure for wood volume estimate (conifers) in the Susa Valley (Piemonte, NW Italy) based on Sentinel 2 Level 2A data and Multi-layer Perceptron (MLP, Rumelhart&Williams, 1985) ANN applications is presented and first results given.

One S2 image per month, along the 2018 main growing season (May – September, table 2), was selected having the minimum cloud cover in the area.  $NDVI = (p_{NIR} - p_R) / (p_{NIR} + p_R)$ , Normalized Difference Vegetation Index, and  $NDWI_G = (p_G - p_{MIR1}) / (p_G + p_{MIR1})$ , Normalized Difference Water Index, were computed from the original bands and used as predictors of BA. Ground observations from 387 plots surveyed in the past years in coniferous stands within the study area were used to train a Multi-layer Perceptron ANN, using the correspondent values of NDVI and NDWI<sub>G</sub> as inputs. Results showed that accuracy of AB estimates by ANN ranges between about 15% and 25%. A preliminary map of AB for the entire study area was finally generated, masking out all those parts of the valley where conifers were not present.

## References

- Dittmann, S., Thiessen, E., Hartung, E., 2017. Applicability of different non-invasive methods for tree mass estimation: A review. *For. Ecol. Manag.* 398, 208–215.
- Dube, T., Mutanga, O., Shoko, C., Adelabu, S., Bangira, T., 2016. Remote sensing of aboveground forest biomass: A review. *Trop. Ecol.* 57, 125–132.
- Fassnacht, F.E., Hartig, F., Latifi, H., Berger, C., Hernández, J., Corvalán, P., Koch, B., 2014. Importance of sample size, data type and prediction method for remote sensing-based estimations of aboveground forest biomass. *Remote Sens. Environ.* 154, 102–114.
- Freitas, S.R., Mello, M.C., Cruz, C.B., 2005. Relationships between forest structure and vegetation indices in Atlantic Rainforest. *For. Ecol. Manag.* 218, 353–362.
- Haywood, A., Stone, C., Jones, S., 2018. The Potential of Sentinel Satellites for Large Area Aboveground Forest Biomass Mapping, in: *IGARSS 2018-2018 IEEE International Geoscience and Remote Sensing Symposium*. IEEE, pp. 9030–9033.
- Jiménez, E., Vega, J.A., Fernández-Alonso, J.M., Vega-Nieva, D., Ortiz, L., López-Serrano, P.M., López-Sánchez, C.A., 2017. Estimation of aboveground forest biomass in Galicia (NW Spain) by the combined use of LiDAR, LANDSAT ETM+ and national forest inventory data. *IForest-Biogeosciences For.* 10, 590.
- Lu, D., Chen, Q., Wang, G., Liu, L., Li, G., Moran, E., 2016. A survey of remote sensing-based aboveground biomass estimation methods in forest ecosystems. *Int. J. Digit. Earth* 9, 63–105.
- Morin, D., Planelis, M., Guyett, D., Viiard, L., Dedieu, G., 2018. Estimation of Forest Parameters Combining Multisensor High Resolution Remote Sensing Data, in: *IGARSS 2018-2018 IEEE International Geoscience and Remote Sensing Symposium*. IEEE, pp. 8801–8804.
- Muukkonen, P., Heiskanen, J., 2005. Estimating biomass for boreal forests using ASTER satellite data combined with standwise forest inventory data. *Remote Sens. Environ.* 99, 434–447.
- Pandit, S., Tsuyuki, S., Dube, T., 2018. Estimating above-ground biomass in sub-tropical buffer zone community forests, Nepal, using Sentinel 2 data. *Remote Sens.* 10, 601.
- Rumelhart, D.E., Hinton, G.E., Williams, R.J., 1985. Learning internal representations by error propagation. California Univ San Diego La Jolla Inst for Cognitive Science.
- Vacchiano, G., Berretti, R., Motta, R., Mondino, E.B., 2018. Assessing the availability of forest biomass for bioenergy by publicly available satellite imagery.
- Wittke, S., Yu, X., Karjalainen, M., Hyyppä, J., Puttonen, E., 2019. Comparison of two-dimensional multitemporal Sentinel-2 data with three-dimensional remote sensing data sources for forest inventory parameter estimation over a boreal forest. *Int. J. Appl. Earth Obs. Geoinformation* 76, 167–178.
- Zhao, P., Lu, D., Wang, G., Wu, C., Huang, Y., Yu, S., 2016. Examining spectral reflectance saturation in Landsat imagery and corresponding solutions to improve forest aboveground biomass estimation. *Remote Sens.* 8, 469.

Maurizio Pollino, Sergio Cappucci, Ludovica Giordano, Domenico Iantosca, Luigi De Cecco, Danilo Bersan, Vittorio Rosato, Flavio Borfecchia  
*ENEA, Italian Agency for New Technologies, Energy and Sustainable Economic Development*

Corresponding author: Pollino M.

Keywords: Seismic Post-emergency Management, LIDAR, active/passive remote sensing, Sentinel2 World View satellites, COPERNICUS, hyperspectral signatures of urban rubble materials, SMA (Spectral Mixture Analysis), Classification & machine learning algorithms.

### 1. Abstract

The methodology implemented in the present study focused on the rubble management support in a urban seismic post-emergency scenario by integrating active (LIDAR) and passive remote sensing techniques based respectively on airborne and satellite platform. The LIDAR data were exploited to provide the geometric features (location and volume) of rubble piles distributed in the center of Amatrice town (Central Italy), stroked by the earthquake of August 24, 2016, using on purpose developed procedure, based on photointerpretation and volumes 3-D modelling. The rubble piles location was based on rapid mapping products of EMS Copernicus services. The subsequent surface characterization of rubble typologies for each heap was derived from the High Resolution multispectral data acquired by the Sentinel-2 HR (High Resolution) and WorldView-3 VHR (Very High Resolution) sensors on polar satellites. The approach used was the Spectral Mixture Analysis (SMA) supported by hyperspectral signatures of the various building materials of interest acquired on field through the ASD FieldSpec pro hand-held radiometer and machine learning algorithms. The implemented methodology allowed us to effectively map the rubble heaps with their volumes and related rubble typologies percentages which supported their optimized management and removal from urban center with the subsequent building waste storage.

### 2. Introduction

Earth Observation (EO) technologies coupled with GIS mapping and modeling techniques (Borfecchia et al., 2016) provide valuable opportunities for effectively supporting all phases of emergency management due to catastrophic events including seismic ones. In the framework of technical-scientific activities for supporting the post event-activities after the earthquake occurred on the August 24, 2016 in Central Italy, we proposed a new EO-based application in order to characterize the urban rubble heaps deriving from buildings affected by partial or total collapse, in the area of Amatrice town, one of the most affected urban areas (Fig. 1).

These activities focused on the optimized management of relevant quantities of urban rubble following seismic event and the implementation of good practices and specific procedures to efficiently plan the subsequent removal and transport operations. The main urban rubble features to be assessed are heaps location and delimitation, volume, weight and typologies of the principal collapsed building materials. However, the volume and variety of disaster waste are often difficult to assess (Lund, 1993; Memon, 2015; Talbot and Talbot, 2013; US EPA, 1993).

The level of buildings damage distribution was initially provided by the Copernicus EMS operational service. The main goals were to estimate: a) the heaps volumes and b) the percentage of the various types of materials characterizing the rubble heaps' surface by using multiplatform remote sensing data. The high spectral and spatial heterogeneity of urbanized areas, which dramatically increase in case of rubble caused by catastrophic



Figure 1 Central Italy (left); Amatrice by Sentinel2 (3-d true color;centre); a rubble heap from aerophotos (right).

earthquakes, sets serious limits on the use of automatic procedures affecting the timeliness and stability of results. Indeed, surveys based on LIDAR and aerophotos from aerial platforms can provide detailed information (Ricci et al., 2011), but are extremely burdensome for the



necessity of continuous monitoring of the emergency areas in order to follow the phenomena evolution. Currently, these needs can better be met by integrating surveys of the last generation satellite network equipped with active (SAR) and passive (multi/hyperspectral) HR/VHR sensors, with data (Baiocchi et al., 2013) provided by other platforms (i.e. UAV- Unmanned Aerial Vehicle).

## 2. Methods

The procedures for the identification of the rubble heaps volumetric estimates, together with the surface main types of debris constituent, follows the general scheme sketched in Fig. 2. The volumes estimation method is based on the use of data taken from the aerial platform in the aftermath of the earthquake by LIDAR, as a point cloud (10 p/m<sup>2</sup>) and high resolution RGB orthophotos/aero-photos (0.30 m). For the development of the methodology for estimating the types of rubble, we exploited a WorldView-3 (WV3) VHR satellite frame, (1.35 m resolution for the 8 (VIS-NIR) multispectral channels; 0.33 m for panchromatic channel), acquired on 08/25/2016, in the aftermath of the first seismic event in Amatrice. Given the spatial and heterogeneity of the urban rubble, typically smaller than the WV3 pixel, the SMA (Spectral Mixture Analysis) approach was adopted using an in situ spectral characterization of building materials. This characterization is based on the radiometric hyperspectral signatures of the urban rubble main constituents acquired through an ASD-FieldSpec Pro hand-held radiometer on pilot areas set in the center of Amatrice, during an on purpose designed survey carried out in December 2016.

### *Volume estimate*

The method for the rapid estimation of the volumes of rubble heaps within the so-called “red zones” (the areas of the Amatrice center, depicted by Cappucci et al., 2017, strongly stroked by the Earthquake and filled by rubble heaps), included the following steps, schematically described as follows:

- data retrieval, homogenization and organization with creation of the reference repository of georeferenced and congruent territorial data for the subsequent phases of the activity;
- production of DTM (Digital Terrain Model) and DSM (Digital Surface Model) from the LIDAR points cloud using specific filtering and devoted processing tools. The photointerpretation and overlay with available aerophotos provided a first verification of the LIDAR DTM/DSM basic products;
- estimates of rubble piles distribution, volumes and contours using an interactive threshold for DSM/DTM differences, visually checked on detailed aerophotos of the area and pre-event plano-altimetric data if available;
- comparison, checking, updating and verification of the piles volumes and contours provided in the context of seismic emergency activities (perimeter of the destroyed, highly damaged buildings indicated in the EMS Copernicus outputs have been exploited for visual checking purposes).

Where the quality of the ortho-photos and DTM/DSM digital models allowed it, a single polygon was considered for each collapsed building; otherwise, the polygon that delimits the area of the piles has been attributed to two or more aggregates of buildings. To each polygon a degree of damage, according to the Copernicus EMS damage grading also checked through photo-interpretation, was assigned: (1) totally destroyed; (2) partially destroyed; (3) doubt.

### *Typology assessment*

The methodology for the extensive evaluation of the types of heaps rubble constituents techniques, encompass the following steps (Fig. 2):

- acquisition and pre-processing (geometric, radiometric and atmospheric corrections, homogenization) of VHR satellite remotely sensed data and auxiliary data;
- design and management of the ground survey for acquisition of hyperspectral signatures related to the various types of materials characterizing the surface of the rubble piles of the historic center of Amatrice by means of ASD portable hyperspectral-radiometer. Acquisition and pre-processing of the spectral signatures and creation of a library related to the main types of materials identified on field. About 140 hyperspectral signatures were acquired mainly for the first five materials, whose spectral signatures differed significantly among the various piles and urban places. The most similar signatures were preprocessed (filtered and normalized in case of calibration faults), averaged and stored in a spectral library. To preserve the spectral variability of the first five materials for each of them four different averaged signatures were included, so as in total 23 signatures are registered in the library.
- analysis and development of SMA (Spectral Mixture Analysis) procedures based on the hyperspectral signatures of the materials present in the library and acquired on site.

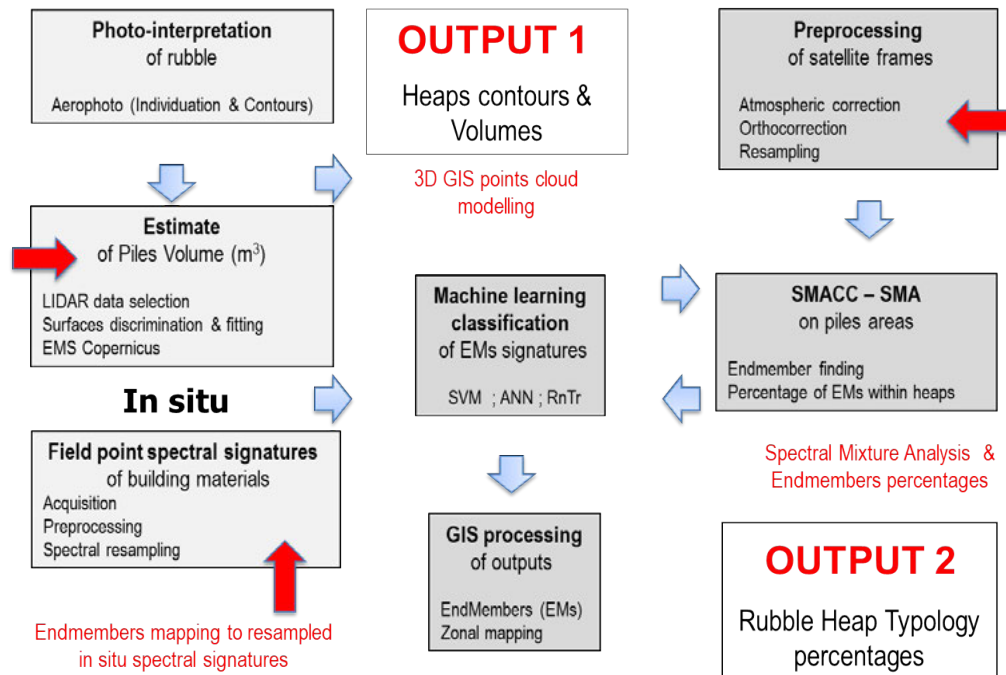


Figure 2. Flow diagram of the implemented procedure. Red arrows indicates main data input and blue arrows shows the used processing chain. The three input group data are: 1) LIDAR point cloud data, RGB aerophotos, Copernicus EMS building damaging grade map; 2) Sentinel-2 and WorldView-3 multispectral data; 3) In situ Hyperspectral signature library

The hyperspectral signatures collected using the ASD FieldSpec Pro hyperspectral radiometer, were resampled to make them compatible with the 8 channels of WV3 sensor. From the WV3 multispectral imagery a small number (9) of pure materials signatures, i.e. endmembers (EM), were derived through Sequential Maximum Angle Convex Cone (SMACC) algorithm from pixels of sample heaps used as reference for the main material classes of urban rubble. SMA was then carried out on the heaps of the entire test area using the above mentioned EMs. The SMA algorithms provide the percentage of these EMs for each pixel within the heaps surface according to soft classification approach.

- Subsequently, the percentages obtained in this way were recombined using the classification of the EMs to the 23 field materials of the library on the basis of their resampled spectral signatures. To this end, after a preliminary test of various machine learning algorithms (i.e. ANN-Artificial Neural Network, RnTr-Random Forest Tree, Knn-K-Nearest Neighbor) the SVM (Support Vector Machine) one allowed us to better discriminate the most representative categories of rubble heaps.
- Finally the characterization of rubble within the test area was obtained through GIS processing (zonal analysis and normalization) executed for each polygon of the heaps layer.

N	Material
1	rubble debris
2	cement
3	tiles
4	bricks
5	natural stones
6	zinc gutter
7	bitumen sheath
9	copper gutter

Table 1. Urban rubble materials typologies identified on field

As a result, the implemented methodology allowed us to suitably assess both the volume for each heap (range between 500 to 1,000 m<sup>3</sup>) and its relative percentages of rubble materials identified during the field survey.

## 2. Results

Nine different principal constituents of urban rubble have been identified on field during the two-days survey of the December 2016, as reported in table 1. In Fig. 3, different component of hyperspectral signatures collected on urban rubble are reported (upper figures). In order to profitably use the multispectral signals acquired by the WorldView-3 satellite system, these on-site hyperspectral signatures, relating to the 23 types of urban rubble were resampled to 8 spectral bands of the WV3 sensor, using the related filter functions available on the satellite owner firm site (lower figures).

Then the 23 resampled signatures of materials typologies were matched (classified) with those of EMs derived from the WV3 data within the rubble heaps using the BVM (Ball Vector Machine; a specific SVM machine learning algorithm; Tsang et al., 2007). Each of EMs was mapped to one of the 23 resampled



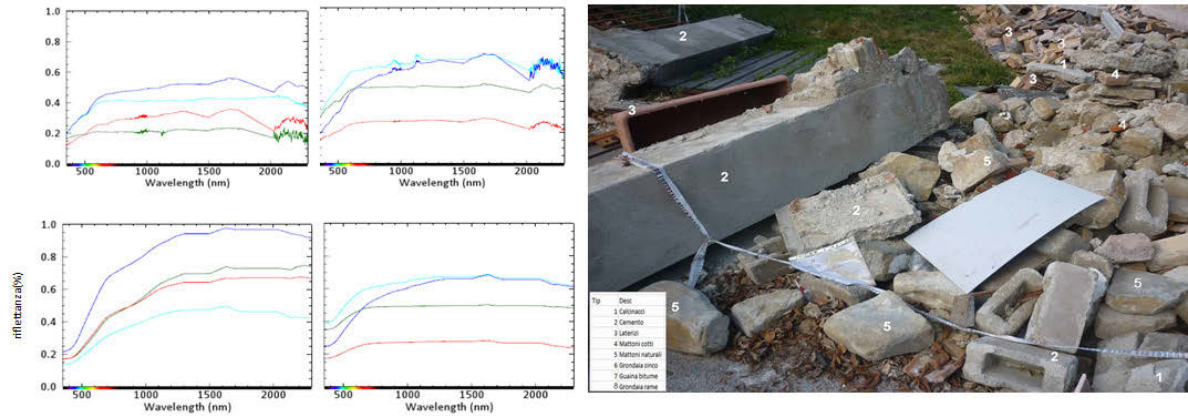


Figure 3. The graphs show the average spectral signatures of 9 types of rubble materials (white numbers of right image) for the 4 groups of measurements in Table 2 (site1-dd 6 in blue; site2-gg6 in green; site1-gg7 in red; site 3-dd7 in blue). The two upper graphs refer to the types of rubble (top left) and cement (top right) after the first pre-processing phase before smoothing by filtering. The two graphs below show the filtered spectral signatures and refer to the brick (left) and cement (right)

signatures corresponding to one of the 9 main typologies of urban rubble materials identified on field. The zonal processing of the raster map derived from the software classification implementing the per pixel distribution of EMs percentages (within the rubble heaps polygons) provided us with the attribute table including volume and typology values (table 2). The assessed distributions of materials typology percentages for the various heaps are shown in Fig.5. The most abundant rubble heap typology (macro class) identified is represented by concrete/debris (range: 40-50%), followed by brick/tiles (range: 25-30%) and local stones (range: 7-17%), with other materials (metal, plastic, roof-tiles, etc.) completing the list (range: 3-25 %). These results are in general agreement with the preliminary information derived from the rubble inventories made during the rubble removal activities (transportation to final disposal).

id_pile	volume (m <sup>3</sup> )	concrete and debris (%)	bricks and tiles(%)	natural stones(%)	others materials (%)
Ar641	2478.63	54	28	10	8
Ar642	1494.47	50	28	12	10
Ar643	3471.36	56	31	6	7
Ar644	4199.4	57	27	10	6
Ar645	1490.97	54	29	10	7
Ar646	2010.39	52	29	10	9
Ar647	865.79	53	30	8	9
Ar648	876.687	56	29	8	7
Ar649	5118.51	54	29	8	8
Ar6410	7140.05	56	30	7	7
Ar6411	1314.63	49	27	10	14
Ar6412	1228.15	55	30	8	7
Ar6413	4612.94	55	29	8	8
Ar6414	1221.36	57	31	7	5

Table 2. For each rubble pile (see Fig. 4) volume and typology of the identified main rubble materials

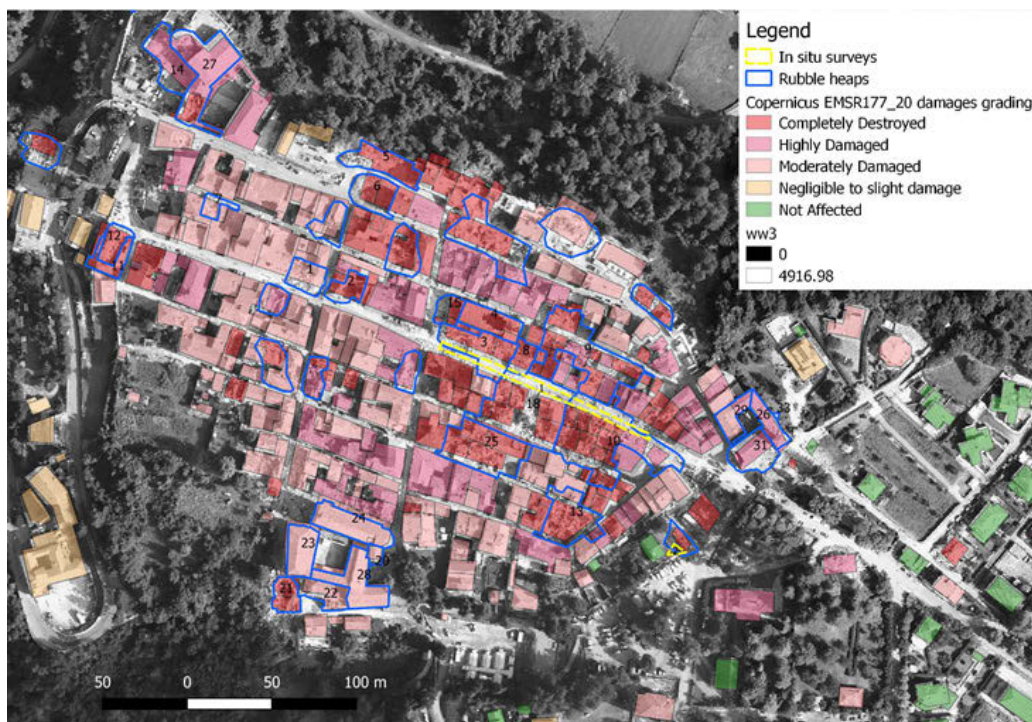


Figure 4. Distribution of rubble heaps and related volumes (Table2) derived from the orthophotos (background) and LIDAR data. The Copernicus EMS building damage grading of is displayed as background



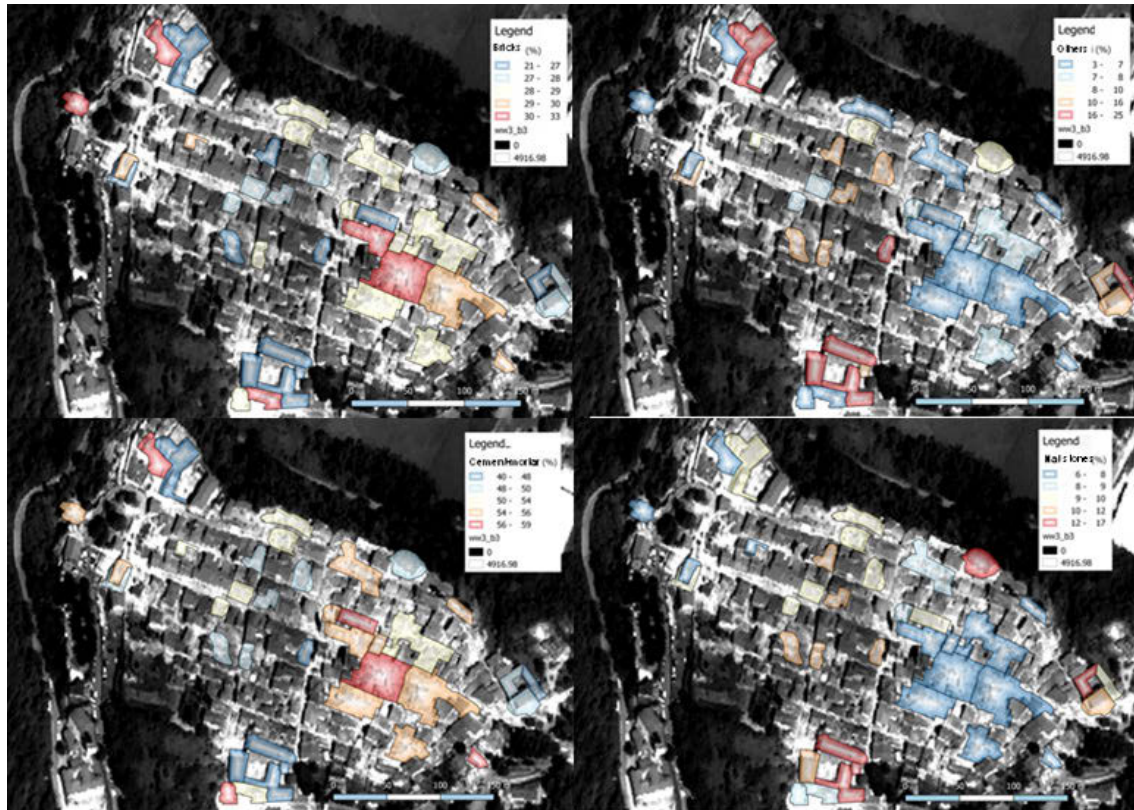


Figure 5. Estimated percentage distributions of the types of rubble heaps found in the center of Amatrice town. The four maps refer respectively to: cement-rubble (lower left), natural bricks (lower right), bricks (upper left) and other building materials (upper right).

## Discussion and Conclusion

In the context of post-event activities related to seismic emergencies, the management of the huge amount of resulting rubble and debris arising in urban areas is one of the major issues which can be suitably supported by EO based monitoring and mapping applications including the last generation of the multi/hyperspectral satellite HR/VHR sensors. The surveys from the aerial platform can provide detailed up to date information, but are extremely expensive for the continuous monitoring of the emergency areas required for controlling the evolution of the earthquake urban scenario.

Preliminary results obtained through the innovative methodology developed in this work, show the applicability of the WV3 satellite VHR data to provide effective surface estimates of the distribution of seismic rubble types in heaps distributed on urban areas. This information can be advantageously integrated with those of related volumes derived from aerial surveys carried out in the aftermath of the earthquake (Table 2; Fig. 4, 5), providing suitably support to management activities of the seismic urban rubble. The stereoscopic acquisition capabilities of VHR satellite sensors could support also the estimation of volumes in monitoring the evolution of the emergency scenario, possibly with a "one-off" calibration based on the LIDAR information deriving from an initial aerial survey.

The original EO based methodology developed here allowed us to produce realistic estimates of the types and volumes of seismic rubble in the historical center of Amatrice. It can be generalized with high degree of automation and can be easily applied to similar situations even with possible improvements deriving from the integration of the SAR (Synthetic Aperture Radar) and hyperspectral data provided by ongoing EO missions (Copernicus Sentinel 1, Cosmo SkyMed, PRISMA, EnMap). Future activities will include a greater exploitation of high-resolution and hyperspectral satellite data, for assessing both volumes and typologies of earthquake rubble heaps, also investigating the possibility to detect hazardous rubble materials (i.e. asbestos).

## Bibliography

- Baiocchi, V., Dominici, D., Mormile, M., 2013. UAV application in post-seismic environment. *Int. Arch. Photogramm. Remote Sens. Spatial Inf. Sci.*, XL-1 W 2, 21–25.
- Borfecchia, F., De Canio, G., De Cecco, L., Giocoli, A., Grauso, S., La Porta, L., Martini, S., Pollino, M., Roselli, I., Zini, A., 2016. Mapping the earthquake-induced landslide hazard around the main oil pipeline

- network of the Agri Valley (Basilicata, southern Italy) by means of two GIS-based modelling approaches. *Nat Hazards*, 81: 759.
- Cappucci, S., De Cecco, L., Gemerei, F., Giordano, L., Moretti, L., Peloso, A., Pollino, M., 2017. Earthquake's rubble heaps volume evaluation: Expeditious approach through earth observation and geomatics techniques. *Lecture Notes in Computer Science*, 10405: 261-277.
- Lund, H. F., 1993. Household Hazardous Wastes. *The McGraw-Hill Recycling Handbook*.
- Memon, M.A., 2015. Disaster waste recovery and utilization in developing countries-Learning from earthquakes in Nepal, 15th Asian Regional Conference on Soil Mechanics and Geotechnical Engineering, ARC 2015: New Innovations and Sustainability, 143-147.
- Ricci, P., Verderame, G.M., Manfredi, G., Pollino, M., Borfecchia, F., 2011. Multilevel approach to large scale seismic vulnerability assessment of reinforced concrete building. *Proceedings of the 14th conference of the Italian National Association of Earthquake Engineering*, 2011, Bari (IT).
- Talbot, B.G., Talbot, L.M., 2013. Fast-responder: Mobile access to remote sensing for disaster response. *Photogramm Eng. Remote Sensing*, Vol. 79, 10, 945-954.
- Tsang, W., Kocsor, A., Kwok, J.T., 2007. Simpler core vector machines with enclosing balls. In *Proceedings of the 24th International Conference on Machine Learning*, 911-918.
- United States Environmental Protection Agency, 1993. *Household Hazardous Waste Management: A Manual for One-Day Community Collection Programs*. EPA530-R-92-026. Washington, D.C. August.
- Ricci, P., Verderame, G. M., Manfredi, G., Pollino, M., Borfecchia, F., De Cecco, L., Martini, S., Pascale, C., Ristore, E., James, V., 2011. Seismic Vulnerability Assessment Using Field Survey and Remote Sensing Techniques. In: B. Murgante et al. *Computational Science and Its Applications - ICCSA 2011*, Santander, Spain, June 20-23, 2011. Berlin-Heidelberg: Springer Verlag. *Proceedings*, II-2, 376-391.

## **Rheticus® Network Alert supporting critical infrastructures: a case study for ACEA - utility operator - within SCIRES project**

Angelo Amodio<sup>1</sup>, Giuseppe Forenza<sup>1</sup>, Daniela Drimaco<sup>1</sup>, Vincenzo Massimi<sup>1</sup>, Francesca Albanese<sup>1</sup>, Christian Bignami<sup>2</sup>, Matteo Albano<sup>2</sup>, Maurizio Pollino<sup>3</sup>, Vincenzo Rosato<sup>3</sup>, Cristiano Cialone<sup>4</sup>

<sup>1</sup> Planetek Italia s.r.l., Via Massaua 12, I-70132 Bari, Italy, e-mail: info@planetek.it

<sup>2</sup> INGV, Via di Vigna Murata, 605, 00143 Roma, Italy

<sup>3</sup> ENEA, Via Anguillarese, 301 - 00123 Roma, Italy

<sup>4</sup> ESA-ECSAT, Fermi Avenue Fermi Ave, Harwell Campus, Didcot OX11 0FD, United Kingdom

Corresponding author: (albanese@planetek.it)

Keywords: Rheticus® Network Alert, infrastructures, Sentinel-1

### **Abstract**

In 2018 ESA Business Application issued an invitation to tender for the design of innovative EO-based services, aiming at improving the resilience of critical infrastructures.

Planetek Italia as prime contractor, ENEA and INGV, proposed a vertical application devoted to the integrated water cycle management support.

The integrated water cycle management relies on different infrastructures: water basin and impoundment, transport and distribution pipelines, wastewater collection, and as interconnected infrastructures, power distribution networks on which the infrastructures rely on for energy supply and power plants that exploits the path of the water to produce energy.

### **1. Overview**

SCIRES aims at developing a vertical application for the integrated water cycle. The application is based on the pipeline monitoring and the impoundment stability that is performed integrating different monitoring data acquired both by satellites technologies (Radar and Optical) and ground sensors with different risk models.

- Pipeline monitoring by using multi-temporal interferometry on S-1 data through the Rheticus® platform, IoT (in-situ sensors) and AI techniques

The service aims at identifying precursor phenomena related to the breaking of pipeline, using Artificial Intelligence methods, that can be responsible for the losses of water, and subsequent water infiltration in the ground and potentially causing damages to the surrounding infrastructures.

- Impoundment Stability

The service is focused on the monitoring by means of mean ground velocity and time series of deformation computed by Rheticus® platform, integrated with in situ geological and geomorphological data. The objective is to provide a comprehensive analysis of surface and near sub-surface deformations and dislocations that affect hydraulic works, such as water impoundments and distribution networks that could be damaged by hazardous events.

Within the project, the services are further integrated within the CIPCast Decision Support System developed by ENEA.

### **2. Planetek Rheticus® Network Alert**

The Sentinel open data together with the power of cloud infrastructures provide players in the EO sector with the unprecedented opportunity to design operational Earth monitoring services. Shifting from the provision of data to the provision of continuous monitoring services (i.e., continuous access to information) is the key point upon which addressing real users' needs in the new Era of Big Data. Moreover, shifting from monitoring services on request to long time information services available under subscription is the real disruptive innovation in the field of EO: end-users pay for the information not for the data. At the forefront of this new innovative model there is Rheticus, a cloud-based hub that processes satellite imagery and geospatial data automatically and delivers geo-information services ready-to-use by end-users. Designed and developed by Planetek Italia, Rheticus moves beyond mapping visualisation, thanks to a broad range of advanced geo-analytics.



The Pipeline monitoring service is based on Rheticus® Network Alert, which is part of the Rheticus® suite of services.

Rheticus® Network Alert is a turnkey web service that helps utility companies in the management of inspections and maintenance activities over their integrated water and sewerage networks. By using satellite radar data to identify ground instabilities, Rheticus Network Alert provides operators with an always updated log of hot spots within their network that can reveal leaking or damaged pipes. Thus, network's operators can act on the information they have. The service provides all the information by means of geoanalytics, maps and reports, released on a monthly basis. Instead of replacing pipes and connectors after major leakage evidence or pipeline collapse, Rheticus® Network Alert allows an 'a priori' approach, supporting and optimizing the field inspection management allowing the identification of those pipes classified as possibly at risk enabling the preventive maintenance before larger problems occur. As a matter of fact, companies better manage their financial resources and reduce service disruptions and/or threats for people.

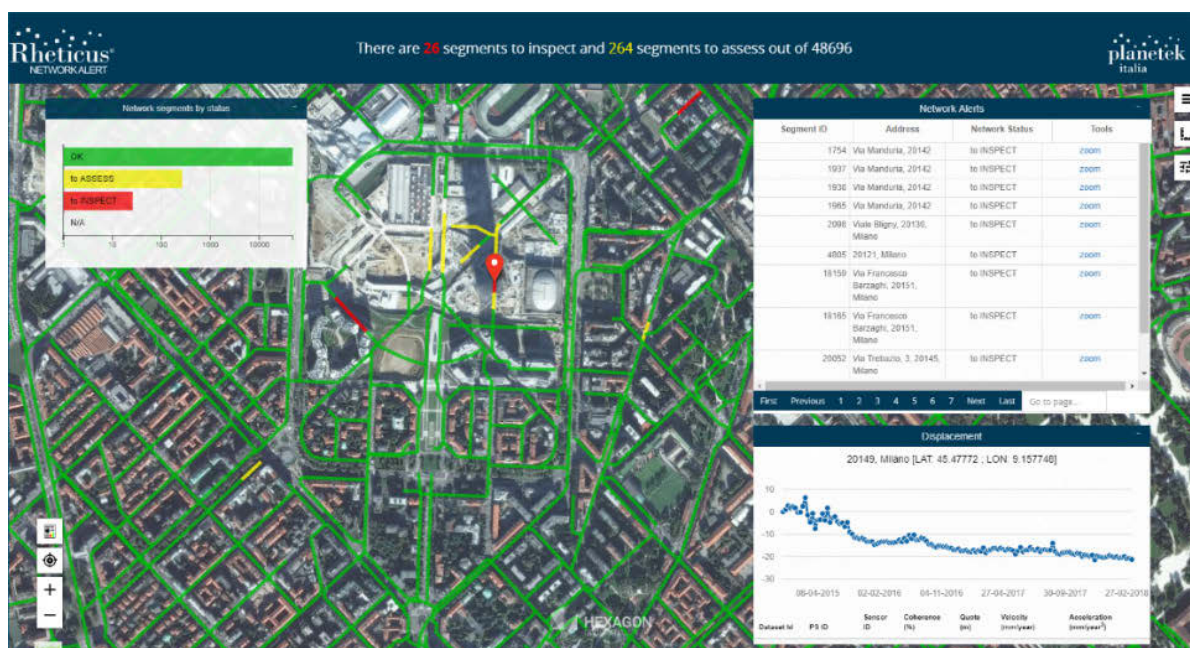


Figura 1. Rheticus® Network Alert User Interface

Key benefits are:

Continuous monitoring of the entire network: support for the management, maintenance and restoration of underground pipeline networks thanks to up-to-date satellite radar data that feeds the BI analysis functions.

- Prevention of possible losses and structural damage: survey of ground surface movements caused by natural subsidence, structural defects and / or pipeline leaks that could affect areas around the network.
- Innovative analysis of networks to optimize investments: thanks to precise and increasing levels of potential damage on each pipeline in the network, maintenance activities and management of inspection priorities are simplified.
- No experience required with GIS systems or satellite data: the results of the complex automatic processing chain are provided to the user through a simple and dynamic interface, allowing them to easily perform analyzes on the network status and obtain precise information on the surface movements that the interest.

### 3. ACEA Case study

#### a) Pipelines monitoring (based on Rheticus® Network Alert)

Within this project, the aim related to the pipeline monitoring is of improving the performance of the existing service, developing a vulnerability model that allows of highlighting the pipelines that needs to be inspected with different level of priority.

Rheticus® Network Alert indicates locations of concern and lets operators to act upon the information, simplify maintenance activities and prioritize inspection.

Thus, the service allows an "a priori" approach, helping to highlight problems before they become critical. As a result, operators better manage their financial resources and reduce service disruptions and/or threats for people.

The typical end-user of the Rheticus® Network alert are the water and sewer maintenance divisions and in

this project ACEA, as current customer of the service, is directly involved. The end-user uses the Rheticus® Network Alert service to select all the pipelines that need to be inspected by the maintenance operators. Once selected all the pipelines that need to be inspected, a verification report that contains all the information that are useful to the field operators is emitted for each pipeline segment.

Rheticus® Network Alert provides updated levels of concern on each segment of an underground pipeline network (water and sewage, including energy supply, oil&gas), based on measurements of displacement of the network itself as well as of the nearby areas. Once the client performs the subscription to the service and provides the extent of the Area of Interest (AoI) together with a georeferenced vector file of the pipeline network (Esri shapefile, KML, DWG/DXF), the service is activated over the customer's AoI.

At service activation, the client gains access to the web platform throughout the subscription duration. The service is available at <https://services.rheticus.eu> with the credentials provided at activation. Standard subscription includes a 12-month historical analysis of surface displacement over the AoI, starting from the subscription date and running backward in time. Once the client logs into the web platform and launches the web application, the pipeline network together with relevant analytics are loaded within a Business Intelligence (BI) dashboard.

Each segment of the network is classified accordingly to the measurements of displacement of the segment itself as well as of the nearby areas measured through satellite radar data.

The status of each segment of the network is represented with three classes/colours that correspond to increasing levels of concern:

- stable segments in green,
- segments to assess in yellow,
- segments to inspect in red.

Clicking on each segment, a pop-up window shows the time-line analysis of displacement related to the selected segment as well as a summary table of all provided parameters, i.e. Sensor ID, Velocity (mm/year), Acceleration (mm/year<sup>2</sup>), Normalised Coherence (%), and Altitude (m).

An overview of the status of the entire network is available on the header of the web interface, as well as on the left-side dynamic bar chart. A detailed report is available on the right-side table of the web interface, providing users with the following information: Segment ID, Address, Network Status, Zoom-to-Feature tool, sorted by Network Status. A right-side menu gives access to the map of PS over the AoI, together with filtering sliders for velocity, acceleration and normalised coherence. Displacement is represented in 3 classes: stable PS in green, PS moving downward along the satellite's LoS in red, and PS moving upward along the satellite's LoS in blue.



Figure 2. Overview of the state of the pipeline network

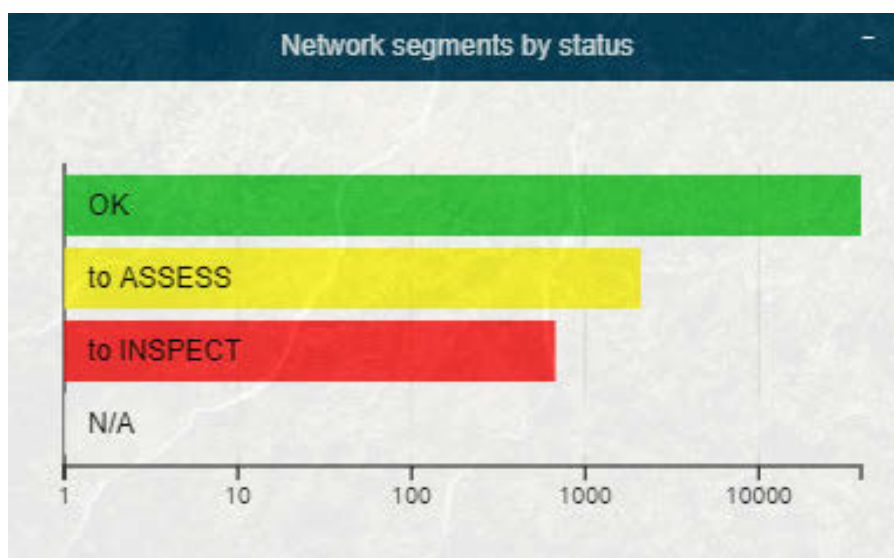


Figure 3. Segments by status

Network Alerts			
Segment ID	Address	Network Status	Tools
67	Via Giuseppe Impastato, 21, 40013	to INSPECT	<a href="#">zoom</a>
68	Via Giuseppe Impastato, 1, 40013	to INSPECT	<a href="#">zoom</a>
71	Via Giuseppe Impastato, 35, 40013	to INSPECT	<a href="#">zoom</a>
73	Via Giuseppe Impastato, 28, 40013	to INSPECT	<a href="#">zoom</a>
75	Via Giuseppe Impastato, 48-50, 40013	to INSPECT	<a href="#">zoom</a>
76	Via Giuseppe Impastato, 28, 40013	to INSPECT	<a href="#">zoom</a>

First Previous 1 2 3 4 5 6 7 Next Last Go to page...

Figure 4. Detailed report on the pipeline network

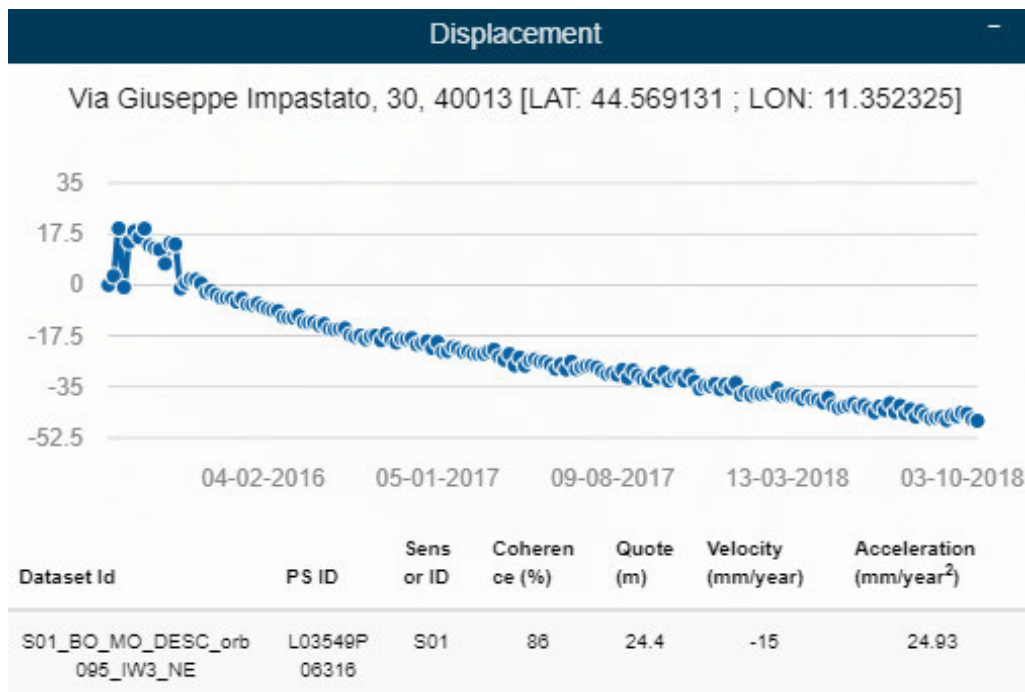


Figure 5. Displacement time series of a pipeline segment computed through multi-temporal Interferometry using the Rheticus® platform

In order to evaluate the performance of the service, it is possible to consider the level of damages on the water and sewer pipelines identified through the field inspection by the water and sewer maintenance operators. The integrated water cycle operators, generally consider the following 5+1 classes of damage level:

- 0: Pipeline in optimal condition
- 1: Pipeline in acceptable condition
- 2: Damaged pipeline
- 3: Pipeline in Bad condition
- 4: Pipeline in really bad condition
- 5: Pipeline with important structural damages

Using Rheticus® Network Alert service, the water and sewer operators improved the monitoring performance with respect to the previous point-based analysis (PSI results) that was performed using the Rheticus® Displacement service, a cloud-based service developed by Planetek Italia that implement the Multi-Temporal Interferometry technique to monitor the stability of the ground and infrastructures. In particular with the Rheticus® Displacement service the water and sewer operators were able to find an average damage class



on their pipelines infrastructures of 1.16 while, thanks to the vertical service Rheticus® Network Alert, the operators currently are able to detect an average damage class of 2.37.

The aim of this project is to further improve the performance of the service, integrating ancillary data within of the AI Rheticus® Network Alert algorithm. With this project we propose both the improvement in the identification of interesting points (PS) characterized by particular displacement trend over time and the interpretation of the ground displacement phenomena through the definition of different clusters of Persistent Scatterers (PS) instead of using the single point-based displacement analysis. These approaches will be accomplished through the AI methods.

During the feasibility analysis some of the most important Artificial Intelligence (AI) methods to study surface deformation using Persistent Scatterers Interferometry (PSI) have been analyzed. Furthermore, techniques to extract useful information coming from PSI and how the analysis of more points (cluster of PSI) can improve standard methodologies of the ground displacement analysis, will be described.

ACEA, as current customer of the Rheticus® Network Alert is continuously proving feedbacks about the service performance and the needed improvement. Thanks to the continuous interaction, the improvements of the service that have demonstrated with this feasibility study and that will be implemented during the demonstration phase have been validated by ACEA that already demonstrated a high-level interest in their implementation on the current service.

## **b. CIPCast DSS**

A new concept of DSS should account for and support all phases of the risk analysis process: event forecast (when applicable/predictable), prediction of reliable and accurate damage scenarios, estimate of the impact that expected damages could have on CI service (in terms of reduction or loss of the service), estimate of the possible consequences. The DSS should also support the identification and definition of preparedness and emergency strategies that, taking into account the different phases of the expected crisis (event, damage, impact and consequence) could be adopted to reduce the impact, speed-up mitigation and healing procedures, ease the recovery phase, thus reducing as much as possible the extent, the severity and the duration of the crisis.

A DSS with such capabilities can also be used as effective simulation tools to perform comprehensive stress tests. This activity would produce educated contingency plans based on the analysis of (synthetic) crisis scenarios instead of being built upon (a few, when available) records of historical events. This will enhance their quality and adapt them to the effective current scenario conditions (in terms of critical assets, available technical tools, etc.).

Thus, CIPCast DSS was conceived as a combination of free/open source software (FOSS) environments including GIS features (GFOSS), which play a major role in the construction of such a tool. In the last few years, the geo-scientific community has been focusing on the use of GIS technologies and techniques for supporting risk assessment and emergency management tasks in case of natural hazardous events. Multisource data and GIS-integrated analysis can contribute to a better planning, providing fundamental information for immediate response. CIPCast DSS is capable to provide a user-friendly geographical user interface (GUI), by means of a specific WebGIS application, for querying and analysing geographic data and thematic maps, produce and evaluate scenarios, etc. The creation of this information consultation tool, enriched by the geospatial component, implies the adoption of specific and suitable GIS and SDI (Spatial Data Infrastructures) architectures that have been developed using GFOSS packages.

SCIRES seeks to extend and enhance the current CIPCast functionalities.

CIPCast produces, on the basis of knowledge of the geographic location of CI elements in a given territory, an expected "damage scenario" by assessing for each element of CI their possible degree of damage depending on the type of event expected (and its intensity), taking into account the "specific vulnerabilities" (i.e. different types of hazard) of each individual infrastructure element (pipes, substation, water pump, etc.). CIPCast, in addition, based on the "scenario of damage", elaborates the "impact scenario", that is, the impact that the expected damage(s) will cause on the affected infrastructure and, in perspective/if needed, on other infrastructures functionally linked to the one directly affected by the event (through the so-called "domino effect"). Based on the "impact scenario" on services, CIPCast produces an estimate of the consequences in terms of service degradation and in terms of impact on citizens, territory and production activities.

Shows the main functional blocks of CIPCast and the relevant components i.e. the GeoDatabase and the Graphic User Interface (WebGIS). CIPCast block gets external data from many different sources (e.g. meteo/hydrological models), to establish the current external conditions. CIPCast estimates the expected manifestation strength for predictable events and, then, elaborates a "damage scenario", correlating the strength of the expected hazard manifestations with the vulnerability of the different CI elements in the

affected areas, in order to estimate the probability that the manifestation could effectively damage (and, in the positive case, to what extent) the CI elements. This, the DSS converts the damages expected for the CI elements into outages of the service. A final step is devoted to inform and support the response, by allowing testing and comparing different strategies for restoring the service by prioritising repairs and deploying physical and human resources.

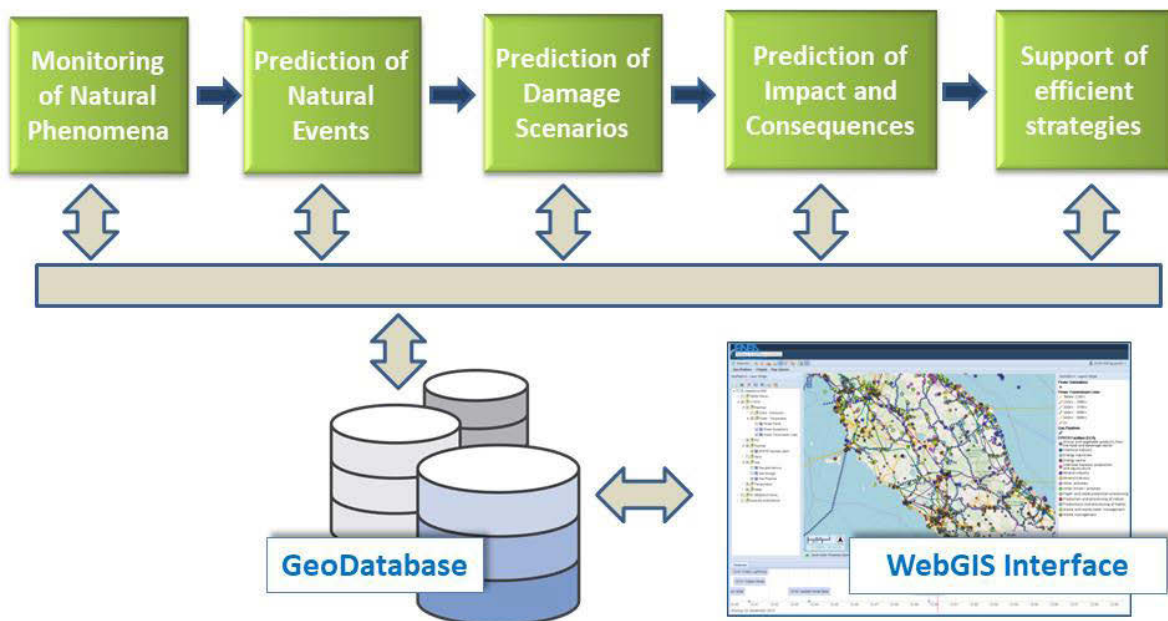


Figure 6: CIPCast workflow

Taking into account the above described features, CIPCast can be used as an operational tool (real-time, risk forecaster, when a disturbance risk may occur based upon weather forecast and live field sensor data). Moreover, the DSS can be exploited as a stress tester enabling to cause synthetic natural events and assessing the resulting chain of events (damages, impacts and consequences).

To summarise, CIPCast can:

- provide CI operators with a large information database;
- predict external threats from natural hazards by using prediction models;
- integrate data coming from available field sensors and EO-based services;
- estimate the expected damages on CI elements, caused by an expected natural event;
- support Operators for actions related to the maintenance and/or recovery (in case of outages) of their infrastructure.

## Conclusions

The SCIRES project, integrating innovative monitoring techniques, AI algorithms and risk models will support the management of the critical infrastructures like the integrated water cycle through the continuous monitoring of the stability water basins, pipeline networks, and the impoundment stability. The aim of the project will be accomplished thanks to the top-down approach that is implemented in the SCIRES platform allowing the multi-scale monitoring of critical infrastructures. The Rheticus® Network Alert service and the CIPCast DSS will simplify the operational application of the system for the management of the critical infrastructures.

## Acknowledgments

Rheticus® is a registered trademark of Planetek Italia srl.

SCIRES project received funds from the AO9305 Open Call for Proposal for IAP – ESA Business Applications.

## References

1. Bovenga, F., Refice, A., Nutricanto, R., Guerriero, L. and Chiaradia, M. T., "SPINUA: A flexible processing chain for ERS/ENVISAT long term interferometry", Proceedings of 2004 ESA-ENVISAT Symposium 1, 1-6 (2004)
2. Bovenga, F., Nutricato, R., Refice, A. and Wasowski, J., "Application of Multi-temporal Differential Interferometry to Slope Instability Detection in Urban/Peri-urban Areas," Engineering Geology 88, 218-

- 239 (2006).
3. S. Samarelli, A. P. Lorusso, L. Agrimano, R. Nutricato, F. Bovenga, D. O. Nitti, M. T. Chiaradia, "Rheticus: an automatic cloud-based geo-information service platform for territorial monitoring", Proceedings of SPIE 10003, SAR Image Analysis, Modeling, and Techniques XVI, 100030M, 7 pages; DOI: 10.1117/12.2241285 (2016)
  4. V. Massimi, G. Forenza, A. Alisiconi, Monitoring the health of water and sewerage networks, NEREUS/ESA/EC The Ever Growing use of Copernicus across Europe's Regions, pages 246-247, November 2018.
  5. V. Massimi, ,Rheticus: Satellite-based Information Services for Utilities, Geomedia, may-june 2018
  6. S. Samarelli, V. Massimi, L. Agrimano, D. Drimaco, R. Nutricato, D. O. Nitti, M. T. Chiaradia. "Rheticus: a cloud-based Geo-Information Service for the Detection and Monitoring of Geohazards and Infrastructural Instabilities", M. T. Chiaradia, S. Samarelli, V. Massimi, R. Nutricato, D. O. Nitti, A. Morea and K. Tijani, AGU Fall Meeting 2017, New Orleans, Louisiana, 11-15 December 2017
  7. V. Massimi, Satellite information-as-a-service, GeoConnexion, November 2017
  8. S. Samarelli, V. Massimi, L. Agrimano, D. Drimaco, R. Nutricato, D. O. Nitti, M. T. Chiaradia "Rheticus®: a cloud-based Geo-Information Service for ground instabilities detection and monitoring based on fusion of Earth observation and INSPIRE data», , In: P. Soille and P.G. Marchetti (Eds.), Proceedings of the 2017 conference on Big Data from Space. BIDS' 2017, EUR 28783 EN, Publications Office of the European Union, Luxembourg, 2017, ISBN 978-92-79-73527-1, ISSN 1831-9424, doi:10.2760/383579, JRC108361



## The Hyperspectral PRISMA Mission and its first results

Rosa Loizzo, Rocchina Guarini, Maria Girolamo Daraio, Ettore Lopinto

*Agenzia Spaziale Italiana*

Corresponding authors: [ettore.lopinto@asi.it](mailto:ettore.lopinto@asi.it); [rocchina.guarini@est.asi.it](mailto:rocchina.guarini@est.asi.it); [MariaGirolamo.Daraio@asi.it](mailto:MariaGirolamo.Daraio@asi.it)

Keywords: PRISMA, Hyperspectral Data, Earth Observation, CAL/VAL, Products, Data Policy

### Abstract

Since March the 22<sup>nd</sup> 2019 the PRekursore IperSpettrale della Missione Applicativa (PRISMA) is in orbit on a sun-synchronous orbit at 615 km for a five years operational lifetime. The PRISMA mission, fully funded by the Italian Space Agency, is based on a technology demonstrator project, aimed at the in space qualification of an innovative hyperspectral payload and at the development of new Earth Observation products and applications.

In the upcoming Earth Observation European scenario PRISMA is expected to be a good opportunity for science and users community to access hyperspectral data, both to develop new application products and to explore technological innovative contribution of hyperspectral data to earth observation, in the perspective of a future hyperspectral operational mission.

PRISMA will provide images acquired by an innovative electro-optical instrument using an Imaging Spectrometer, able to acquire in contiguous spectral bands ranging from 400 to 2500 nm, optically integrated with a medium resolution Panchromatic Camera (PAN). The PRISMA payload uses pushbroom scanning technique to collect PAN/HYP image strips up to 1800 km in length and along sub-satellite track. Several additional data (e.g. calibration data, etc.), as necessary, is also provided for the on ground processing. The Users can access the PRISMA system via web, either to submit new image acquisition requests and/or to access the catalogue browser, to search for images already acquired and to require products from archived data.

This paper will report the status of the PRISMA mission and will present the commissioning phase and preliminary mission exploitation plan.

### 1. Introduction

PRISMA is an innovative Earth Observation mission fully funded by Italian Space Agency (ASI), based on an innovative electro-optical instrument, combining a hyperspectral sensor with a medium-resolution panchromatic camera. PRISMA was launched on 22 March 2019 on board the VEGA rocket.

PRISMA is potentially of great interest, both for scientific community and for end users because it could provide an innovative contribution to Earth Observation, thanks to the capability to acquire worldwide lot of data with a very high spectral resolution and in a wide range of frequencies. The combined hyperspectral and panchromatic products give the capability of recognition of the geometric characteristics of a scene and may provide detailed information about the chemical composition of materials and objects on the Earth surface, giving enormous impacts to remote sensing applications.

The combined use of HYP and PAN is expected to give an innovative contribution mainly in the field of:

- forest analysis (e.g., forest disturbance, forest fires, forest classification, biomass analysis);
- precision agriculture (e.g., crop mapping, crop rotation, crop stress analysis, fertilization);
- inland and coastal waters (e.g., Water quality, chlorophyll monitoring, alga bloom);
- climate change and environmental research (e.g., desertification, deforestation, vegetation stress, environmental degradation and hazards);
- raw material exploration and mining;
- soil degradation and soil properties.

This paper will report the main PRISMA mission characteristics and performances after the launch, preliminary commissioning activities and early mission exploitation plan.

### 2. PRISMA Architecture

The PRISMA system includes Ground and Space facilities able to perform all the functions requested to provide image acquisition planning on targets of interest, data acquisition and downloading to ground station, processing and products delivering to the end user [1].

In the following figure (Figure 1) the mission architecture is presented:

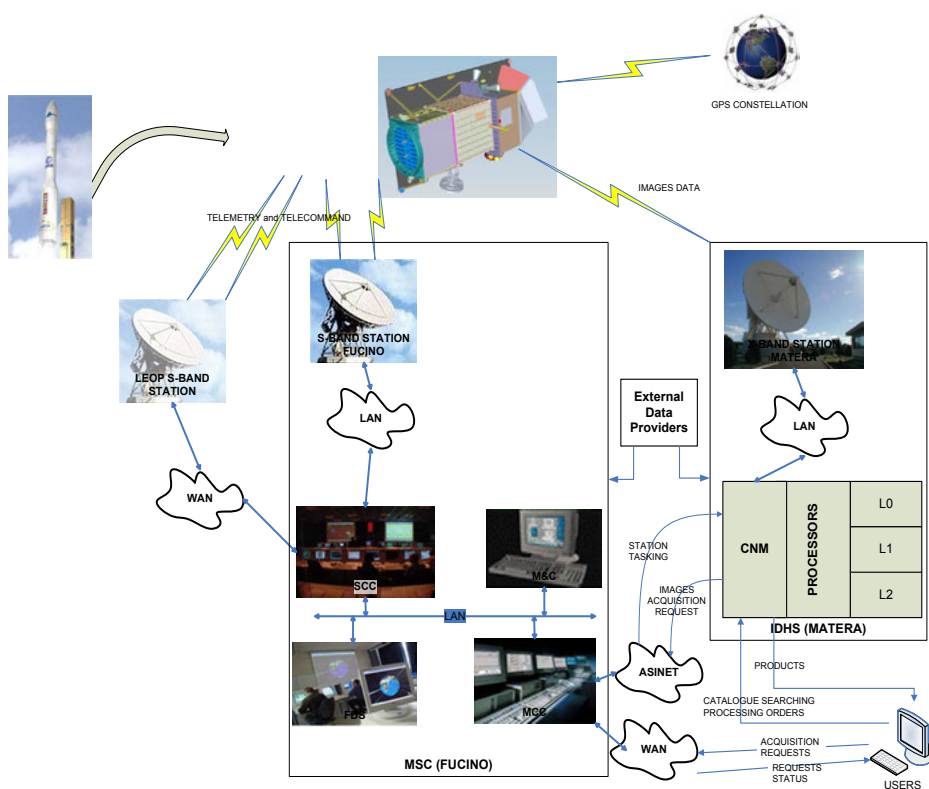


Figure 1. PRISMA Mission Architecture

## 2.1 Area of Interest

PRISMA provides the capability to acquire, downlink and archive images of all Hyperspectral/Panchromatic channels totaling 200,000 km<sup>2</sup> daily over the Primary Area of Interest (Figure 2).

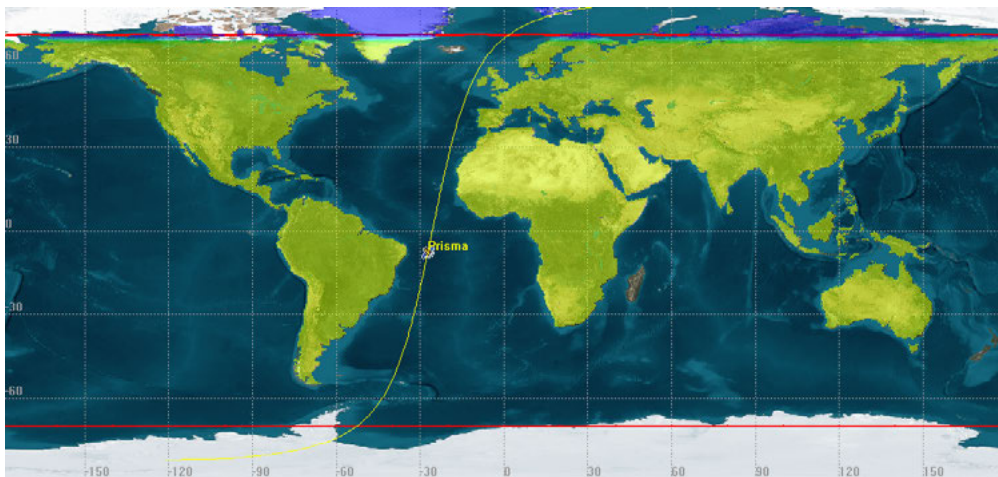


Figure 2. Area of Interest

The Area of Interest is defined as:

- Longitude: in the range 180°W - 180°E
- Latitude: in the range 70°S - 70°N

## 2.2. Commissioning phase

The commissioning phase will allow the in-flight verification and calibration of the payload and the full validation of the System (Space Segment, Ground Segment and ILS&OPS Segment) before releasing the products to the user community. During both the commissioning and the operational phase, a series of imaging campaigns designed to assess the PRISMA performance and to generate image products is envisaged.

<i>Thematic areas</i>	<i>Site</i>
<i>Coastal Water</i>	<i>Lampedusa, Venezia</i>
<i>Snow</i>	<i>Torngnon, Plateau Rosa</i>
<i>Inland water</i>	<i>Lago Trasimeno, Lago di Garda</i>
<i>Agricultural areas</i>	<i>Grosseto, Basilicata, Tavoliere delle Puglie, Ferrara</i>
<i>Forests</i>	<i>Lavarone</i>



Table 1. Italian test sites

After the end of the commissioning phase, actually expected to end in late July 2019, it is foreseen a structured three years CAL/VAL activity, which will be performed on instrumented sites distributed in Italy in support to:

- the performance characterization of the instrument;
- the verification and maintenance of mission performance over time;
- the effective use of data.

A systematic validation process is foreseen both during the commissioning phase and during the operational phase. The Validation involves the assessment of the accuracy of data and products, over the relevant spatial, temporal and spectral domains. The overall approach for validation is based on an extensive use of ground-based data, including airborne surveys with VNIR-SWIR scanner possibly coupled with thermal LWIR multispectral data and field activities contemporary to the PRISMA acquisitions. The test sites have been selected according to the peculiar thematic areas of interest for the mission (Table 1).

International test site are still under agreement.

### 3. Space Segment

The PRISMA space segment consists in a single small class spacecraft. The PRISMA payload is a hyperspectral/panchromatic camera with VNIR (Visible and Near-InfraRed) and SWIR (ShortWave InfraRed) detectors.

The expected performance and characteristics for the mission are reported in the following table (Table 2):

<b>Orbit</b>	SSO 615 km 10:30 LTDN
<b>Lifetime</b>	5 ys
<b>Revisit time</b>	4.8 days (roll max 20.7 and descending orbit)
<b>Onboard Data Storage</b>	448 Gbit
<b>Downlink data rate</b>	310 Mbps
<b>Imaging capacity</b>	200.000 km <sup>2</sup> /day Pushbroom, strip = 1800km
<b>Pointing accuracy</b>	0.5 km
<b>Response time</b>	= 10.8 days Overall latency < 9.5 days
<b>Target access opportunities over the P-AoI</b>	duration/day: 234 minutes (average, off nadir pointing) over full daily orbit
<b>Repeat cycle</b>	29 days (430 orbits)
<b>Geolocation accuracy</b>	0.2 km
<b>Spectral calibration accuracy</b>	± 0.1 nm
<b>Spectro-Radiometric Accuracy</b>	5% with Radiometric Quantization 12 bit
<b>SNR Requirements</b>	VNIR: > 160:1 (>450:1 at 650nm)
	SWIR: > 100:1 (>360:1 at 1550nm)
	PAN: > 240:1

Table 2. PRISMA main characteristics



It consists of an Imaging Spectrometer, able to acquire in a continuum of spectral bands ranging from 400 to 2500 nm, and a medium resolution Panchromatic Camera (PAN) [2].

The PRISMA Hyperspectral sensor utilizes the prism to obtain the dispersion of incoming radiation on a 2-D matrix detectors in order to acquire several spectral bands of the same ground strip. The “instantaneous” spectral and spatial dimensions (across track) of the spectral cube are given directly by the 2-D detectors, while the “temporal” dimension (along track) is given by the satellite motion (pushbroom scanning concept). The PDHT will store the acquired data in its internal memory and download it to the ground station in Matera via a dedicated X-band link.

#### 4. Ground Segment

The PRISMA GS consists of the following main elements:

- MCC – Mission Control Center;
- SCC – Satellite Control Center;
- IDHS - Image Data Handling Segment/Center.

The MCC consists of a unique subsystem, the Mission Planning System (MPS). It is the G/S element responsible for the scheduling of on board operations and for coordinating ground activities, performing overall mission planning, allocating resources and solving conflicts.

The SCC includes the Satellite Control System (SCS), the Flight Dynamics System (FDS), the S-band TT&C Station (TT&C) and the G/S Network (Communication infrastructure connecting the PRISMA G/S centers and facilities).

The IDHS is in charge of performing all the chain from the Users requests management to the delivery of final products, including reception of images data from the satellite and their processing. It includes different elements:

- Centro Nazionale Multimissione (CNM);
- L0 Processor;
- L1 Processor;
- L2 Processor;
- Calibration facility;
- GCP DB.

The CNM provides all ground segment functions related to catalogue browsing, image ordering from catalogue, standard products processing and product delivery. It includes the X-band ground station used to receive the payload data downloaded by the PRISMA satellite.

The user will access the PRISMA services via web through a unique access point named CNM Access System (CAS) permitting a Single Sign-On (SSO) authentication and then the access to the User Interaction Subsystem (UIS). The UIS provides end users with web-based interfaces for user management, accessing services relevant to catalogue browsing and query, products ordering, processing requests and help desk.

##### 4.1 PRISMA Products

The Ground Segment data processing provides at Sensor Radiance (Level 1 products) or at Surface Reflectance obtained by applying atmospheric correction (L2b product) and geolocation (L2c/2d products). Users can order new acquisition or catalogue products [3] of the TOA (Top Of Atmosphere) radiometrically and geometrically calibrated HYP and PAN radiance images and/or the Geolocated and Geocoded Atmospherically corrected HYP and PAN reflectance images.

In detail the deliverable standard products are:

- Level 0 (HYP/PAN) - formatted data product with appended metadata, including ancillary data and file formatting information (Archived data);
- Level 1 (HYP/PAN) - radiometrically corrected and calibrated radiance data in physical units. This product provides: Top-of-Atmosphere Spectral Radiance; Cloud mask; Sun-glint Mask; Calibration and characterization data used and Classification Mask;
- Level 2b - Geolocated at Ground Spectral Radiance Product (HYP/PAN);
- Level 2c - Geolocated At-surface Reflectance Product (HYP/PAN). This product includes Aerosol Characterization Product (VNIR), Water Vapour Map Product (HYP) and Cloud Characterization;
- Level 2d - Geocoded version of the level 2c products (HYP PAN).

#### 5. Mission Exploitation

PRISMA is a scientific and demonstrative mission, it will play a significant role in the upcoming international scenario of Earth Observation thanks to the development of New Data Processing (methods & techniques enabling new applications or services), New Products (e.g. Data Fusion), Pre-operational downstream services,

Exploitation Platforms. Access to mission data is regulated by the PRISMA mission data policy document [4].

### 5.1 Data Access

The access to PRISMA products will be controlled and based on user registration, and a license to use shall be signed, it will contain the terms and conditions of the service. User will be allowed to require new acquisition and/or products from catalogue based on archived data. The access to new acquisition request and products will be subject to limits of quota and priority. Products of level 0 will be accessible only to users belonging to ASI, in order to preserve the industrial know-how underlying the development of the mission. Product of higher level (L1 and L2) will be accessible to all users. Currently it is not considered access to new acquisition request for commercial users.

### 5.2 Data Policy

The PRISMA Data Policy document establishes technical and legal principles to regulate access to mission products, in accordance with foreign policy and domestic security. It is based on the following guidelines:

To allow a wide use of products in order to validate the technology, maximize the return on investment and support the development of skills in an innovative sector.

To promote the development of domestic competences, in view of future opportunities at European and international level.

Promote scientific use and experimentation of innovative application services.

To allow the development of commercial demonstration services, on the basis of archive data (as actually foreseen) and in accordance with the characteristics of the mission.

The data policy document also provides the categorization of users and possible uses of products. Every PRISMA mission user can assigned to one of the followings categories:

- A. ASI as system owner and entity carrying out the maintenance of system in operating conditions and the safeguarding of national security;
- B. Domestic Istituzional User (Universities, Research centres, Local authorities, Agencies, etc.);
- C. Foreign Istituzional User (Universities, Research centres, Int. authorities, Agencies, etc.);
- D. Generic users.

Possible uses of products will be:

Scientific Use: research and study activities;

Institutional Use: innovative, public utility and non-profit applications;

Commercial Use: projects with commercial purposes, currently based exclusively on archive data.

PRISMA products will be free for new acquisition request and for archived products in the following cases:

Category A users

Scientific Use from Category B

Institutional-Application Use from Category B, only on Italian regions

Scientific use and Institutional-Application Use by non-Italian user, limited by a quota and in the framework of Agreements or others initiatives (e.g. Announcement Of Opportunities, Open Calls, etc).

In remaining cases (e.g. commercial use) products will be subject to a fee.

## 6. Conclusion


PRISMA is an innovative Earth Observation Italian mission aiming at acquiring and delivering hyperspectral and panchromatic images of the earth as an original contribution to remote sensing applications.

Earth Observation is recognized as a key instrument to support monitoring actions at local and global scale aimed to ensure environmental sustainability of human activities. An innovative role is represented by PRISMA Mission in term of development of new analysis methodologies which involve the capability to observe not only the geometric features but also the chemical-physical ones of the targets of interest.

PRISMA will provide high quality hyperspectral products (images) on specific individual targets requested by the users, free of charge and with a mostly open access.

## Bibliografia

- [1] Guarini, R., Loizzo, R., Longo, F., Mari, S., Scopa, T., Varacalli, G., 2017. Overview Of The PRISMA Space And Ground Segment And Its Hyperspectral Products. Proceedings of the IEEE IGARSS (International Geoscience and Remote Sensing Symposium) Conference, Fort Worth, Texas, USA, July 23–28.
- [2] Meini, M., Fossati, E., Giunti, L., Molina, M., Formaro, R., Longo, F., Varacalli G., 2015. The PRISMA Mission Hyperspectral Payload. IAC-15-B1.3.7, 66th International Astronautical Congress, Jerusalem, Israel.

- 
- [3] Guarini, R., Loizzo, R., Facchinetti, C., Longo, F., Ponticelli, B., Faraci, M., Dami, M., Cosi, M., Amoruso, L., De Pasquale, V., Taggio, N., Santoro, F., Colandrea, P., Miotti, E., Di Nicolantonio, W., 2018. PRISMA hyperspectral mission products. IGARSS (International Geoscience and Remote Sensing Symposium) Conference, Valencia, Spain, July 22-27.
- [4] Loizzo, R., Daraio, M., Guarini, R., Longo, F., Lorusso, R., Dini, I., Lopinto, E., 2019 (Proceedings In Press). PRISMA Mission Status and Perspective. IGARSS (International Geoscience and Remote Sensing Symposium) Conference, Yokohama, Japan, July 28 - August 2.



## Copernicus S2 to support CAP control policies in agriculture

Filippo Sarvia, Enrico Borgogno-Mondino

*University of Torino, DISAFA, L.go Braccini 2, Grugliasco, TO I-10095, Italy*

Corresponding author: Filippo Sarvia

Keywords: Copernicus S2, control policies, Common Agricultural Policy, Crop monitoring

### 1. Introduction

Natural disasters cost farmers in developing countries billions of dollars each year. Drought is the most significant threat, followed by floods, forest fires, storms, pests, pathogens, etc. According to a new report by the United Nations Food and Agriculture Organization (FAO), between 2005 and 2015, natural disasters cost the agricultural sectors of developing countries \$ 96 billion in damaged crops or lost. The report of the conference of March 15 in Rome / Hanoi convened by the Vietnamese government in collaboration with the FAO revealed that half of this damage, 48 billion, concerned Asia. 83% of all the economic losses caused by the drought documented by the FAO study were absorbed by agriculture, with a value of 29 billion dollars. The European Union supports agricultural production in the countries of the Community by providing aid, contributions and premiums to producers. These disbursements, financed by the EAGF (European Agricultural Guarantee Fund) and the EAFRD (European Agricultural Fund for Rural Development), are managed by Member States through the Paying Agency (PA), established pursuant to Reg. (EC) n. 885/2006 (Art. 18). With the legislative decree n. 165/99, in Italy, the Agea (Agency for Agricultural Payments) was established to carry out the functions of Coordination Body and Paying Agency (PA). The Agea, as Coordination Body, is, among other things, charged with: a) supervising and coordinating the Paying Agency; b) verification of the consistency of their activity with the community guidelines; c) the promotion of the harmonized application of Community legislation and the related authorization, provision and accounting procedures for Community aid by Paying Agency ([www.agea.gov.it](http://www.agea.gov.it)). In Italy, Paying Bodies have been set up for many (but not all) regions, with tasks of authorization and control of payments, execution of payments, accounting for payments.

The compliance of these activities with EU legislation is guaranteed by constant and in-depth audits carried out by the Internal Control: this, constantly in contact with AGEA, MIPAAFT (Ministry of Agricultural, Food, Forestry and Tourism Policies), and the EU, is a structure completely free from the "operational" sectors, super partes and directly reporting to the Management. For the efficient and innovative management of all activities, the paying agencies have their own Information Systems developed with the collaboration of private parties. In Piedmont this role is performed by the Information System Consortium (CSI - Instrumental body for IT services of the Piedmont Region).

The technical-administrative controls carried out by ARPEA concern two types, the first is aimed at the beneficiaries of the contributions paid (the farmers) and consists in verifying the data declared in the application and ascertaining the real requirements and obligations imposed by the legislation in force; the second level of control is instead addressed to all the functions that are delegated by the external paying agency and allow to check compliance with the agreements, coordinate the delegates, test their own procedures and highlight the critical points with reference to the correct application of the law Community and national level. The checks are carried out on a sample extracted according to precise criteria and retrace the main phases implemented by the delegated agency during the first-degree checks. If the definition of the companies subjected to on-the-spot control does not derive from a timely notification internal or external to the Agency, the Control Function Office proceeds to extract a control sample to be verified in the current year. The number of the sample to be extracted derives, except for justified exceptions, from the Annual Control Plan. Based on community recommendations, the sample must be extracted in part according to risk criteria and partly according to criteria of randomness. It is to be hoped that the ratio of the practices extracted will settle at around 80% about extraction on a risk basis and 20% for practices on a random basis. Depending on the size of the sample and the risk criteria to be considered, it is possible to assign specific risk classes to the practices being extracted, so that those on a random basis are more likely to be extracted, in relation to the attribution of a highest risk criterion (1st level control manual).

Controls may be preceded by a notice from the Agency, provided it does not interfere with their purpose and effectiveness. The notice cannot exceed 14 days (Article 25 of the Reg. (EU) n. 809/2014). As regards instead

the measures connected to animals, the notice cannot exceed 48 hours, except in duly justified cases. In all cases, the Control Function has the right to provide or not the notice to the companies concerned regarding the execution of on-the-spot checks.

In general, the checks are carried out at national level, on all applicants 5% is checked based on an algorithm that randomly chooses the samples according to the parameters described above. The basic elements of control are identified with: compliance of the surface with the requirements established by the legislation concerning the definition of "permissible hectare" (EU Reg. 1307/2013); compliance with all eligibility criteria, possession of the requirements, commitments and other obligations inherent in the aid scheme; verifying the accessibility of the surfaces and maintaining them in a state suitable for grazing or cultivation; verification of the performance of a cultivation practice at least annually on the surface subject to verification, responding to the declared use restrictions; measurement of the effective area used for agricultural and / or cultivation activities and verification of compliance with the conditionality requirements set by the regulations.

## **2. The graphic application**

The graphic application from 2016 is based on geospatial tools. The Reg. (EU) n 809/2014 establishes that, in the case of aid applications for area aid schemes (for example basic payment, greening, coupled support and payment for small farmers) or of applications for payment for the support measures related to the surface, the Member State provides the beneficiary with a pre-established template in electronic format and the corresponding graphic material through a software application, based on a geographic information system (GIS) (graphic application based on on geospatial instruments - GSAA). The introduction of the graphical request took place gradually: in 2016 it concerned a number of beneficiaries corresponding to that necessary to cover at least 25% of the area determined for the basic payment scheme during the previous year; in 2017 it concerned a number of beneficiaries corresponding to that necessary to cover at least 75% of the total area determined for the basic payment scheme during the previous year and in 2018 the graphical request should have covered the entire national territory.

The system allows the observation of the surface subject to CAP payments with a simultaneous economic saving due to the reduction of on-site controls. The physical inspections in the field remain necessary if the collected evidence does not allow the determination of the eligibility for the requested aid (MIPAAFT, 2018 direct payments monitoring).

## **3. Use of Copernicus S2 for the monitoring of agricultural crops**

Crop monitoring in all European countries, via satellite data, allows a blanket check of all support requests for the provision of aid, contributions and premiums to farmers. The final model and therefore the automation of the process is being studied and still needs appropriate calibrations in relation to environments of different cultivation development. Some Member States have already launched pilot projects to explain the phenological trend of crops in different areas within the national context. Many studies state that satellite remote sensing effectively meets the requirements of large-scale vegetation mapping (Xie et al., 2008 and Inglada et al., 2015). Moreover, many of the datasets of the global archives of satellite images are freely accessible, therefore they can represent a valid support tool especially if used together with field data to optimize reading (Brown and all., 2013).

The data available on the market for monitoring cultures are different (Zhang et al., 2003; Sakamoto et al., 2005; Veloso et al., 2017 and Wardlow et al., 2008). As far as the monitoring of the cultural phenological development is concerned, spectral indices are used (for example NDVI Leprieur et al., 1994) appropriately calculated through the different satellite bands (Didan et al., 2015).

Sometimes, after calculating the appropriate spectral indices, an operation of filtering and interpolation of the temporal index profiles is necessary in order to correctly appreciate the image (Liu et al., 2006 and Chen et al., 2004). Finally, with a valid product, it will be possible to proceed with the extraction of the phenological parameters that could possibly be used by the paying agency during the checks on the declarations of the farmers. The main parameters that are used during the control phase with remote data are related to the beginning, the end and the peak of the growing season of the crop (Testa et al., 2018; Testa et al., 2014; Jayawardhana et al., 2016) and related to some agronomic practices such as: the plowing, the growth of the crop in the considered period, the presence of the crop at the time declared by the farmer, the activity of some agricultural practices by the farmer and the harvesting or crop removal. In 2018 AGEA started an experimental field in Foggia for the determination of control markers on the national territory, subsequently,

in 2019, ARPEA established a second one in Vercelli in order to identify the possible differences with the first. The objective of these pilot projects is to succeed, at best, in obtaining a model for functional control by the end of the year 2019.

#### 4. Discussion and conclusion

These proposals are configured as a pilot experience that, if properly calibrated in a territorial context and appropriately engineered, could be configured as an operational prototype for the control of declarations of European incentive applications. It is emphasized that the proposed methodology, however advanced, does not exempt from the need to maintain a constant dialogue between ordinary practices and field observations and satellite data. The veracity and reliability of remote deductions cannot be different, for example, from statements made by farmers.

With the inclusion of the graphic application for European contributions, the future development of this methodology will always be greater. Furthermore, it is advisable to carry out cultivation growth plans monitored both by field and satellite in order to obtain a stable model that can accurately describe all the cultivation development. Once the scheme is in place, it will be good if this is constantly monitored over time as the variables involved vary constantly both spatially and temporally.

It should be remembered that the use of this technique therefore has the purpose of providing a tool applicable to the investigation of vast areas through which the legislator is able to identify any crop presence in relation to the phenomenon investigated and therefore offer control or an efficient, economically competitive and immediate service. It should be remembered that the use of this technique cannot and must not ignore an accurate control of the field, a precise recording of crucial events and cultivation operations, but must be added to these to make the management, monitoring and coordination of the simplest, fastest and most effective agricultural dynamics.

#### Bibliografia

- Brown, J. C., Kastens, J. H., Coutinho, A. C., de Castro Victoria, D., & Bishop, C. R. (2013). Classifying multiyear agricultural land use data from Mato Grosso using time-series MODIS vegetation index data. *Remote Sensing of Environment*, 130, 39-50.
- Didan, K. (2015). MOD13Q1 MODIS/Terra vegetation indices 16-day L3 global 250m SIN grid V006. NASA EOSDIS Land Processes DAAC.
- Inglada, J., Arias, M., Tardy, B., Hagolle, O., Valero, S., Morin, D., ... & Koetz, B. (2015). Assessment of an operational system for crop type map production using high temporal and spatial resolution satellite optical imagery. *Remote Sensing*, 7(9), 12356-12379.
- Jayawardhana, W. G. N. N., & Chathurange, V. M. I. (2016). Extraction of agricultural phenological parameters of Sri Lanka using MODIS, NDVI time series data. *Procedia food science*, 6, 235-241.
- Sakamoto, T., Yokozawa, M., Toritani, H., Shibayama, M., Ishitsuka, N., & Ohno, H. (2005). A crop phenology detection method using time-series MODIS data. *Remote sensing of environment*, 96(3-4), 366-374.
- Testa, S., Mondino, E. C. B., & Pedrolì, C. (2014). Correcting MODIS 16-day composite NDVI time-series with actual acquisition dates. *European Journal of Remote Sensing*, 47(1), 285-305.
- Testa, S., Soudani, K., Boschetti, L., & Mondino, E. B. (2018). MODIS-derived EVI, NDVI and WDRVI time series to estimate phenological metrics in French deciduous forests. *International journal of applied earth observation and geoinformation*, 64, 132-144.
- Veloso, A., Mermoz, S., Bouvet, A., Le Toan, T., Planells, M., Dejoux, J. F., & Ceschia, E. (2017). Understanding the temporal behavior of crops using Sentinel-1 and Sentinel-2-like data for agricultural applications. *Remote sensing of environment*, 199, 415-426.
- Wardlow, B. D., & Egbert, S. L. (2008). Large-area crop mapping using time-series MODIS 250 m NDVI data: An assessment for the US Central Great Plains. *Remote sensing of environment*, 112(3), 1096-1116.
- Xie, Y., Sha, Z., & Yu, M. (2008). Remote sensing imagery in vegetation mapping: a review. *Journal of plant ecology*, 1(1), 9-23.
- Zhang, X., Friedl, M. A., Schaaf, C. B., Strahler, A. H., Hodges, J. C., Gao, F., ... & Huete, A. (2003). Monitoring vegetation phenology using MODIS. *Remote sensing of environment*, 84(3), 471-475.



Matteo Albano, Simone Atzori, Christian Bignami, Marco Moro, Marco Polcari, Stefano Salvi,  
Cristiano Tolomei and Salvatore Stramondo  
*Istituto Nazionale di Geofisica e Vulcanologia, Italy*

Corresponding author: Salvatore Stramondo

Keywords: InSAR, Volcano, Earthquake, Crustal deformation

## 1. Abstract

The detection and analysis of crustal deformations are one of the most important ways for observing, modelling and understanding the natural phenomena occurring in the Earth surface. Generally, the main causes of natural deformations are earthquakes and volcanic processes, often destructive and very dangerous for human beings. Therefore it is easy to understand why the study and monitoring of such ground movements is a key topic. To this aim, the improvements of satellite Earth Observation data and methods over the last three decades, have provided unprecedented perspectives to measure crustal movements with short temporal sampling, good accuracy and wide spatial coverage. In particular, multi-temporal Synthetic Aperture Radar (SAR) satellite data sets and Interferometric SAR (InSAR) techniques have demonstrated the capacity to collect information on the dynamics of the deformation occurring during the various phases of the seismic and volcanic cycles.

## 2. Introduction

During the last 25 years, Interferometric Synthetic Aperture Radar (InSAR) image processing technique has become a widely used method for the detection of small ground movements (Bürgmann et al., 2000). Especially during the last 10 years, the increased availability of new SAR instruments and satellite constellations has stimulated a steady improvement of processing algorithms, providing measurement accuracies able to identify both small and large ground deformation signals (Stramondo et al., 2016).

Satellite SAR data provide a way to cover large areas with ever better revisiting times, at lower costs than airborne data, and are thus best suited for the monitoring of earthquakes and volcanoes. InSAR can provide surface deformation maps with high spatial resolutions (5–80 m) over large areas. Secondly, InSAR is particularly sensitive to vertical displacements and finally, it is a remote-sensing technique and as such it does not require field work and can be available practically worldwide.

Going back to the past SAR data, ESA (European Space Agency) was the main source of useful imagery thanks to the ERS-1, ERS-2 and ENVISAT-ASAR sensors (C-band, 5.3 GHz), which all together span nearly 20 years, from the end of 1991 to July 2011. For the main parts of the missions, the repeat cycle of both ERS and ASAR was 35 days. Presently a C-band Canadian sensor (Radarsat-2), two German X-band instruments (TerraSAR-X and TanDEM-X), the Japanese L-band PALSAR-2 sensor onboard ALOS-2, the ESA C-band Sentinel-1A/B SAR, and the four COSMO-SkyMed X-band sensors managed by the Italian Space Agency (ASI) are operational systems. SAR satellite constellations today achieved 1 to 6 days of temporal sampling. Such sensors with different revisit times and working at different frequency bands allow us focusing the key role of InSAR for the management and mitigation of seismic and volcanic risk as well as providing an input data for the modelling of the seismic and volcanic sources.

## 3. InSAR techniques and results

SAR-based ground deformation measurements rely on repeat-pass acquisitions carried out by L-, C-, and X-band microwave SAR sensors. The standard two-pass approach (Massonnet et al., 1993) includes image coregistration, interferogram formation and filtering, removal of the topographic phase contribution using an external Digital Elevation Model (DEM), 2D phase unwrapping and conversion to displacement.

The InSAR technique can measure the projection of the deformation vector onto the Line of Sight (LoS) direction. According to radar wavelength, spatial coverage and revisit time, several ground deformation phenomena can be analyzed thus supporting hazard assessment purposes. Indeed, InSAR-based studies have been extensively applied in the study of tectonic processes (Atzori et al., 2009; Stramondo et al., 2011; Cheloni et al., 2017) and volcanic activity (Palano et al., 2008; Foulmelis et al., 2013; Trasatti et al., 2015).

Once archives of SAR images acquired by different sensors, operating in different frequency bands became available, it was possible to develop multi-temporal InSAR algorithms with the aim of monitoring ground movement. Several multi-temporal InSAR techniques have been proposed in the last decade, which exploit the redundancy offered by tens or hundreds of image pairs. The output of these techniques is a mean ground

velocity map and the relative displacement time-series, temporally referred to the first acquisition date of the image stack, and spatially referred to a reference point or area within the radar coverage. Moreover, the stacking methodologies have the advantage to estimate and remove the turbulent tropospheric delays by data redundancy and low-pass temporal filtering. The existing algorithms fall into two broad categories, namely the Persistent Scatterer (PS) (Ferretti et al., 2001) and the Small Baseline (SBAS) (Berardino et al., 2002) approaches.

#### 4. Applications

Concerning the applications in active tectonics, it is worth noting the strong improvements in terms of available data, different wavelength, and processing algorithms. Since the very first applications worldwide, Landers earthquake (Massonnet et al., 1998), and in Italy, Colfiorito earthquake sequence (Stramondo et al., 1999), InSAR demonstrated the capability to be employed for measuring surface signature from short, medium and large scale events. It can be representative of situation enhancement how scientists managed the most recent earthquake sequences in Italy. During Colfiorito 1997-1998, satellite view was ensured by ERS1 and 2 ESA missions, C-band sensors with 35 days revisiting time (Stramondo et al., 1999). Technologies for InSAR and for processing algorithms were at their early stages (Figure 1a). In 2009, the L'Aquila earthquake sequence, COSMO-SkyMed mission was operating. This allowed the very first 3-bands (X-, C-, L-) interferometry (Stramondo et al., 2011) a large amount of data, the capability to investigate much deeply the effects (Figure 1b). In the 2016-2017 Amatrice-Visso-Norcia-Campotosto sequence, InSAR techniques have been intensively applied to follow the evolution of the very complex displacement field all along the sequence (Cheloni et al., 2017) (Figure 1c).

InSAR data have been also exploited to image the ground deformations associated with volcanic eruptions. On December 24, 2018, the Etna volcano began a very intense eruption, characterised by significant lava flows, ash and gas emissions, and a seismic swarm triggered by the intrusion of the magma in the volcano. Two days later, an earthquake of Mw 4.9 occurred at a depth of approximately 1 km along the volcano southeastern flank, causing damages and several ground fractures in some villages and also in Catania city. SAR data collected by Sentinel-1 (S1) sensors acquired along both the ascending and

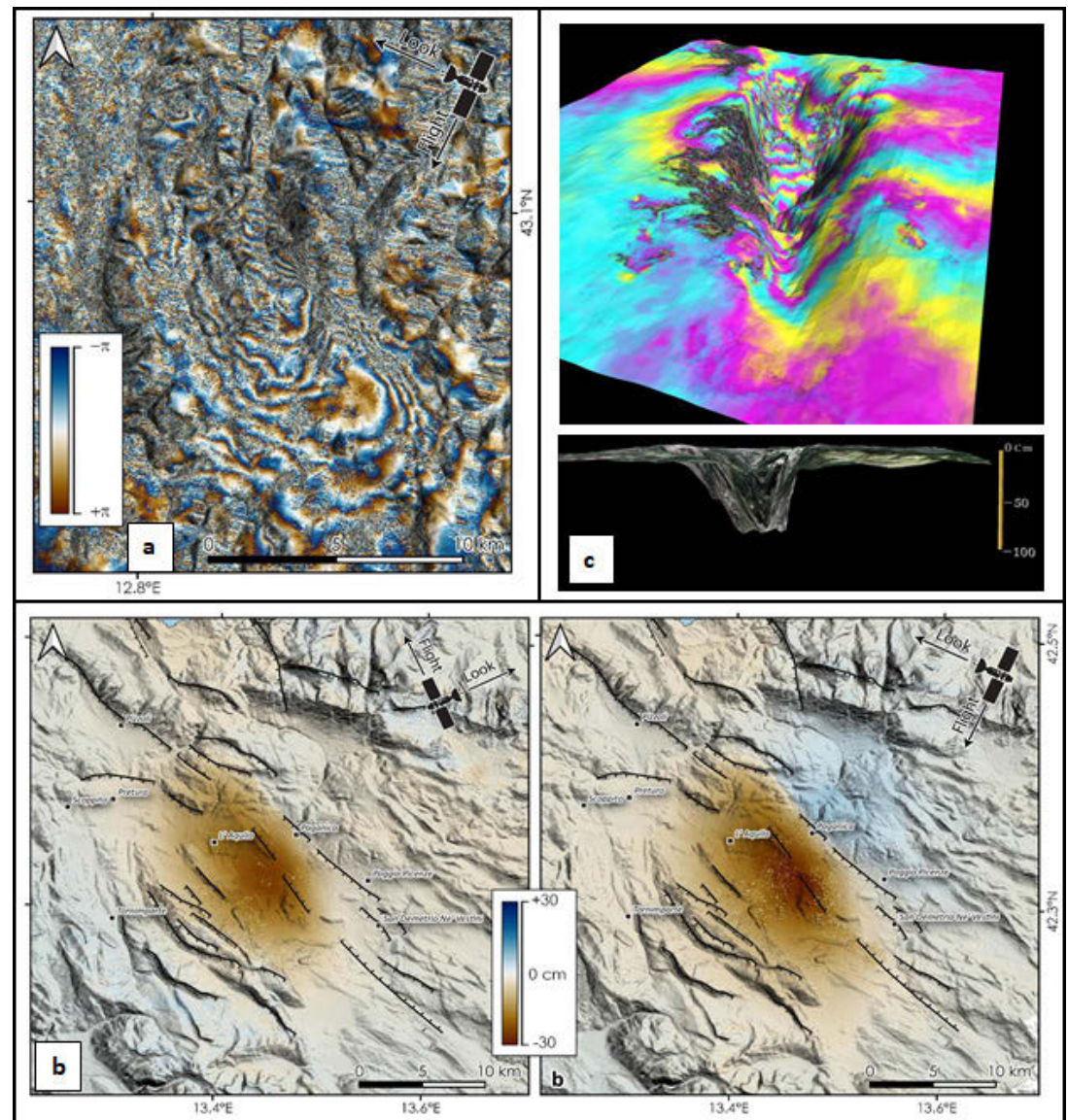


Fig. 1: a) Wrapped ERS1-2 descending coseismic interferogram related to the Colfiorito earthquake. b) Unwrapped ascending (left panel) and descending (right panel) coseismic ground displacement from ENVISAT data related to the L'Aquila 2009 earthquake. c) Wrapped Co-seismic interferogram (upper panel) related to the 2016-2017 Central Italy seismic sequence (Amatrice, Visso and Norcia earthquakes), superimposed to the enhanced vertical ground deformation (lower panel). InSAR analysis allowed estimating subsidence of the Castelluccio Plain of the order of 1 m



descending tracks allowed to constrain the ground displacement induced by the Etna eruption and the earthquake (1 and 2 in Figure 2 a and b). The most important signal is related to the deformation of the Etna summit due to the opening of a dyke and the related magma ascent. The deformation involves a large portion of the volcano flanks, reaching more than 40 cm and 65 cm along west and east directions, respectively. The deformation pattern related to the concurrent Mw 4.9 (2 in Figure 2) earthquake was generated by the slip of the Fiandaca-Pennisi Fault (FPF) and resulted in a mainly horizontal movement of ~15 cm toward east and 20 cm toward west directions. The interferograms also allowed to detect a small-scale landslide occurring along the southwestern flank of the volcano, at ~23 km away from the Etna eruption event (3 in Figure 2).

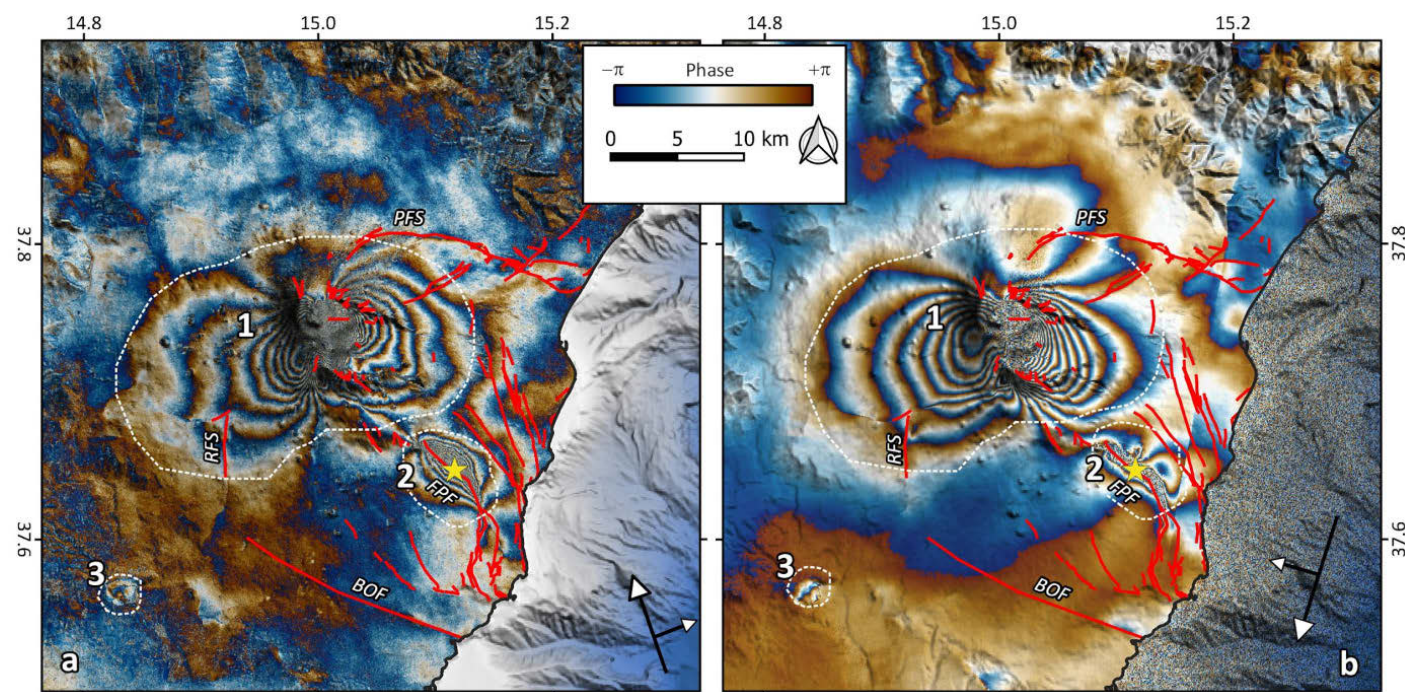


Fig 2. Ascending (a) and descending (b) InSAR results for the December 2018 Etna eruption. Ground deformations due to the volcano eruption (1), the Mw 4.9 earthquake (yellow star) (2) and the seismically induced landslide (3)

## 5. Conclusions/Discussion

The progressive increase of SAR data availability, the extended coverage of each frame, the shortening of temporal sampling resulted in a strong increase of the observation of ground deformation worldwide. The huge amount of studies involving InSAR demonstrated that providing new, high-quality, data allowed scientists to achieve the objective of improving their knowledge of natural phenomena. Furthermore InSAR is now widely used for developing and testing analytical and numerical models of seismic and volcanic processes. The long-term Sentinel-1 missions (up to at least 2030), together with its free and open data policy, implies that such data will continue to be among the main source for ground deformation studies. Such peculiarities make multi-band InSAR-based analysis and its synergic use with other data sources, such as GNSS or Leveling data, an important tool for improving the knowledge of natural and/or anthropogenic phenomena ongoing on Earth's surface.

## Bibliografia

- Atzori, S., Hunstad, I., Chini, M., Salvi, S., Tolomei, C., Bignami, C., Stramondo, S., Trasatti, E., Antonioli, A., Boschi, E., 2009. Finite fault inversion of DInSAR coseismic displacement of the L'Aquila earthquake (central Italy). *Geophys. Res. Lett.* 36 (2009).
- Berardino P., Fornaro G., Lanari R. and Sansosti E.; 2002: A new algorithm for surface deformation monitoring based on small baseline differential SAR interferograms. *IEEE Trans. Geosci. Remote Sens.*, 40, 2375-2383.
- Bürgmann, R., Rosen, P. A., and Fielding, E. J. (2000). Synthetic aperture radar interferometry to measure Earth's surface topography and its deformation. *Annu. Rev. Earth Planet. Sci.* 28, 169–209. doi: 10.1146/annurev.earth.28.1.169.
- Cheloni, D.; De Novellis, V. et al. (2017). Geodetic model of the 2016 Central Italy earthquake sequence inferred from InSAR and GPS data. *Geophys.Res.Lett.*, 44, 6778-6787.
- Ferretti A., Prati C. and Rocca F.; 2001: Permanent scatterers in SAR interferometry. *IEEE Trans. Geosci. Remote Sens.*, 39, 8-20.



- Foumelis, M., Trasatti, E., Papageorgiou, E., Stramondo, S., Parcharidis, I., 2013. Monitoring Santorini volcano (Greece) breathing from space. *Geophys. J. Int.* 193, 161–170.
- Massonnet, D., and Feigl, K. L. (1998). Radar interferometry and its application to changes in the Earth's surface. *Rev. Geophys.* 36, 441–500. doi: 10.1029/97RG03139.
- Palano, M., Puglisi, G., Gresta, S., 2008. Ground deformation patterns at Mt.Etna from 1993 to 2000 from joint use of InSAR and GPS techniques. *J. Volcanol. Geotherm. Res.* 169, 99–120.
- Stramondo, S., Tesauro, M., Briole, P., Sansosti, E., Salvi, S., Lanari, R., Anzidei, M., Baldi, P., Fornaro, G., Avallone, A., Buongiorno, M.F., Franceschetti, G. and Boschi, E., 1999, The September 26, 1997 Colfiorito, Italy, earthquakes: modeled co-seismic surface displacement from SAR interferometry and GPS, *Geophys. Res. Lett.* 26(7), 883–886
- Stramondo, S., Chini, M., Bignami, C., Salvi, S., Atzori, S., 2011. X-, C-, and L-band DInSAR investigation of the April 6, 2009, Abruzzi earthquake. *IEEE Geosci. Remote Sens. Lett.* 8, 49–53.
- Stramondo S., Trasatti E., Albano M., Moro M., Chini M., Bignami C., Polcari M., Saroli M., Uncovering deformation processes from surface displacements, *Journal of Geodynamics*, Invited Review Article, August 2016.
- Trasatti, E., Polcari, M., Bonafede, M., Stramondo, S., 2015. Geodetic constraints to the source mechanism of the 2011–2013 unrest at Campi Flegrei (Italy) caldera. *Geophys. Res. Lett.* 42, 3847–3854.

## **Ottawa Flooding 2019 April/May– Processing of Sentinel-1 imagery with PCI Geomatica for hydraulic risk management**

Vera Costantini

*Sysdeco Italia srl*

Keywords: flooding, risk management, Sentinel-1, PCI Geomatica

Heavy rains hit eastern Canada from the end of April and for many weeks, causing severe flooding. The first flooding of Ottawa River was on April 26<sup>th</sup>.

Sentinel-1 data is of great help in providing a quick response to this type of emergency because it is easily available and can be processed with different software, including Geomatica of PCI Geomatics, whose Sysdeco is the unique Italian distributor. One of PCI Geomatics company's headquarters is in Ottawa, so our partners from PCI rushed to generate a map of the first flood and made it public online to help with the emergency response, using Sentinel-1 images. Here we show the results of this analysis which we took further by classifying the river area before the flooding with object-based analysis, applying Coherence Change detection on Sentinel-1 multitemporal images, extracting shape polygons of the flooded areas and more.

## **EO multitemporal data for semi-automatic agricultural monitoring: the new Common Agricultural Policy application**

Fabio Volpe, Livio Rossi

*e-geos, Roma*

To guarantee a correct supply of CAP - Common Agriculture Policy funds, the Italian Agency AGEA uses a complex geographic information system that collects data on the national agricultural territory and from the agricultural producers. The Copernicus satellite constellation (Sentinel) has opened new approaches for a systematic monitoring of the agronomic parcels, allowing semi-automatic check of the overall crop declaration correctness and of the environmental protection applied.

An operational pilot has been successfully performed over Foggia province (south of Italy), automatically processing more than 450,000 agricultural parcels, using more than 200 Sentinel images collected in 2017 and 2018. For completing and closing the entire monitoring phases, a new innovative APP on mobile phone for acquiring secure, protected and certified ground photos (GEOTAGGED agro-parcels) has been created by eGEOS. The presentation will summarize the major hints of how this complex EO based system works



Sara Zollini<sup>1</sup>, María Cuevas-González<sup>2</sup>, Donatella Dominici<sup>1</sup>, Oriol Monserrat<sup>2</sup>, Maria Alicandro<sup>1</sup>

<sup>1</sup> - DICEAA, Department of Civil, Environmental Engineering and Architecture, Via Gronchi 18, 67100 L'Aquila, Italy

<sup>2</sup> - Centre Tecnològic de Telecomunicacions de Catalunya (CTTC), Division of Geomatics, Av. Gauss 7, E-08860 Castelldefels, Barcelona, Spain

Corresponding author: Cuevas-González, M.

Keywords: Remote sensing, Sentinel, SAR, shoreline extraction

### 1. Introduction and state of art

The monitoring of the territory has nowadays a central role not only in research fields but also for emergency management and planning interventions in risk areas. With the developments in technology, the means to monitor the territory are increasingly becoming more specific and precise for all types of applications (Alicandro et al. 2019; Bellone et al. 2016; Dominici et al. 2017; Gomez & Purdie 2016; Mills et al. 2005; Sawaya et al. 2003; Shalaby & Tateishi, 2007; Xu et al. 2010).

In the geomatics field, information can be acquired, modelled, interpreted, processed and stored using in-situ techniques (classic topography), spatial positioning techniques (GNSS), photogrammetry, laser scanning, optical and radar remote sensing, Geographic Information System (GIS), etc. (Gomarasca, 2009).

Focusing in remote sensing field, the advantage to have free and relatively easy – to – use satellite images, both optical and radar, allows to explore vast areas of the territory in a timely fashion.

The European Space Agency (ESA) launched the Sentinel missions within the Copernicus project, whose main purpose is to support European operational and policy needs of the Global Monitoring for Environmental Security (GMES) program ([https://m.esa.int/About\\_Us/Ministerial\\_Council\\_2012/Global\\_Monitoring\\_for\\_Environment\\_and\\_Security\\_GMES](https://m.esa.int/About_Us/Ministerial_Council_2012/Global_Monitoring_for_Environment_and_Security_GMES)).

The Sentinel–1 satellite was the first of five missions that ESA is developing and it is formed by a constellation of two Synthetic Aperture Radar (SAR) polar orbiting satellites (Sentinel – 1A and Sentinel – 1B) which acquire data in C–band. The SAR enables to acquire imagery during day and night and in all weather conditions, because it operates in the microwave wavelength (<https://sentinel.esa.int/web/sentinel/missions/sentinel-1>). Sentinel–1 are used for many application fields, like soil moisture mapping (Malenovsky et al. 2012), sea ice monitoring (Pedersen et al. 2015; Nagler et al. 2015), landslide detection (Barra et al. 2016; Dai et al. 2016), volcanoes monitoring (González et al. 2015), etc.

In this work, Sentinel – 1 imagery is exploited for coastal monitoring, in particular, shoreline mapping in the Italian coast. Italy is the European country with the longest coastline at risk of erosion. With a coast of over 7500 km, about 2400 km are at this risk, which represent about a third of the Italian coasts ([http://www.isprambiente.gov.it/it/progetti/acque-interne-e-marino-costiere-1/progetti-conclusi/copy\\_of\\_progetti-conclusi](http://www.isprambiente.gov.it/it/progetti/acque-interne-e-marino-costiere-1/progetti-conclusi/copy_of_progetti-conclusi); <http://cadsealand.cinfai.it/default.htm>). Estimating shoreline variations is a crucial point for safe navigation, coastal resource management, coastal environment protection, sustainable coastal development and urban planning (Taha & Elbeih, 2010).

It is well known that the coastal environment is a dynamic ecosystem which is really difficult to map. The shoreline is defined as the line of contact between land and water (Misra & Balaji, 2015). In this project, we will develop an integral monitoring for the coastal area in Ortona (Italy). First of all, deformation and velocity maps of the Ortona territory will be generated using interferometric techniques and exploiting Sentinel – 1A/B, Single Look Complex, IW acquisition mode. Secondly, SAR Sentinel-1 and Optical Sentinel-2 data will be integrated for the instantaneous shoreline mapping. Finally, a land cover map will be produced by means of an object based classification using methods and algorithms like “multivariate filter-based feature selection method”, “random forest metrics”, “genetic algorithms”, “bayesian information criterion”, etc. All these layers, together with ancillary data, will be integrated and analysed to produce a general vulnerability map of the Ortona coastal area.

### 2. The project and future developments

Deformation and velocity maps have been estimated using Sentinel–1 images covering the period from October 19, 2014 to December 21, 2018. The product type is Level-1 Single Look Complex (SLC) and the acquisition mode is Interferometric Wide (IW) swath. The total number of the images is 179. IW acquisition mode acquires data with a 250 km swath at 5 m by 20 m spatial resolution (<https://sentinel.esa.int/web/sentinel/user-guides/sentinel-1-sar/acquisition-modes/interferometric-wide-swath>). The interferometric processing chain developed by the Remote Sensing Department of Centre Tecnològic de Telecomunicacions

de Catalunya (CTTC) was used in this work.

A total of 178 interferograms were generated and used in the analysis.

A Sentinel-1 amplitude image of the area of Ortona (CH, Italy) is showed in Fig. 1.

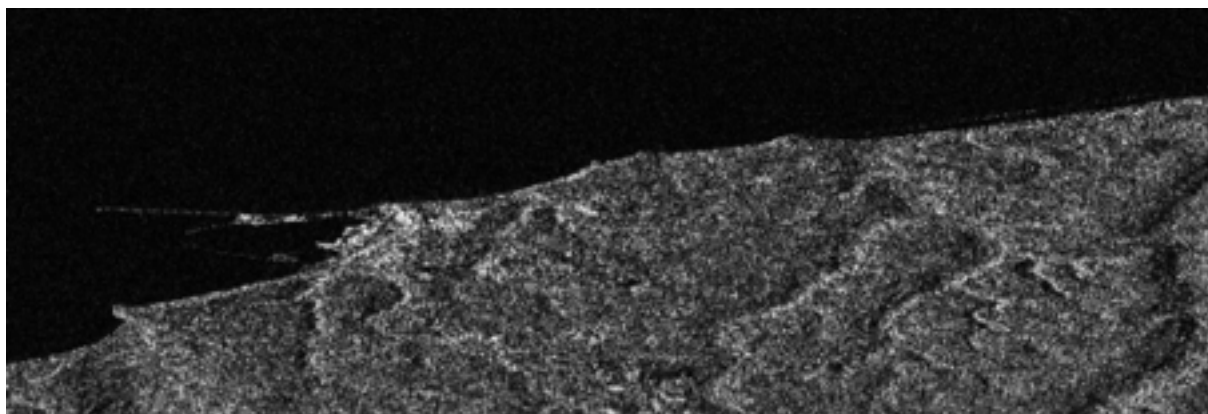


*Figure 1. Amplitude image in radar geometry of the area of Ortona (Italy). December 15, 2018, Descending Orbit*

In the meantime, the shoreline mapping has been carried on, using 7 Sentinel-1 images before a storm event (happened on January 18, 2017) and 7 Sentinel-1 images after. The number of the images is necessary to correct the speckle. The Level-1 GRD, IW images are chosen (for more information about the used data see <https://sentinel.esa.int/web/sentinel/user-guides/sentinel-1-sar/product-types-processing-levels/level-1>).

The idea of the project is to extract the shoreline maps before and after the event in order to see variations of it. A series of shorelines will be extracted to analyse their behaviour. At first, a pre-processing is performed, aimed at emphasizing the contrast between land and sea. Then, specific algorithms will be used to extract the shoreline. Many algorithms and methods have already been used for this application, like the Lee algorithm (Marghany & Hashim, 2010), the edge detection and segmentation methods (Braga et al., 2013; Pradan et al., 2018), the PCNN algorithm (Palazzo et al., 2011), etc.

Once extracted the shoreline with SAR images, it will be compared to the vectorised shoreline of the pre-treated image.

A similar study will be performed using the Sentinel – 2 images. The purpose is to extract instantaneous shoreline from Sentinel-1 and Sentinel-2 separately and, then, from the fusion between them. The obtained results will be compared and discussed, both qualitatively and quantitatively.

In the end, using an object based classification, a land cover map of the area is performed.

The availability of a free and ready – to – use products helps the rapid and low – cost monitoring of the territory in various applications fields, allowing a management also in emergency situations.

## References

- Alicandro, M., Candigliota, E., Dominici, D., Immordino, F., Quaresima, R., & Zollini, S. (2019). Alba Fucens Archaeological Site: Multiscale and Multidisciplinary Approach for Risk Assessment and Conservation. ISPRS-International Archives of the Photogrammetry, Remote Sensing and Spatial Information Sciences, 4211, 47-53.
- Barra, A., Monserrat, O., Mazzanti, P., Esposito, C., Crosetto, M., & Scarascia Mugnozza, G., 2016. First insights on the potential of Sentinel-1 for landslides detection. Geomatics, Natural Hazards and Risk, 7(6), 1874-1883.
- Braga, F., Tosi, L., Prati, C., & Alberotanza, L. (2013). Shoreline detection: capability of COSMO-SkyMed and high-resolution multispectral images. European Journal of Remote Sensing, 46(1), 837-853.
- Bellone, T., Dabove, P., Manzino, A. M., & Taglioretti, C., 2016. Real-time monitoring for fast deformations using GNSS low-cost receivers. Geomatics, natural hazards and risk, 7(2), 458-470.
- CADSEALAND, Online at <http://cadsealand.cinfai.it/default.htm> [Accessed on May 20, 2019]
- Dai, K., Li, Z., Tomás, R., Liu, G., Yu, B., Wang, X., ... & Stockamp, J., 2016. Monitoring activity at the Daguangbao mega-landslide (China) using Sentinel-1 TOPS time series interferometry. Remote Sensing of Environment, 186, 501-513.
- Dominici, D., Alicandro, M., Rosciano, E., & Massimi, V., 2017. Multiscale documentation and monitoring of l'aquila historical centre using uav photogrammetry. International Archives of the Photogrammetry, Remote Sensing & Spatial Information Sciences, 42.
- ESA Global Monitoring For Environment and security (GMES) Online at [https://m.esa.int/About\\_Us/Ministerial\\_Council\\_2012/Global\\_Monitoring\\_for\\_Environment\\_and\\_Security\\_GMES](https://m.esa.int/About_Us/Ministerial_Council_2012/Global_Monitoring_for_Environment_and_Security_GMES) [Accessed on March

- 18, 2019]
- ESA Sentinel Online, Home, Missions, Sentinel – 1 Online at <https://sentinel.esa.int/web/sentinel/missions/sentinel-1> [Accessed on May 17, 2019]
- ESA Sentinel Online, Home, User Guides, Sentinel-1 SAR, Acquisition Modes, Interferometric Wide Swath <https://sentinel.esa.int/web/sentinel/user-guides/sentinel-1-sar/acquisition-modes/interferometric-wide-swath> [Accessed on March 21, 2019]
- ESA Sentinel Online, Home, User guide, Sentinel – 1 SAR, Product Types and Processing Levels, Level-1 <https://sentinel.esa.int/web/sentinel/user-guides/sentinel-1-sar/product-types-processing-levels/level-1> [Accessed on May 25, 2019]
- González, P. J., Bagnardi, M., Hooper, A. J., Larsen, Y., Marinkovic, P., Samsonov, S. V., & Wright, T. J., 2015. The 2014–2015 eruption of Fogo volcano: Geodetic modeling of Sentinel-1 TOPS interferometry. *Geophysical research letters*, 42(21), 9239-9246.
- Gomarasca, M. A., 2009. Basics of geomatics. Springer Science & Business Media.
- Gomez, C., & Purdie, H., 2016. UAV-based photogrammetry and geocomputing for hazards and disaster risk monitoring—a review. *Geoenvironmental Disasters*, 3(1), 23.
- ISPRA, Istituto Superiore per la Protezione e la Ricerca Ambientale, Online at [http://www.isprambiente.gov.it/it/progetti/acque-interne-e-marino-costiere-1/progetti-conclusi/copy\\_of\\_progetti-conclusi](http://www.isprambiente.gov.it/it/progetti/acque-interne-e-marino-costiere-1/progetti-conclusi/copy_of_progetti-conclusi) [Accessed on May 20, 2019]
- Marghany, M., & Hashim, M. (2010). Different polarised topographic synthetic aperture radar (TOPSAR) bands for shoreline change mapping. *International Journal of Physical Sciences*, 5(12), 1883-1889.
- Malenovský, Z., Rott, H., Cihlar, J., Schaepman, M. E., García-Santos, G., Fernandes, R., & Berger, M., 2012. Sentinels for science: Potential of Sentinel-1,-2, and-3 missions for scientific observations of ocean, cryosphere, and land. *Remote Sensing of Environment*, 120, 91-101.
- Mills, J. P., Buckley, S. J., Mitchell, H. L., Clarke, P. J., & Edwards, S. J., 2005. A geomatics data integration technique for coastal change monitoring. *Earth Surface Processes and Landforms: The Journal of the British Geomorphological Research Group*, 30(6), 651-664.
- Misra, A., & Balaji, R., 2015. A study on the shoreline changes and Land-use/land-cover along the South Gujarat coastline. *Procedia Engineering*, 116, 381-389.
- Nagler, T., Rott, H., Hetzenecker, M., Wuite, J., & Potin, P., 2015. The Sentinel-1 mission: New opportunities for ice sheet observations. *Remote Sensing*, 7(7), 9371-9389.
- Palazzo, F., Baiocchi, V., Del Frate, F., Giannone, F., Dominici, D., Latini, D., ... & Remondiere, S. (2011). Remote Sensing as a Tool to Monitor and Analyse Abruzzo Coastal Changes: Preliminary Results from the ASI COSMO-Coast Project. In 5th EARSeL Workshop on Remote Sensing of the Coastal Zone Proceedings.
- Pedersen, L. T., Saldo, R., & Fenger-Nielsen, R., 2015, July. Sentinel-1 results: Sea ice operational monitoring. In 2015 IEEE International Geoscience and Remote Sensing Symposium (IGARSS) (pp. 2828-2831). IEEE.
- Sawaya, K. E., Olmanson, L. G., Heinert, N. J., Brezonik, P. L., & Bauer, M. E., 2003. Extending satellite remote sensing to local scales: land and water resource monitoring using high-resolution imagery. *Remote sensing of Environment*, 88(1-2), 144-156.
- Shalaby, A., & Tateishi, R., 2007. Remote sensing and GIS for mapping and monitoring land cover and land-use changes in the Northwestern coastal zone of Egypt. *Applied Geography*, 27(1), 28-41.
- Taha, L. G. E. D., & Elbeih, S. F., 2010. Investigation of fusion of SAR and Landsat data for shoreline super resolution mapping: the northeastern Mediterranean Sea coast in Egypt. *Applied Geomatics*, 2(4), 177-186.
- Xu, J., Wang, H., Luo, Y., Wang, S. Q., & Yan, X. Q., 2010. Deformation monitoring and data processing of landslide based on 3D laser scanning. *Rock and Soil Mechanics*, 31(7), 2188-2191.





**ENEA**

Promotion and Communication Service

*enea.it*

Graphic design and layout: Flavio Miglietta

Printed in June 2019  
at ENEA Frascati Research Center

ISBN 978-88-8286-377-7

**ENEA**  
Servizio Promozione e Comunicazione

giugno 2019